Geochronology and geochemistry of a Kimban diorite, drill hole LED001, Lake Gilles, eastern Gawler Craton

Stacey McAvaney and Elizabeth Jagodzinski

Government of South Australia
Department for Manufacturing, Innovation, Trade, Resources and Energy

Report Book
2012/00010

Geochronology and geochemistry of a Kimban diorite, drill hole LED001, Lake Gilles, eastern Gawler Craton

Stacey McAvaney and Elizabeth Jagodzinski

Geological Survey of South Australia
Resources and Energy Group

April 2012

Report Book 2012/00010

Government of South Australia
Department for Manufacturing, Innovation, Trade, Resources and Energy

Resources and Energy Group
Department for Manufacturing, Innovation, Trade, Resources and Energy
Level 7, 101 Grenfell Street, Adelaide
GPO Box 1264, Adelaide SA 5001
Phone +61 8 8463 3037
Email dmitre.minerals@sa.gov.au
www.minerals.dmitre.sa.gov.au

South Australian Resources Information Geoserver (SARIG)
SARIG provides up-to-date views of mineral, petroleum and geothermal tenements and other geoscientific data. You can search, view and download information relating to minerals and mining in South Australia including tenement details, mines and mineral deposits, geological and geophysical data, publications and reports (including company reports).
www.sarig.dmitre.sa.gov.au

Preferred way to cite this publication
McAvaney, S. and Jagodzinski E. 2012. *Geochronology and geochemistry of a Kimban diorite, drill hole LED001, Lake Gilles, eastern Gawler Craton*, Report Book 2012/00010. Department for Manufacturing, Innovation, Trade, Resources and Energy, South Australia, Adelaide.

CONTENTS

TABLES

FIGURES

Geochronology and geochemistry of a Kimban diorite, drill hole LED001, Lake Gilles, eastern Gawler Craton

Stacey McAvaney and Elizabeth Jagodzinski

1. INTRODUCTION

The geology of the Lake Gilles area in the south west of the Port Augusta 250k map sheet is poorly understood (Fig. 1). Outcrop of basement rocks in the area is sparse and typically occurs along the margins of the salt lake where it is highly weathered. The rocks consist of an interlayered sequence of orthogneiss and amphibolite and minor paragneisses which are tight to isoclinally folded about subhorizontal axes trending NNW (Reid et al., 2008). The gneisses are intruded by undeformed granitoids, pegmatites and dolerites. In departmental mapping all these rocks were originally assigned to the lower Palaeoproterozoic Cleve Metamorphics (Dalgarno et al., 1968), and were subsequently differentiated into the Hutchison Group and Lincoln Complex granitoids (Weste, 1996).

Recent geochronology of a foliated leucogranite on the northern shore of Lake Gilles yielded a crystallisation age of ~2529±4 Ma, (Fraser et al., 2010), suggesting that these gneisses are equivalent to the Sleaford Complex. Migmatitic and mylonitic gneisses on the northwestern shore of Lake Gilles are along strike from the Minbrie Gneiss to the south on the WHYALLA 1:250 000 map sheet, a sequence of migmatitic gneisses deformed during the Kimban Orogeny (Parker and Flint, 1983), which also has a precursor age similar to that of the Sleaford Complex (Fanning et al., 2007; Fraser and Neumann, 2010).

Recent geochronology near Iron Knob has revealed the presence of Mesoarchaean crust (Fig. 1). The Cooyerdoo Granite, a weakly foliated to gneissic I-type granite, crops out to the south on either side of the Middleback Range (Fraser et al., 2010; McAvaney, 2012). The granite has a crystallisation age of ~3150 Ma and contains inherited zircons up to ~3300 Ma in age and a D_{TM} between 3400 and 3200 Ma (Fraser et al., 2010). The foliated leucogranite on the northern shore of Lake Gilles contains inherited zircons 3150 Ma and on a neodymium isotope evolution diagram it lies within the trend of the Cooyerdoo Granite, suggesting that the leucogranite was derived from partial melting of the Cooyerdoo Granite during the Sleafordian Orogeny. It is believed that the Cooyerdoo Granite extends in the subsurface as far west as the Kalinjala Mylonite Zone (Fraser et al., 2010), a Kimban-aged structure evident in the TMI (Fig. 1).

Despite this recent progress, many geological questions about the area still remain, such as the age of the younger intrusives, whether the paragneisses within the sequence are Sleafordian equivalents or structurally interleaved Hutchison Group, whether Sleafordian metamorphism is preserved, whether the Slefordian equivalents intrude the Cooyerdoo Granite or another sequence, and whether the Cooyerdoo Granite is exposed. Due to the paucity of fresh outcrop a detailed study employing petrology (descriptions from Purvis, 2009; Purvis, 2010), geochemistry and geochronology were carried out on a recent diamond hole drilled near Lake Gilles, in the hope of answering some of these questions.

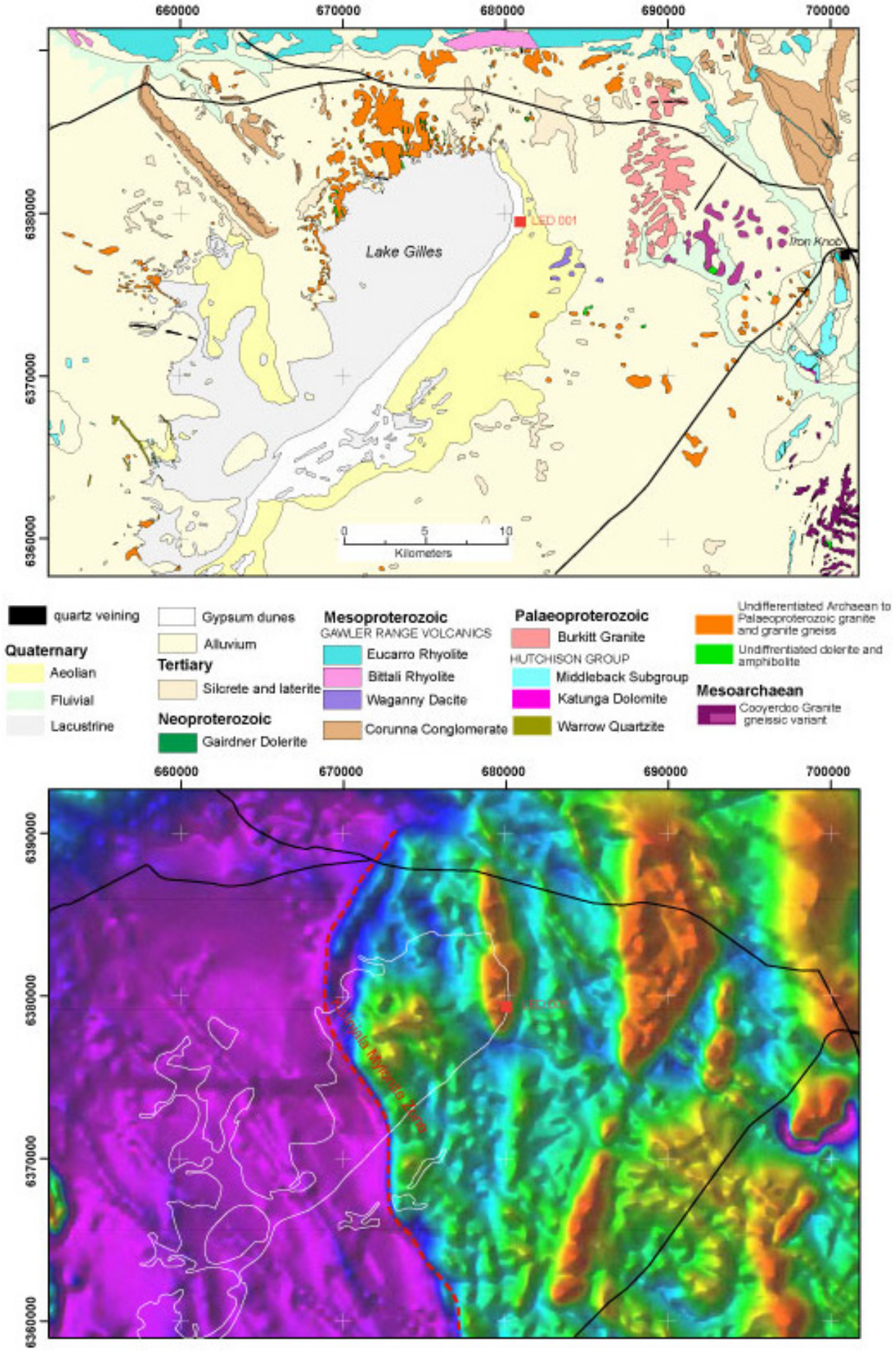

Figure 1. Geology (a) and TMI (b) of the Lake Gilles area, showing location of drill hole LED001.

2. DRILL HOLE LED 001

Drill hole LED 001 (DH No. 229988) is a PACE (Plan for Accelerating Exploration)-funded diamond hole drilled by Intermet Resources to test a magnetic feature while exploring for gold and base metals on their Lake Gilles Tenement (EL 3466) in 2007 (Faulkner, 2007) (Fig. 1). The hole is located approximately 20 km west of Iron Knob on the north-eastern edge of Lake Gilles, and was drilled at an angle of 60° due west to a depth of 676.0 m. The drillhole intersected a diorite pluton which intrudes a finely layered metasediment and fine grained mafic rocks, and is itself intruded by intermediate and mafic volcanics (see graphic log in Fig. 2, and Table 1 summarising intrusive relationships). The diorite is believed to define the magnetic high visible in the regional magnetics (Fig. 1).

3. DIORITE

The drill hole intersects a diorite pluton from 72.5 m down to the bottom of the hole at 676 m. The pluton contains two major lithologies, a smaller granodiorite in the shallower part of the pluton and a larger diorite in the deeper part of the pluton (Fig. 2). At the beginning of the hole the granodiorite and diorite are interlayered with sharp contact boundaries (Fig. 3a), such as at 76.10 m and 78.35 m, but at 103.10 m fingers of the granodiorite intrude the diorite (Fig. 3b) and a xenolith of diorite occurs within the granodiorite above the contact. Thus, the granodiorite is presumably a late stage phase of the pluton.

3.1 PETROLOGY

The granodiorite is medium to coarse-grained, and composed of plagioclase, potassium feldspar and quartz with minor hornblende and biotite (Figs 4a and 4b). Plagioclase occurs as euhedral crystals 0.5–7 mm long, and is surrounded by interstitial quartz grains up to 2 mm in diameter, and potassium feldspar grains up to 4 mm in diameter which locally encloses plagioclase, opaque oxide and quartz (Purvis, 2010). Scattered mafic clots consist of biotite up to 1.5 mm long and brown hornblende up to 2 mm long (Purvis, 2010). Grains and aggregates of magnetite and titanate occur, as well as prisms of apatite which is commonly adjacent to oxide or mafic silicate grains, and rare zircon (Purvis, 2010).

The diorite plots as a diorite, quartz-diorite and quartz-monzonite on a Quartz-Alkali Feldspar-Plagioclase diagram (Fig. 5). The diorite is predominantly medium to coarse-grained (Fig. 3c) and is composed typically of plagioclase, hornblende and biotite with minor, quartz, oxide and titanite (Figs 4c and 4d), and occasionally also either potassium feldspar or clinopyroxene (Figs 4e and 4f). Euhedral plagioclase crystals are up to 6 mm long and 4 mm wide and are occasionally weakly aligned, and hornblende crystals are up to 2.5 mm long and are surrounded by interstitial poikilitic biotite up to 4 mm, minor granular quartz, disseminated titanite and magnetite associated with apatite and rare zircon (Purvis, 2010). Pyroxene grains are up to 4 mm wide and are occasionally preserved, but are more often represented by aggregates of actinolite and hornblende or actinolite and chlorite (Purvis, 2010). When potassium feldspar occurs it is poikilitic and interstitial (Purvis, 2010).

Within the diorite there is a fine-grained and porphyritic phase at 324.50–327.45 m which has sharp contacts with the surrounding coarser-grained rock (Fig. 2). It is composed of plagioclase phenocrysts up to 4 mm long in a groundmass of plagioclase and granular hornblende with minor interstitial biotite, quartz, potassium feldspar, titanite, apatite and oxide (Fig. 3d; Purvis, 2010). Leucocratic bands ranging in thickness from less than 5 cm to 1 m are common in the diorite between 520 and 550 m depth (Fig. 3e). A gabbroic phase at 417.0–420.0 m has gradational contacts with the surrounding diorite and is composed predominantly of pyroxene and plagioclase up to 5 mm in grainsize (Purvis, 2009) (Fig. 3f).

The diorite is undeformed, but for a distinct interval of protomylonitic diorite gneiss at approximately 338 m (Fig. 2) which is strongly foliated and contains mylonitic lamellae of quartz and potassium feldspar interstitial to plagioclase, hornblende and biotite (Purvis, 2010).

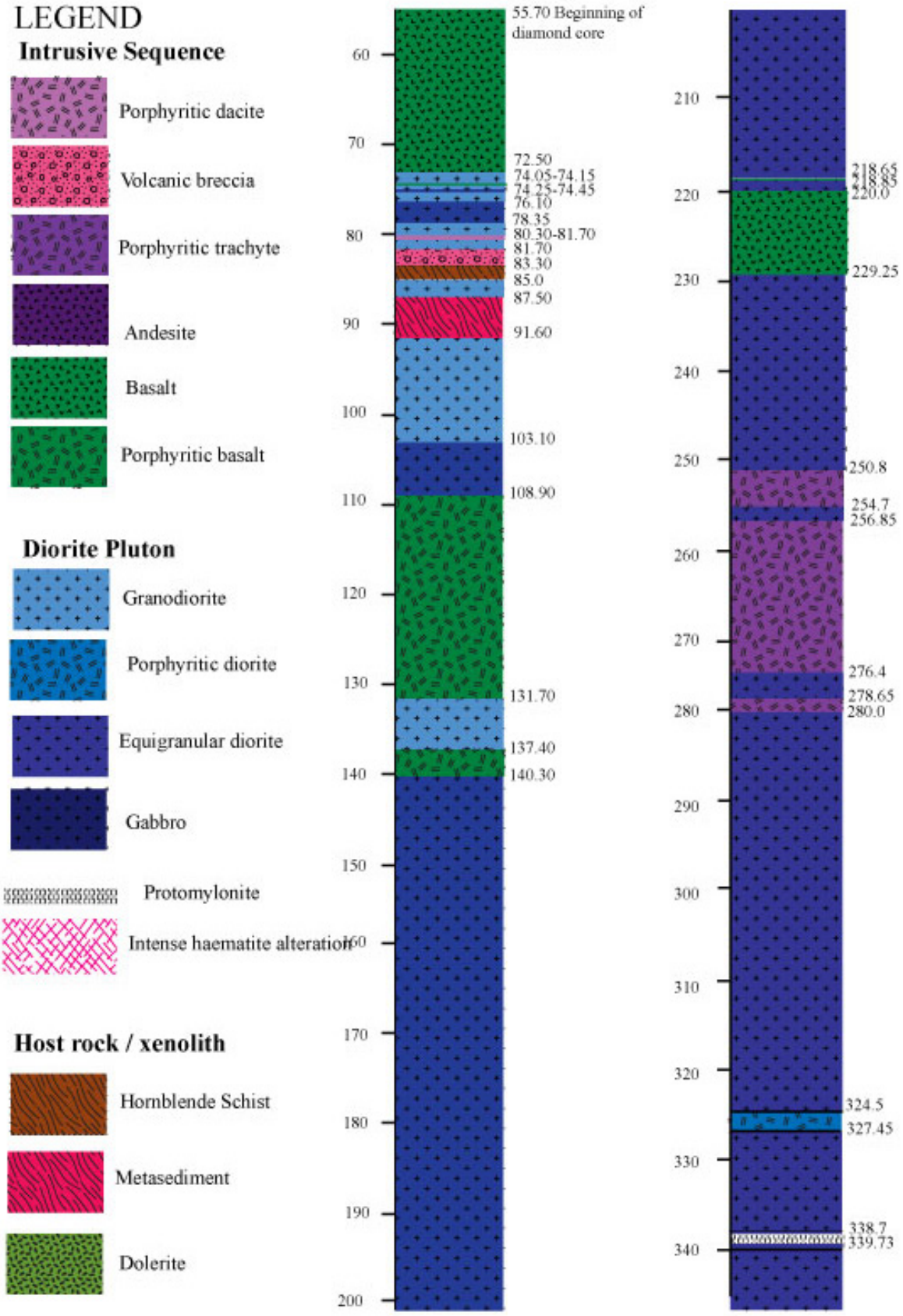
LEGEND
Intrusive Sequence
Porphyritic dacite
Volcanic breccia
Porphyritic trachyte
Andesite
Basalt
Porphyritic basalt
Diorite Pluton
Granodiorite
Porphyritic diorite
Equigranular diorite
Gabbro
Protomylonite
Intense haematite alteration
Host rock / xenolith
Hornblende Schist
Metasediment
Dolerite
55.70 Beginning of diamond core
72.50
74.05-74.15
74.25-74.45
76.10
78.35
80.30-81.70
81.70
83.30
85.0
87.50
91.60
103.10
108.90
131.70
137.40
140.30
218.65
220.0
229.25
250.8
254.7
256.85
276.4
278.65
280.0
324.5
327.45
338.7
339.73

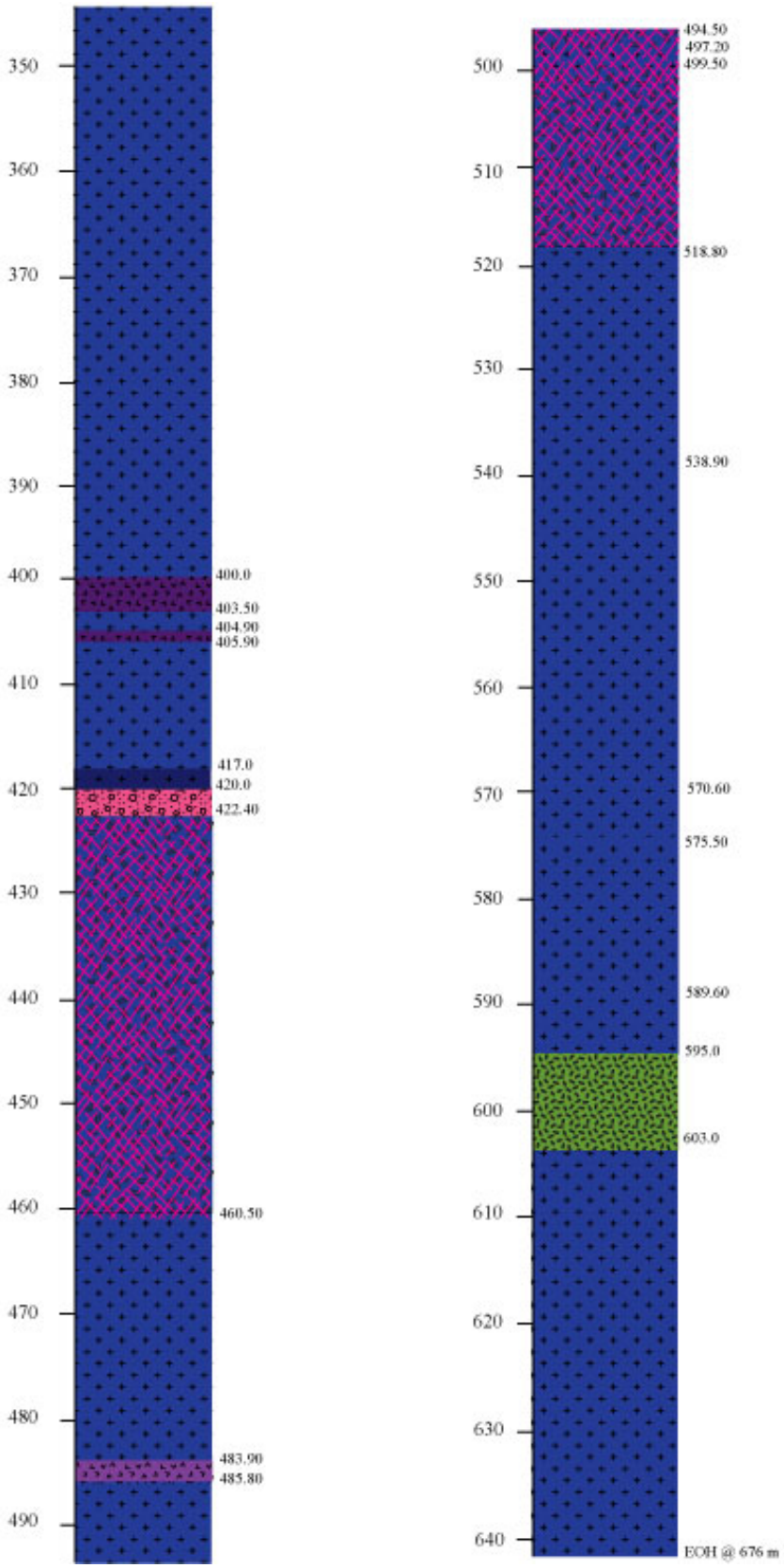

Figure 2. Graphic log of drill hole LED001.

The diorite has undergone alteration including replacement of primary mineralogy and subsequent veining, which is likely to be associated with the volcanics which intrude it (Gifkins et al., 2005). Intense haematite-staining of plagioclase occurs in intervals of the diorite, particularly between 422–460 m and 499–518 m (Fig. 2), often flanking fractures or pegmatite veins, and gives the rock a strong pink colour (Figs 6a – 6c). Mafic silicates are weak to strongly altered, with hornblende replaced by chlorite and leucoxene, biotite replaced by chlorite and epidote with minor leucoxene and titanite and pyroxene replaced by actinolite and hornblende or actinolite and chlorite (Purvis, 2010). The diorite is also intruded by chlorite veins (Figs 6c and 6d), pegmatite veins (Figs 6e and 6f) and calcite veins.

Table 1. Intrusive relationship with diorite

Unit	**Core Interval** (m)	**Relation-ship with diorite**	**Notes**
Aphyric basalt I	Start of diamond core (55.70) – 72.50	Intrusive	Broken core at contact Chloritic alteration in basalt at contact
Aphyric basalt II	74.05 – 74.15	Intrusive	Thin vein intruding diorite, probably associated with Aphyric basalt I
Porphyritic dacite	80.00 – 80.30	Intrusive	Upper contact ambiguous Lower contact sharp with recrystallisation of biotite along contact with diorite Alteration in diorite below volcanic
Volcanic breccia I	81.70 – 83.30	Intrusive	Contains fragments of diorite and schist
Hornblende Schist I	83.30 – 85.0	Intruded	Broken core at both contacts Diorite vein intruding schist
Porphyritic basalt I	108.90 – 131.70	Ambiguous	Upper contact at broken core Basalt altered for the first 10cm below upper contact
Porphyritic basalt II	137.40 – 140.30	Ambiguous	Upper contact ambiguous Lower contact at broken core
Aphyric basalt III	218.65 – 218.85	Intrusive	Upper contact invaded by pegmatite dyke Lower contact intrusive Basalt is brecciated and chlorite-altered
Aphyric basalt IV	220.00 – 229.25	Ambiguous	Upper contact at broken core Lower contact intruded by calcite vein Basalt is brecciated and chlorite-altered
Porphyritic trachyte I	250.80 – 254.70	Intrusive	Contacts at broken core Purple-brown cooling margin at contacts
Porphyritic trachyte II	256.85 – 276.40	Intrusive	Contacts at broken core Purple-brown cooling margin at contacts
Porphyritic trachyte III	278.65 – 280.0	Intrusive	Apophyses of volcanic intruding diorite Purple-brown cooling margin at contacts
Andesite I	400.0 – 403.50	Intrusive	Apophyses of volcanic intruding diorite Volcanic vein in diorite
Andesite II	404.90 – 405.90	Intrusive	Sharp ambiguous contacts Probably associated with Andesite I
Volcanic breccia II	420.0 – 422.40	Intrusive	
Andesite III	483.90 – 485.80	Intrusive	Apophyses of volcanic intruding diorite
Dolerite I	595.0 – 603.0	Intruded	Enclaves of dolerite in diorite above contact Diorite veins intruding dolerite

3.2 GEOCHRONOLOGY

A sample of the diorite (R1708863) from the interval 158.7–160.15 m was selected for geochronology.

Table 2. Sample Information 1708863

GA fieldsites number:	2109662		
Collector:	S McAvaney		
Analyst:	E Jagodzinski		
Stratigraphic Unit:	unassigned		
Location GDA94:	680450	6381003	Zone 53
Location Lat-Long:	32° 41” 38.23”	136° 55’ 29.69”	
250K map sheet	PORT AUGUSTA (SH5304)		
100K map sheet	UNO (6232)		
Location:	DDH LED1 (#229988), 158.7–160.15 m		
Mount:	GA 6144		
Date analysed:	14-18 Oct 2010		
Machine:	SHRIMP IIe (GA) LIMS session 100134		
OG1 standard age (α)*	3463.1 ± 2.0 Ma (0.99846)		
IMF correction applied?	Yes		
Interpreted age:	1742 ± 6 Ma		
Age type:	Magmatic crystallisation		

*α is a correction for instrumental mass fractionation (IMF) defined by Stern et al. (2009).

3.2.1 ANALYTICAL DETAILS

Zircons from sample R1708863 were mounted in epoxy resin, together with three zircon standards. Absolute U and Th concentrations were estimated by comparison with the M257 zircon standard (840 ppm ^{238}U). Temora 2 ($^{206}Pb^*/^{238}U$ = 0.0668 [416.8 Ma], Black et al. 2003), was included to calibrate the $^{206}Pb/^{238}U$ ratio and monitor the accuracy of the ^{204}Pb common-Pb correction. Fifty five analyses of the Temora standard were obtained during the session, and have an external spot-to-spot (reproducibility) uncertainty of 0% (1σ) and a $^{238}U/^{206}Pb^*$ calibration uncertainty of 0.14% (1σ). A more realistic Pb/U external error of 1.0% (1σ) has been assigned for data reduction.

The OG1 standard (3465.4 ± 0.6 Ma, Stern et al. 2009) was used to monitor $^{207}Pb^*/^{206}Pb^*$ reproducibility and accuracy, and yielded an age of 3463.1 ± 2.0 Ma (MSWD = 1.2, probability of fit = 0.19, n = 30 of 31).

Data were reduced and analysed using Squid 2 and Isoplot V3.71 (Ludwig 2001, Ludwig 2003), using decay constants recommended by Steiger and Jäger (1977). Common Pb corrections were applied to all analyses using contemporaneous common Pb isotopic compositions determined according to the Pb isotopic model of Stacey and Kramers (1975). Mean ages are reported with 95% confidence intervals.

3.2.2 ZIRCON CHARACTERISTICS

The zircon in this sample is very similar in appearance to the TEMORA zircon standard, which derives from the medium- to coarse-grained, low silica (48%), mafic, Middledale Gabbroic Diorite (Black et al. 2003). As with Temora, the separated zircon represents coarse grain fragments, about 200 μm in size, with both euhedral and repressed crystal faces, suggesting that the zircon formed late in the crystallisation sequence (Fig. 7). Sector zoning is present in some grains and the oscillatory zoning is generally quite broad. The crystals are clear, and in very good condition, with few cracks and inclusions and no cores. The low uranium content of the crystals (average = 115 ppm) explains the absence of radiation damage. Th/U ratios are >1 (0.9–1.64, average = 1.3).

Fractionated mafic rocks commonly have Th/U >1.0. In the absence of monazite, a greater amount of Th is incorporated into the zircon crystal structure than is usual in felsic igneous rocks, which typically have between 0.1–1.0 Th/U.

3.2.3 SAMPLE DATA

Thirty four grains were analysed. All data are near concordant (≤ 6% discordant, Fig. 8) and all analyses are indistinguishable in age (Fig. 9). They yield a weighted mean $^{207}Pb/^{206}Pb$ age of 1740 ± 6 Ma (MSWD = 1.4, probability of equivalence = 0.06). When corrected for IMF the age becomes 1742 ± 6 Ma. This is the best estimate for the crystallisation age of the diorite intrusion.

Figure 3. Photos of diorite. (a) Sharp contact between granodiorite (left) and diorite (right). (b) Granodiorite apophyses intruding diorite. (c) Medium grained equigranular

diorite. (d) Porphyritic diorite. (e) Leucosome within diorite. (f) Gabbroic phase overprinted in places by haematite alteration.

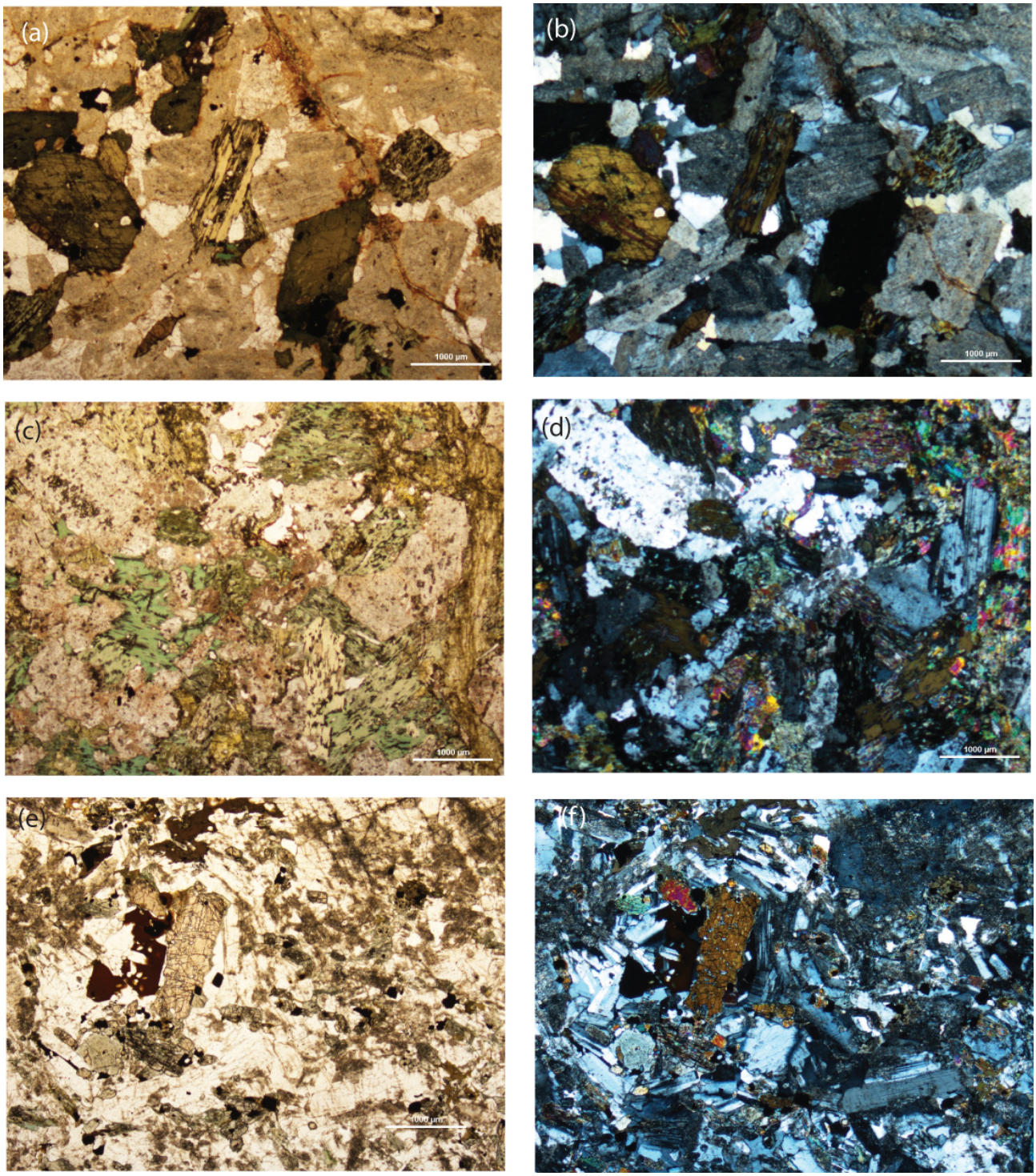

Figure 4. Photomicrographs of diorite. Granodiorite phase viewed under (a) plane polarised and (b) cross polarised light. Hornblende-dominant phase of diorite viewed under (c) plane polarised and (d) cross polarised light. Clinopyroxene-bearing phase of diorite viewed under (e) plane polarised and (f) cross polarised light.

Table 3. SHRIMP analytical results for zircon from R1708867: diorite intrusion

Spot	% $206Pb_c$	U ppm	Th ppm	232Th /238U	238U /206Pb*	206Pb* /238U	±%	207Pb* /235U	IMF-corr 207Pb* /235U	±%	207Pb* /206Pb*	IMF-corr 207Pb* /206Pb*	±%	207Pb /206Pb Age	IMF-corr 207Pb /206Pb Age	± Ma	% Disc
863.17.1.1	0.15	103	156	1.56	3.21	0.312	1.49	4.484	4.491	1.73	0.10439	0.10455	0.88	1704	1706	16	-3
863.10.1.1	0.12	111	176	1.64	3.25	0.308	1.49	4.449	4.456	1.71	0.10484	0.10500	0.85	1712	1714	16	-1
863.1.1.1	0.10	65	68	1.08	3.30	0.303	1.74	4.396	4.403	2.04	0.10516	0.10533	1.08	1717	1720	20	1
863.20.1.1	0.13	81	105	1.33	3.28	0.304	1.60	4.415	4.422	1.88	0.10517	0.10533	0.98	1717	1720	18	0
863.3.1.1	0.11	100	118	1.23	3.24	0.309	1.54	4.476	4.483	1.78	0.10519	0.10535	0.88	1718	1720	16	-1
863.23.1.1	0.11	70	79	1.16	3.26	0.307	1.69	4.457	4.464	1.98	0.10536	0.10553	1.04	1721	1723	19	-0
863.24.1.1	0.01	140	221	1.63	3.20	0.313	1.39	4.548	4.555	1.55	0.10540	0.10556	0.68	1721	1724	12	-2
863.25.1.1	0.19	71	94	1.36	3.18	0.315	1.68	4.577	4.584	2.28	0.10544	0.10561	1.54	1722	1725	28	-3
863.26.1.1	0.16	93	140	1.56	3.26	0.307	1.55	4.468	4.475	1.82	0.10555	0.10571	0.94	1724	1727	17	-0
863.4.1.1	0.16	70	79	1.17	3.26	0.307	1.70	4.474	4.481	2.02	0.10579	0.10596	1.08	1728	1731	20	0
863.29.1.1	0.03	226	243	1.11	3.23	0.309	1.26	4.512	4.519	1.37	0.10579	0.10596	0.54	1728	1731	10	-1
863.12.1.1	0.00	68	59	0.90	3.19	0.314	1.70	4.582	4.589	1.95	0.10585	0.10601	0.95	1729	1732	17	-2
863.8.1.1	0.03	99	149	1.55	3.28	0.305	1.54	4.449	4.456	1.76	0.10585	0.10602	0.84	1729	1732	15	1
863.27.1.1	0.10	96	96	1.04	3.24	0.308	1.54	4.503	4.510	1.78	0.10593	0.10610	0.89	1731	1733	16	-0
863.6.1.1	0.12	98	123	1.30	3.25	0.308	1.56	4.501	4.508	2.13	0.10594	0.10610	1.44	1731	1733	26	-0
863.33.1.1	0.15	64	67	1.08	3.19	0.313	1.76	4.582	4.589	2.09	0.10602	0.10619	1.13	1732	1735	21	-2
863.7.1.1	0.11	118	141	1.23	3.25	0.307	1.47	4.496	4.503	1.68	0.10608	0.10624	0.81	1733	1736	15	0
863.19.1.1	--	112	166	1.53	3.22	0.310	1.47	4.548	4.555	1.66	0.10634	0.10650	0.77	1738	1740	14	-0
863.31.1.1	0.08	119	124	1.08	3.19	0.314	1.45	4.602	4.609	1.63	0.10637	0.10653	0.76	1738	1741	14	-1
863.5.1.1	0.06	154	241	1.62	3.30	0.303	1.38	4.442	4.449	1.55	0.10641	0.10658	0.71	1739	1742	13	2
863.21.1.1	0.05	152	218	1.49	3.27	0.305	1.37	4.486	4.493	1.52	0.10654	0.10670	0.67	1741	1744	12	1
863.32.1.1	0.03	178	169	0.98	3.27	0.306	1.33	4.496	4.503	1.46	0.10654	0.10671	0.61	1741	1744	11	1
863.15.1.1	0.00	108	112	1.08	3.19	0.313	1.50	4.601	4.608	1.69	0.10660	0.10676	0.78	1742	1745	14	-1
863.18.1.1	0.01	149	204	1.41	3.22	0.310	1.37	4.562	4.569	1.52	0.10667	0.10683	0.65	1743	1746	12	0
863.28.1.1	0.01	153	233	1.58	3.24	0.309	1.45	4.544	4.551	1.63	0.10683	0.10699	0.73	1746	1749	13	1
863.34.1.1	--	113	130	1.19	3.18	0.314	1.46	4.631	4.638	1.66	0.10694	0.10710	0.77	1748	1751	14	-1
863.2.1.1	0.07	175	214	1.26	3.25	0.308	1.34	4.549	4.556	1.49	0.10714	0.10730	0.64	1751	1754	12	1

Spot	% $206Pb_c$	ppm U	ppm Th	232Th /238U	238U /206Pb*	206Pb* /238U	±%	207Pb* /235U	IMF-corr 207Pb* /235U	±%	207Pb* /206Pb*	IMF-corr 207Pb* /206Pb*	±%	207Pb /206Pb Age	IMF-corr 207Pb /206Pb Age	± Ma	% Disc
863.11.1.1	0.03	103	128	1.28	3.29	0.304	1.52	4.500	4.507	1.72	0.10740	0.10757	0.81	1756	1759	15	3
863.14.1.1	0.04	155	174	1.16	3.28	0.304	1.37	4.512	4.519	1.53	0.10750	0.10767	0.68	1758	1760	12	3
863.16.1.1	--	97	115	1.22	3.26	0.307	1.53	4.553	4.560	1.73	0.10754	0.10771	0.81	1758	1761	15	2
863.30.1.1	0.00	91	118	1.34	3.27	0.306	1.54	4.539	4.546	1.74	0.10770	0.10786	0.80	1761	1764	15	3
863.22.1.1	0.07	98	144	1.51	3.29	0.304	1.53	4.532	4.539	1.75	0.10807	0.10823	0.85	1767	1770	15	4
863.13.1.1	--	110	133	1.24	3.27	0.306	1.49	4.584	4.591	1.68	0.10857	0.10874	0.77	1776	1778	14	3
863.9.1.1	0.08	101	123	1.26	3.34	0.300	1.52	4.506	4.513	1.75	0.10908	0.10925	0.86	1784	1787	16	6

Data are 1σ precision. Pbc and Pb* indicate the common and radiogenic portions, respectively.
All Pb data are common Pb corrected based on measured ^{204}Pb (after Stacey and Kramer 1975), then corrected for instrumental mass fractionation (IMF)
Both uncorrected data, and IMF-corrected data (grey columns) are presented.

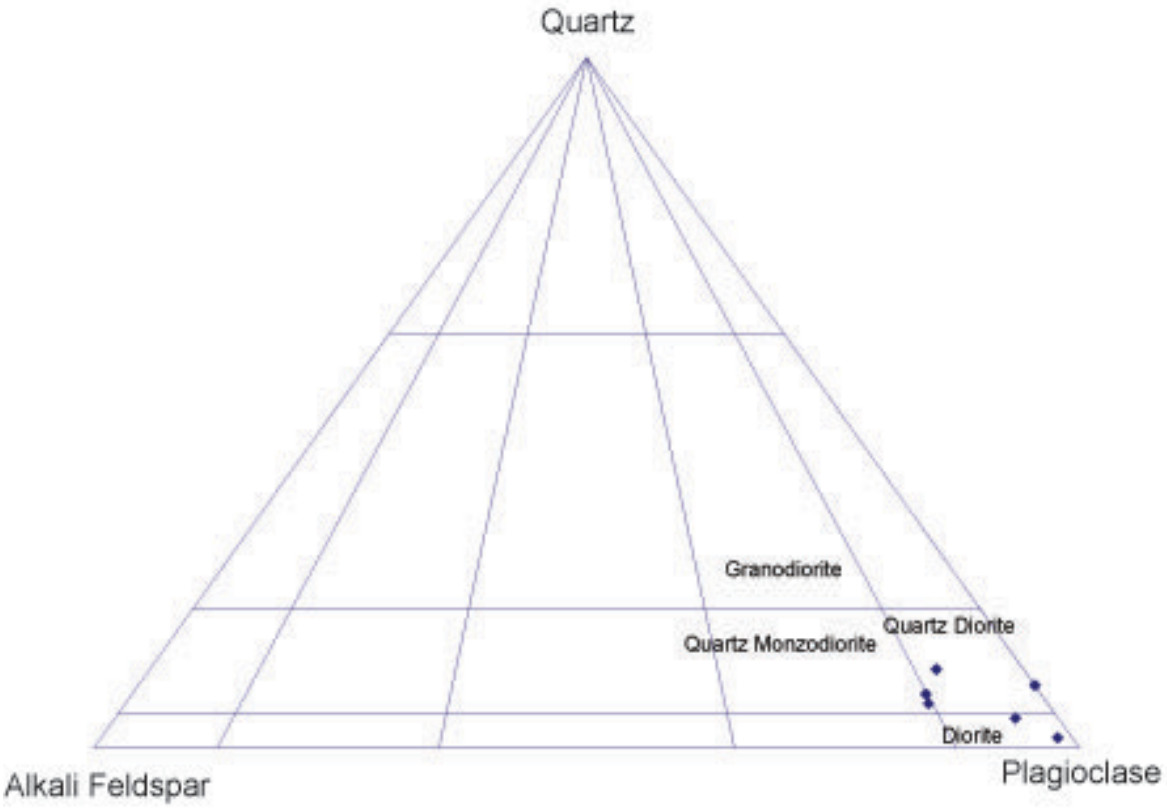

Figure 5. Quartz-Alkali Feldspar-Plagioclase diagram for diorite. Adapted from (Purvis, 2010).

3.3 GEOCHEMISTRY

Despite being classified as a diorite on petrological grounds (Fig. 5), the pluton is monzonitic when classified geochemically using a total-alkalis vs silica (TAS) diagram (Fig. 10). This may be due to the net addition of Na and K in the rock during albitisation and sericification of plagioclase. Despite alteration, the diorite shows typically linear trends on Harker diagrams, which suggest that all compositional phases of the diorite are part of a single magma source (Figs 11 and 12). All samples of the diorite share a similar trace and REE (Rare Earth Element) signature, but for the leucocratic banding which is more depleted in P, Ti and REE. Compared to primitive mantle the diorite is depleted in Rb, Nb, P, Zr, Ti and Y and enriched in Pb and Yb (Fig. 13a). The diorite is more enriched in LREE relative to HREE, which suggests fractional crystallisation and/or crustal contamination and has a positive Yb anomaly (Fig. 13b).

3.4 DISCUSSION

The diorite in LED001 belongs to the suite of both felsic and mafic rocks which intruded the Palaeoproterozoic volcano-sedimentary successions and Archaean rocks of the southern Gawler Craton during the Kimban Orogeny (Parker, 1993). Those of closest comparable age include the 1742±19 Ma Burkitt Granite (Fraser and Neumann, 2010), a hornblende-bearing syenite which crops out directly to the east of LED001 (Fig. 1), a 1738±4 Ma garnet-bearing leucogranite exposed to the west of Lake Gilles (Fraser and Neumann, 2010), and the 1736±6 Ma Middlecamp Granite (Fraser and Neumann, 2010), a foliated granite to the south in the Cleve Hills.

Figure 6. Alteration and veining of diorite. (a) Interval of core (left to right is down hole) showing diorite affected by bands of haematite alteration (pink sections) and intruded by pegmatite veins. (b) Haematite alteration flanking fractures in diorite. (c) Haematite alteration in diorite discolouring plagioclase phenocrysts, cross-cut by chlorite vein. (d) Patch of chloritic alteration overprinting carbonate vein. (e) Large coarse grained pegmatite vein intruding diorite. (f) Small pegmatite veins intruding diorite.

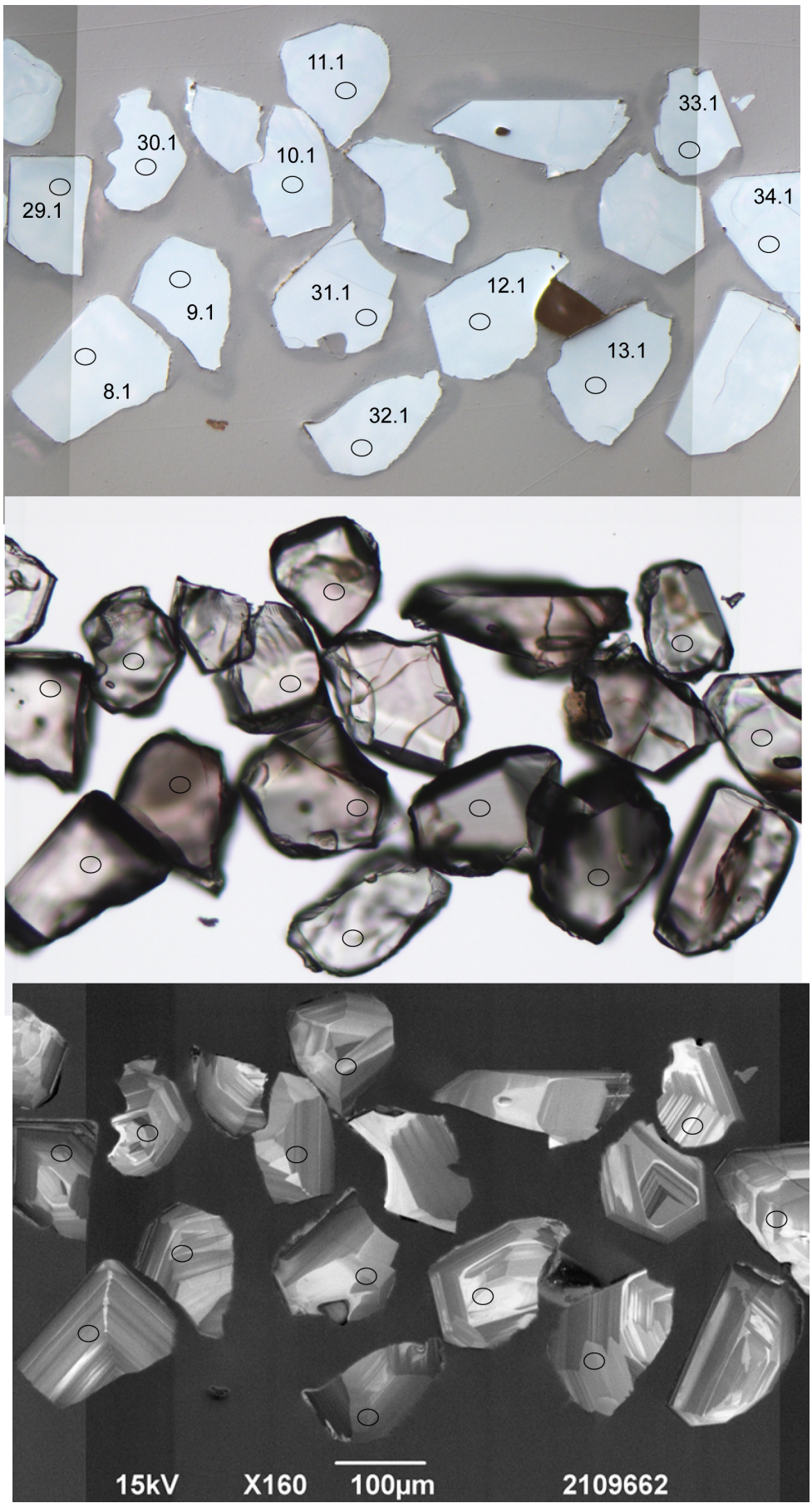

Figure 7. Representative zircon from sample R1708863, showing the location of SHRIMP analyses annotated with their $^{207}Pb/^{206}Pb$ ages: **reflected light (top), transmitted light (middle) and CL (bottom) images.**

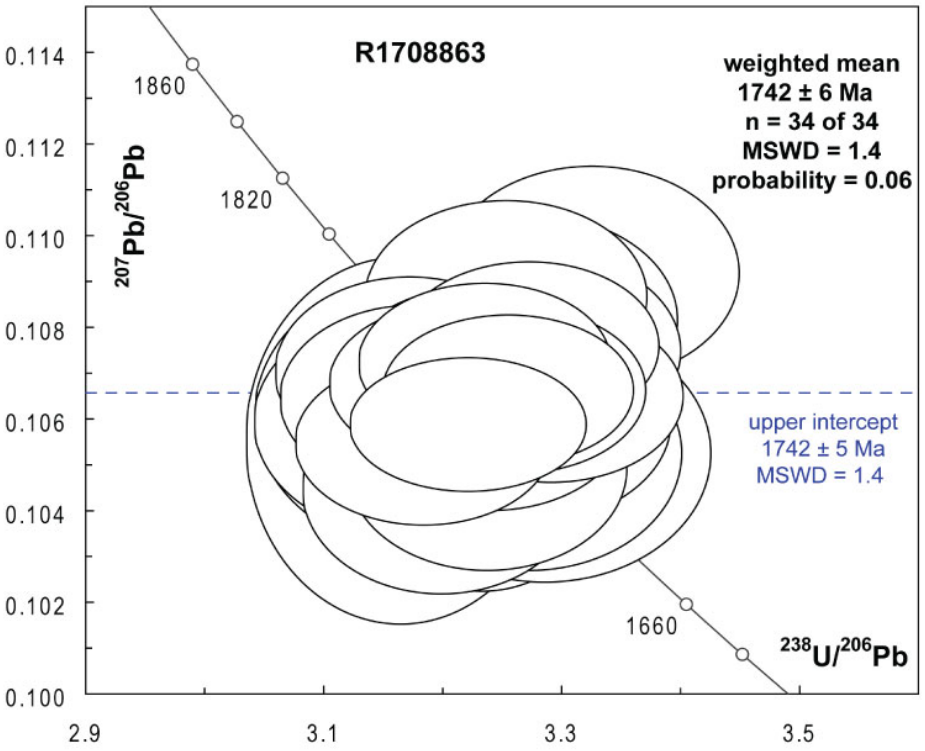

Figure 8. Tera-Wasserburg Concordia diagram for sample R1708863, generated using IMF-corrected $^{207}Pb/^{206}Pb$ ratios. When the lower intercept is anchored at the origin, the upper Concordia intercept age agrees well with the weighted mean age of the zircons.

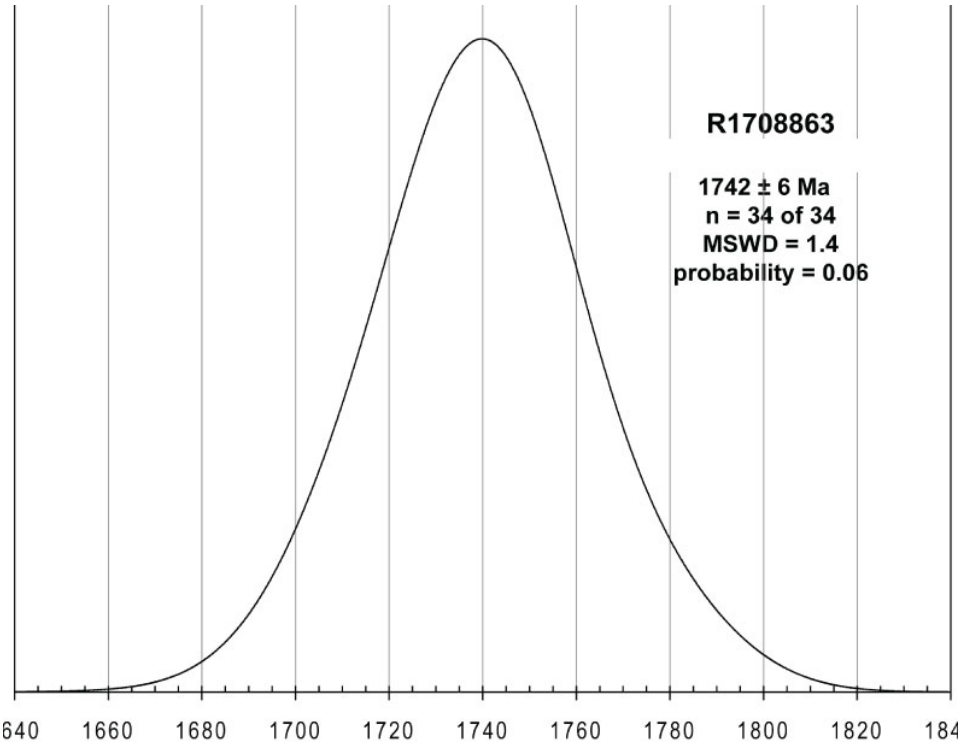

Figure 9. Probability density diagram for all analyses. The simple Gaussian distribution indicates that the analyses form a single age population.

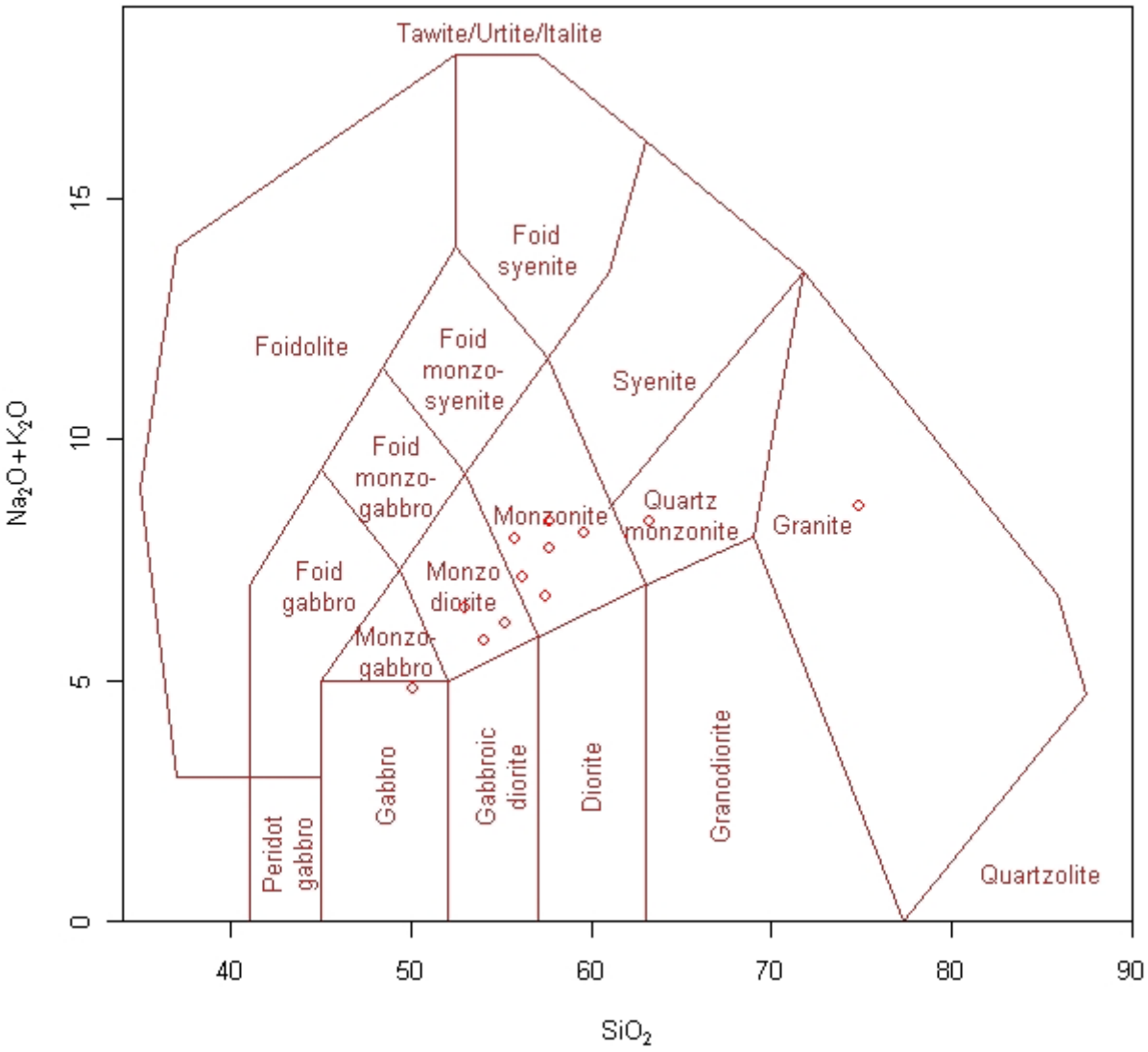

Figure 10. Chemical classification plot of diorite (Middlemost, 1985). Plotted in GCDkit v2.3 (Janousek, 2008).

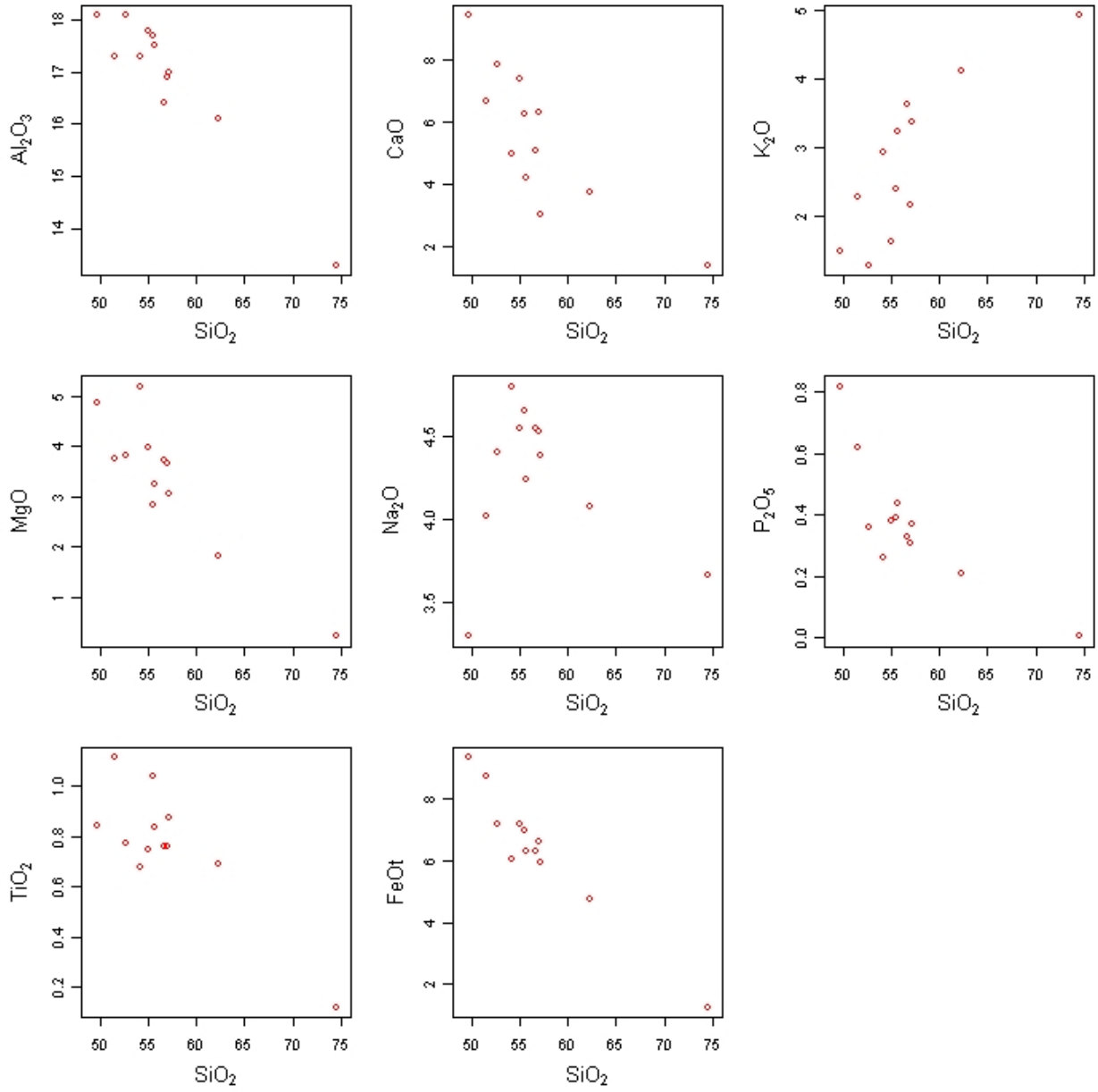

Figure 11. Variation of major elements with wt% SiO_2 of diorite. Plotted in GCDKit v2.3 (Janousek, 2008).

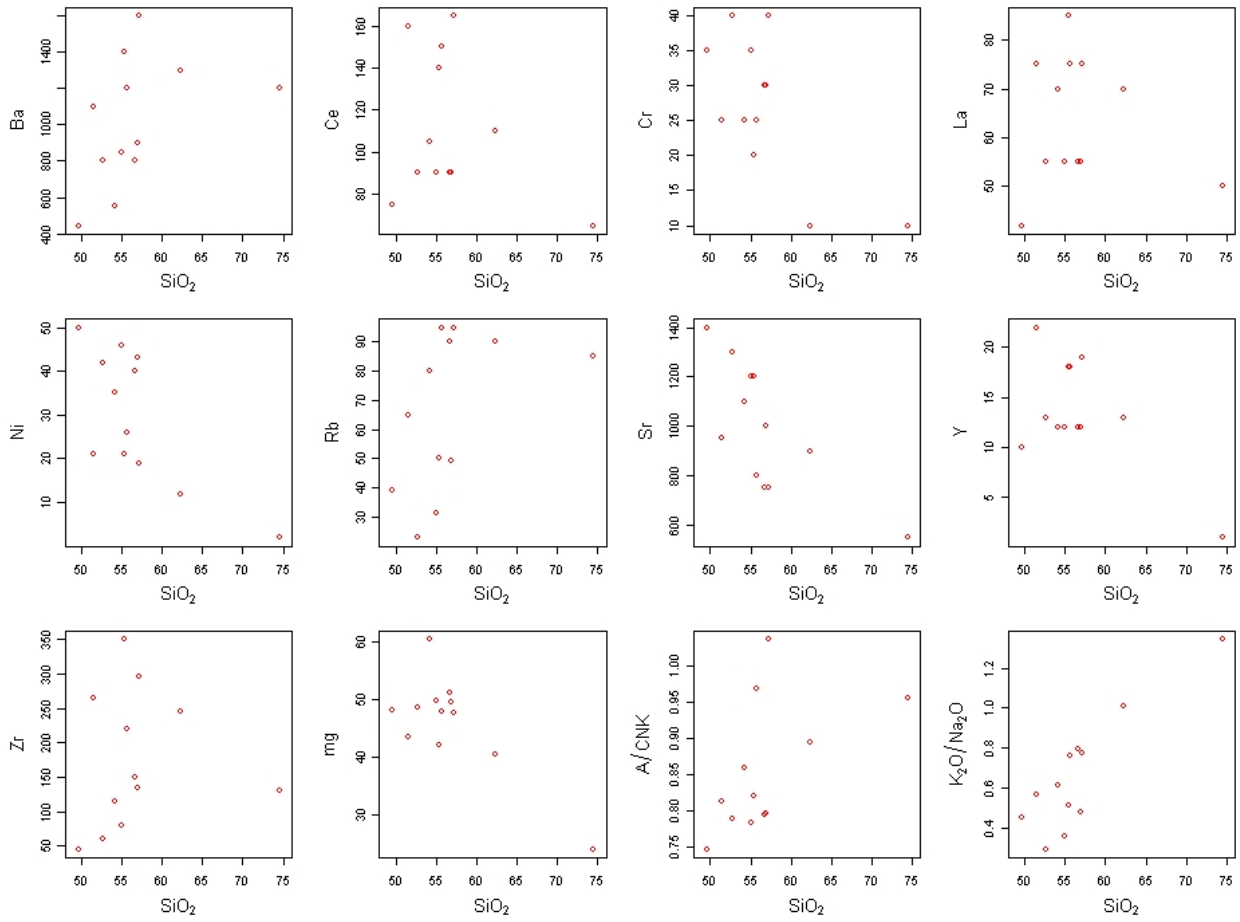

Figure 12. Variation of trace elements with SiO_2 wt% of diorite. Plotted in GCD Kit v2.3 (Janousek, 2008).

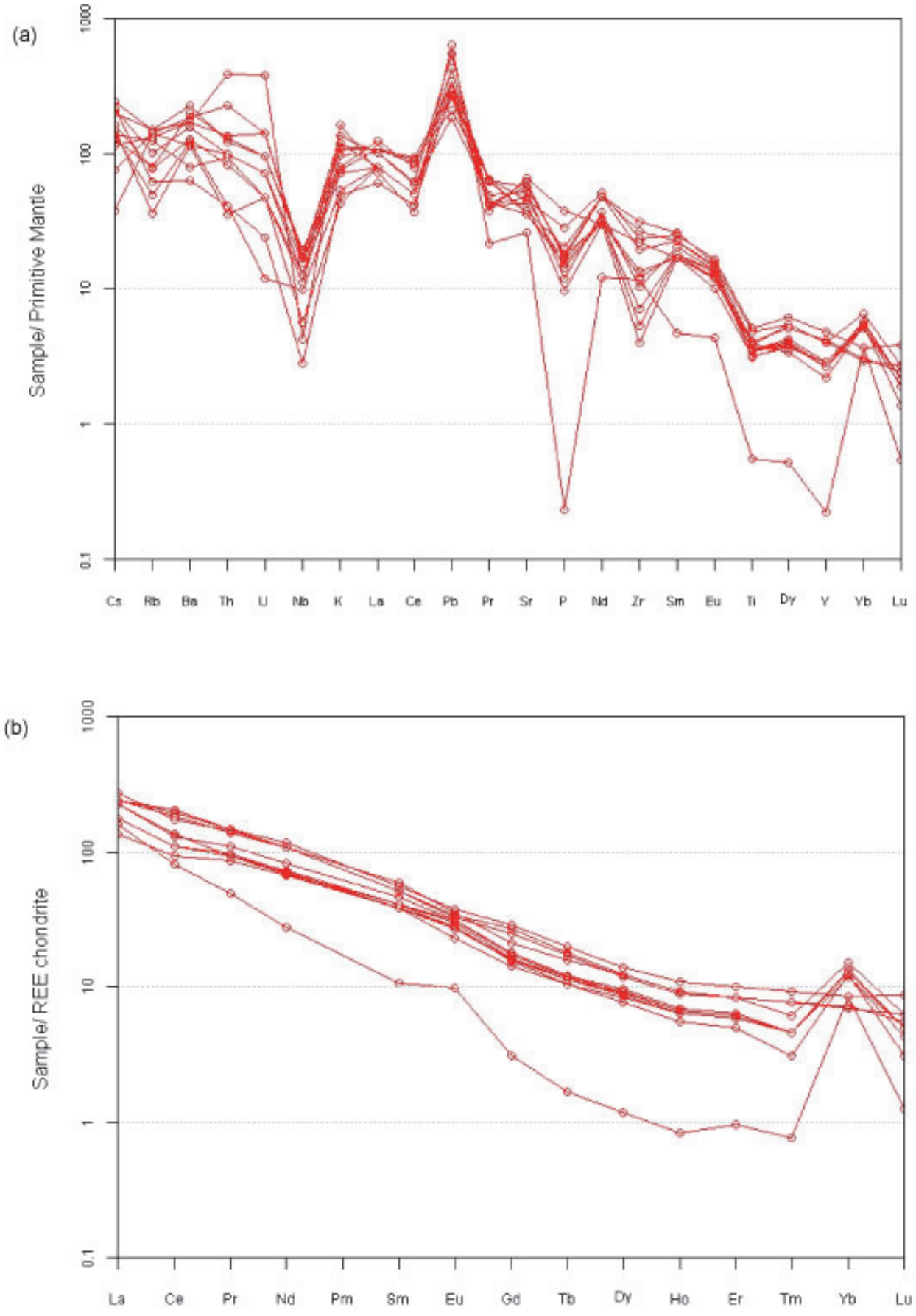

Figure 13. (a) Trace element spidergram normalised to primitive mantle (Sun and McDonough, 1989) and (b) REE spidergram normalised to chondrite of lithologies within monzonite pluton (Bonython, 1984).

4. METASEDIMENT

Within the diorite between 87.5 and 91.60 m is an interval of fine grained grey and pink laminated metasediment (Figs 2 and 14a), which may be either a large enclave or the host rock to the diorite. The contacts between the diorite and metasediment are sharp (Fig. 14b), and the upper 50 cm of the metasediment is affected by haematite alteration, which is also found in the diorite and may be associated with younger felsic intrusives (see below).

4.1 PETROLOGY

The metasediment is composed of lenticular layers between less than 1 mm to 7 mm wide defined by alternating quartz and plagioclase-rich layers (Figs 14c and 14d) (Purvis, 2010). Plagioclase is weakly haematite-stained, sericitised or albitised (Purvis, 2010). Minor foliated biotite is altered to chlorite and leucoxene, and apatite and zircon occur as rare accessory phases. Purvis (2010) suggests that the precursor of the metasediment is a layered quartzofeldspathic sandstone.

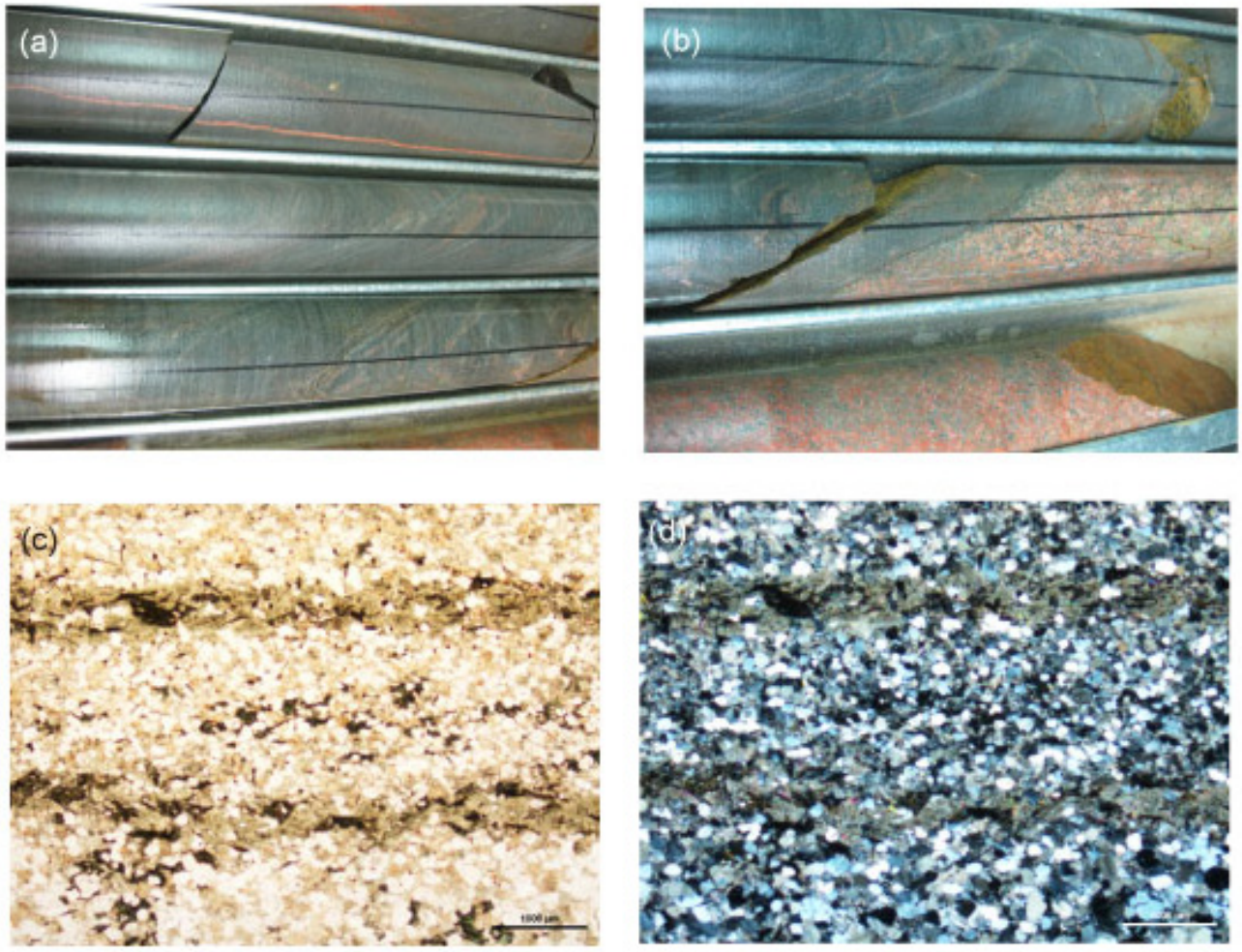

Figure 14. Photos of metasediment. (a) Interval of core (left to right is down-hole) showing layering within the metasediment. (b) Interval of core (left to right is down-hole) showing contact between metasediment and quartz-monzonite. Photomicrographs of metasediment in (c) plane polarised and (d) cross polarised light showing layering defined by alternating quartz-rich and plagioclase-rich bands.

4.2 GEOCHRONOLOGY

A sample of the metasediment was selected from the interval 90.0–91.4 m (R1708858).

Table 4. Sample Information 1708858

GA fieldsites number:	2109661		
Collector:	S McAvaney		
Analyst:	E Jagodzinski		
Stratigraphic Unit:	unassigned		
Location GDA94:	680450	6381003	Zone 53
Location Lat-Long:	32° 41” 38.23”	136° 55’ 29.69”	
250K map sheet	PORT AUGUSTA (SH5304)		
100K map sheet	UNO (6232)		
Location:	DDH LED1 (#229988), 90–91.4 m		
Mount:	GA 6144		
Date analysed:	14-18 Oct 2010		
Machine:	SHRIMP IIe (GA) LIMS session 100134		
OG1 standard age (α)*	3463.1 ± 2.0 Ma (0.99846)		
IMF correction applied?	Yes		
Interpreted age:	1855 ± 6 Ma		
Age type:	Maximum age of deposition		

*α is a correction for instrumental mass fractionation (IMF) defined by Stern et al. (2009).

4.2.1 ANALYTICAL DETAILS

Zircons from sample R1708858 were mounted in epoxy resin, together with three zircon standards. Absolute U and Th concentrations were estimated by comparison with the M257 zircon standard (840 ppm ^{238}U). Temora 2 (^{206}Pb*/^{238}U = 0.0668 [416.8 Ma], Black et al. 2003), was included to calibrate the ^{206}Pb/^{238}U ratio and monitor the accuracy of the ^{204}Pb common-Pb correction. Fifty five analyses of the Temora standard were obtained during the session, and have an external spot-to-spot (reproducibility) uncertainty of 0% (1σ) and a ^{238}U/^{206}Pb* calibration uncertainty of 0.14% (1σ). A more realistic Pb/U external error of 1.0% (1σ) has been assigned for data reduction.

The OG1 standard (3465.4 ± 0.6 Ma, Stern et al. 2009) was used to monitor ^{207}Pb*/^{206}Pb* reproducibility and accuracy, and yielded an age of 3463.1 ± 2.0 Ma (MSWD = 1.2, probability of fit = 0.19, n = 30 of 31).

Data were reduced and analysed using Squid 2 and Isoplot V3.71 (Ludwig 2001, Ludwig 2003), using decay constants recommended by Steiger and Jäger (1977). Common Pb corrections were applied to all analyses using contemporaneous common Pb isotopic compositions determined according to the Pb isotopic model of Stacey and Kramers (1975). Mean ages are reported with 95% confidence intervals.

4.2.2 ZIRCON CHARACTERISTICS

The small zircons are about 100 μm in size. A few grains preserve more euhedral morphologies but most consist of subrounded and rounded grains with pitted surfaces caused by sedimentary abrasion (Fig. 15). Only some grains have rims and they vary in character (e.g. grains 2, 3, 1, 24, 29 and 59), suggesting they do not represent a single metamorphic event post-dating sedimentation.

4.2.3 SAMPLE DATA

Sixty three analyses were made on 60 grains, producing ages ranging between ca 1830–2160 Ma, with one significantly older 2510 Ma grain (Fig. 16). Two analyses are notably imprecise (Fig. 17a). Analysis 28.1.1 is concordant, and the imprecision reflects the low uranium content of the grain (21 ppm). Discordant analysis 29.1.1 intersected a high Th, high common Pb inclusion at depth, and the apparent age produced by this analysis is not reliable and not considered further. One analysis (3.1.1) straddled a core and rim, producing an isotopic mixing age of no geological significance.

The dominant zircon population is the youngest, and constrains the maximum age of deposition at 1855 ± 6 Ma (n = 43, MSWD = 1.3, probability = 0.09). One analysis (25.1.1) has a younger apparent age of ca 1798 Ma, but this is not taken to be the maximum depositional age as a duplicate analysis of the grain falls within the main detrital population (Fig. 17b). The slightly young age probably reflects a minor component of non-recent Pb loss. Five analyses merge with the group but are statistically older, and might represent slightly older inherited zircon, about 1885 Ma in age. Three rims wide enough to analyse (grains 3, 16, 59, Fig. 15) do not record metamorphism post-dating sedimentation.

4.3 GEOCHEMISTRY

The metasediment is composed of 57.8 wt% SiO_2, 19.3 wt% Al_2O_3, 7.48 wt% Fe_2O_3, 5.28 wt% K_2O, 3.26 wt% MgO and 2.2 wt% Na_2O. Relative to primitive mantle, it is enriched in Pb and depleted in Ba, Nb, Sr, P, Eu and Ti (Fig. 18a). The metasediment is moderately enriched in LREE [$(La/Sm)_n$ = 4.64], has a fairly flat HREE pattern [$(Ga/Yb)_n$ = 2.08] and a negative Eu anomaly (Eu/Eu* = 0.177) (Fig. 18b). It has a similar trace and REE signature to Hutchison Group lithologies, in particular to samples of the Yadnarie and Mangalo Schists in the Lincoln-Cleve Uplands (Szpunar et al., 2011) and to the Post-Archaean Australian Shale (PAAS) (Taylor and McLennan, 1985) (Fig. 18).

4.4 DISCUSSION

The detrital zircon population of the metasediment shares similarities with a number of members of the Hutchison Group; the Yadnarie Schist, the Cook Gap Schist at Tumby Bay and the Mangalo Schist from Cleve, which all have a dominant ~1850 Ma peak, although a number of these samples also have ~1790 Ma zircon (Szpunar et al., 2011). Szpunar et al. (2011) included these members of the Hutchsion Group within a recently reclassified Cleve Group containing the Yadnarie Schist, Mount Shannon Iron Formation, Mangalo Schist and Cook Gap Schist outside the Middleback Ranges, distinguishing it from older Hutchison Group sediments in the Middleback Ranges and Darke Peak area on the grounds of a U-Pb and Lu-Hf zircon and Sm-Nd isotopic study.

Table 5. SHRIMP analytical results for zircon from R1708858: metasediment

Spot	% $206Pb_c$	U ppm	Th ppm	232Th /238U	206Pb* /238U	±%	207Pb* /235U	IMF-corr 207Pb* /235U	±%	207Pb* /206Pb*	IMF-corr 207Pb* /206Pb*	±%	207Pb /206Pb Age	IMF-corr 207Pb /206Pb Age	± Ma	% Disc
858.25.1.1	--	193	71	0.38	0.327	1.36	4.946	4.954	1.49	0.10976	0.10993	0.62	1795	1798	11	-2
858.51.1.1	0.60	302	106	0.36	0.318	1.27	4.897	4.904	1.63	0.11172	0.11190	1.03	1828	1830	19	3
858.25.2.1	--	274	81	0.30	0.330	1.28	5.084	5.092	1.39	0.11180	0.11197	0.53	1829	1832	10	-1
858.44.1.1	0.24	259	75	0.30	0.314	1.32	4.843	4.851	1.49	0.11183	0.11200	0.70	1829	1832	13	4
858.57.1.1	0.05	190	100	0.54	0.336	1.37	5.190	5.198	1.50	0.11198	0.11215	0.63	1832	1835	11	-2
858.11.1.1	--	139	98	0.73	0.331	1.46	5.127	5.135	1.62	0.11224	0.11241	0.71	1836	1839	13	-1
858.21.1.1	0.11	109	50	0.48	0.327	1.56	5.064	5.072	1.78	0.11226	0.11244	0.85	1836	1839	15	1
858.9.1.1	0.01	261	137	0.54	0.328	1.27	5.087	5.095	1.37	0.11232	0.11249	0.51	1837	1840	9	0
858.50.1.1	0.02	150	56	0.38	0.337	1.46	5.220	5.228	1.61	0.11238	0.11255	0.70	1838	1841	13	-2
858.41.1.1	0.10	164	117	0.74	0.324	1.41	5.024	5.031	1.58	0.11248	0.11265	0.70	1840	1843	13	2
858.26.1.1	0.12	364	152	0.43	0.317	1.20	4.921	4.929	1.30	0.11248	0.11265	0.50	1840	1843	9	4
858.49.1.1	0.01	256	203	0.82	0.332	1.28	5.156	5.164	1.38	0.11253	0.11270	0.51	1841	1843	9	-1
858.52.1.1	0.05	219	107	0.50	0.336	1.32	5.217	5.225	1.68	0.11254	0.11271	1.03	1841	1844	19	-2
858.23.1.1	0.09	182	70	0.40	0.323	1.37	5.009	5.017	1.52	0.11262	0.11279	0.66	1842	1845	12	2
858.18.1.1	1.37	281	158	0.58	0.325	1.27	5.046	5.054	2.04	0.11266	0.11283	1.59	1843	1846	29	2
858.36.1.1	0.15	364	145	0.41	0.329	1.23	5.117	5.125	1.34	0.11273	0.11290	0.53	1844	1847	10	1
858.58.1.1	0.08	148	81	0.57	0.332	1.46	5.172	5.180	1.64	0.11285	0.11303	0.73	1846	1849	13	-0
858.22.1.1	--	120	61	0.53	0.333	1.51	5.181	5.189	1.68	0.11295	0.11312	0.75	1847	1850	13	-0
858.7.1.1	0.03	153	86	0.58	0.326	1.42	5.086	5.094	1.57	0.11298	0.11316	0.67	1848	1851	12	2
858.35.1.1	0.04	183	121	0.68	0.330	1.37	5.146	5.154	1.51	0.11305	0.11323	0.64	1849	1852	12	1
858.13.1.1	0.12	104	68	0.67	0.336	1.56	5.240	5.248	1.78	0.11322	0.11339	0.86	1852	1854	15	-1
858.37.1.1	0.10	141	64	0.46	0.333	1.47	5.203	5.211	1.65	0.11323	0.11340	0.75	1852	1855	14	-0
858.47.1.1	0.07	152	42	0.29	0.329	1.45	5.135	5.143	1.62	0.11324	0.11342	0.73	1852	1855	13	1
858.54.1.1	0.01	404	216	0.55	0.335	1.20	5.241	5.249	1.40	0.11337	0.11355	0.72	1854	1857	13	-1
858.19.1.1	--	265	137	0.53	0.331	1.26	5.169	5.177	1.36	0.11338	0.11356	0.50	1854	1857	9	1
858.3.3.1	0.03	307	47	0.16	0.337	1.25	5.274	5.282	1.35	0.11342	0.11360	0.51	1855	1858	9	-1

Spot	% $206Pb_c$	U ppm	Th ppm	232Th /238U	206Pb* /238U	±%	207Pb* /235U	IMF-corr 207Pb* /235U	±%	207Pb* /206Pb*	IMF-corr 207Pb* /206Pb*	±%	207Pb /206Pb Age	IMF-corr 207Pb /206Pb Age	± Ma	% Disc
858.53.1.1	0.01	177	91	0.53	0.334	1.39	5.220	5.228	1.52	0.11348	0.11366	0.62	1856	1859	11	-0
858.10.1.1	0.06	151	86	0.59	0.327	1.42	5.119	5.126	1.58	0.11355	0.11372	0.70	1857	1860	13	2
858.8.1.1	0.08	233	127	0.56	0.303	1.74	4.752	4.759	1.99	0.11374	0.11391	0.97	1860	1863	18	9
858.60.1.1	--	228	182	0.82	0.331	1.32	5.189	5.197	1.45	0.11376	0.11393	0.61	1860	1863	11	1
858.48.1.1	--	220	93	0.43	0.328	1.31	5.150	5.158	1.43	0.11385	0.11402	0.56	1862	1865	10	2
858.31.1.1	--	196	141	0.74	0.333	1.34	5.235	5.243	1.46	0.11387	0.11405	0.57	1862	1865	10	0
858.1.1.1	0.01	202	113	0.58	0.329	1.29	5.162	5.170	1.39	0.11390	0.11407	0.52	1862	1865	9	2
858.6.1.1	0.68	338	45	0.14	0.329	1.22	5.165	5.173	1.39	0.11398	0.11416	0.67	1864	1867	12	2
858.45.1.1	0.01	142	87	0.63	0.324	1.47	5.093	5.101	1.64	0.11412	0.11429	0.72	1866	1869	13	4
858.40.1.1	0.05	144	121	0.87	0.335	1.47	5.270	5.278	1.63	0.11417	0.11434	0.71	1867	1870	13	0
858.43.1.1	0.03	170	71	0.43	0.333	1.40	5.249	5.258	1.53	0.11420	0.11438	0.63	1867	1870	11	1
858.12.1.1	--	156	65	0.43	0.339	1.41	5.347	5.355	1.55	0.11434	0.11452	0.65	1870	1872	12	-1
858.14.1.1	--	253	131	0.53	0.323	1.28	5.088	5.096	1.39	0.11434	0.11452	0.53	1870	1872	10	4
858.46.1.1	0.05	228	127	0.58	0.334	1.31	5.273	5.281	1.44	0.11443	0.11461	0.58	1871	1874	10	1
858.56.1.1	0.04	190	126	0.69	0.340	1.36	5.366	5.374	1.49	0.11445	0.11463	0.61	1871	1874	11	-1
858.27.1.1	0.12	273	175	0.66	0.321	1.26	5.073	5.081	1.54	0.11452	0.11470	0.89	1872	1875	16	5
858.39.1.1	0.21	171	112	0.67	0.312	1.39	4.940	4.947	1.58	0.11476	0.11494	0.76	1876	1879	14	8
858.17.1.1	0.18	85	36	0.44	0.332	1.69	5.254	5.262	1.97	0.11487	0.11505	1.01	1878	1881	18	2
858.5.1.1	--	164	91	0.57	0.330	1.40	5.246	5.255	1.54	0.11528	0.11546	0.64	1884	1887	12	3
858.59.1.1	0.00	263	71	0.28	0.335	1.28	5.327	5.335	1.37	0.11539	0.11557	0.50	1886	1889	9	1
858.16.2.1	0.15	685	55	0.08	0.306	1.10	4.875	4.883	1.15	0.11553	0.11571	0.33	1888	1891	6	10
858.30.1.1	--	93	51	0.56	0.336	1.63	5.366	5.374	1.84	0.11574	0.11592	0.84	1891	1894	15	1
858.55.1.1	--	168	72	0.44	0.338	1.41	5.423	5.431	1.55	0.11642	0.11660	0.65	1902	1905	12	2
858.3.1.1	0.11	260	104	0.41	0.310	1.27	5.009	5.017	1.38	0.11727	0.11745	0.53	1915	1918	10	10
858.38.1.1	0.07	187	26	0.14	0.342	1.36	5.544	5.552	1.49	0.11751	0.11769	0.61	1919	1921	11	1
858.15.1.1	0.02	168	92	0.56	0.340	1.39	5.533	5.541	1.52	0.11818	0.11836	0.62	1929	1932	11	3
858.2.1.1	0.03	255	99	0.40	0.343	1.28	5.621	5.630	1.37	0.11894	0.11912	0.50	1940	1943	9	2
858.33.1.1	--	189	130	0.71	0.351	1.36	5.792	5.801	1.48	0.11960	0.11979	0.58	1950	1953	10	1

Spot	% $206Pb_c$	U ppm	Th ppm	232Th /238U	206Pb* /238U	±%	207Pb* /235U	IMF-corr 207Pb* /235U	±%	207Pb* /206Pb*	IMF-corr 207Pb* /206Pb*	±%	207Pb /206Pb Age	IMF-corr 207Pb /206Pb Age	± Ma	% Disc
858.42.1.1	0.02	284	111	0.40	0.349	1.26	5.767	5.775	1.34	0.11974	0.11992	0.47	1952	1955	8	1
858.3.2.1	0.02	189	181	0.99	0.338	1.30	5.613	5.622	1.42	0.12032	0.12051	0.55	1961	1964	10	5
858.24.1.1	--	253	61	0.25	0.360	1.28	6.080	6.089	1.37	0.12257	0.12276	0.48	1994	1997	8	1
858.32.1.1	0.03	149	180	1.25	0.363	1.44	6.173	6.183	1.57	0.12345	0.12364	0.64	2007	2009	11	1
858.34.1.1	0.08	200	121	0.63	0.365	1.35	6.279	6.289	1.46	0.12481	0.12500	0.57	2026	2029	10	1
858.28.1.1	0.00	21	14	0.70	0.379	2.90	6.673	6.683	4.00	0.12770	0.12790	2.76	2067	2069	49	-0
858.16.1.1	0.05	134	53	0.41	0.390	1.49	6.904	6.915	2.03	0.12855	0.12875	1.39	2078	2081	24	-2
858.29.1.1	0.92	484	275	0.59	0.298	6.10	5.338	5.347	7.05	0.12987	0.13007	3.54	2096	2099	62	22
858.20.1.1	--	91	51	0.58	0.398	1.63	7.386	7.397	1.79	0.13452	0.13472	0.73	2158	2160	13	-0
858.4.1.1	0.04	179	128	0.74	0.471	1.38	10.719	10.736	1.61	0.16504	0.16530	0.84	2508	2511	14	1

Data are 1σ precision. Pbc and Pb* indicate the common and radiogenic portions, respectively.
All Pb data are common Pb corrected based on measured ^{204}Pb (after Stacey and Kramer 1975), then corrected for instrumental mass fractionation (IMF)
Both uncorrected data, and IMF-corrected data (grey columns) are presented.

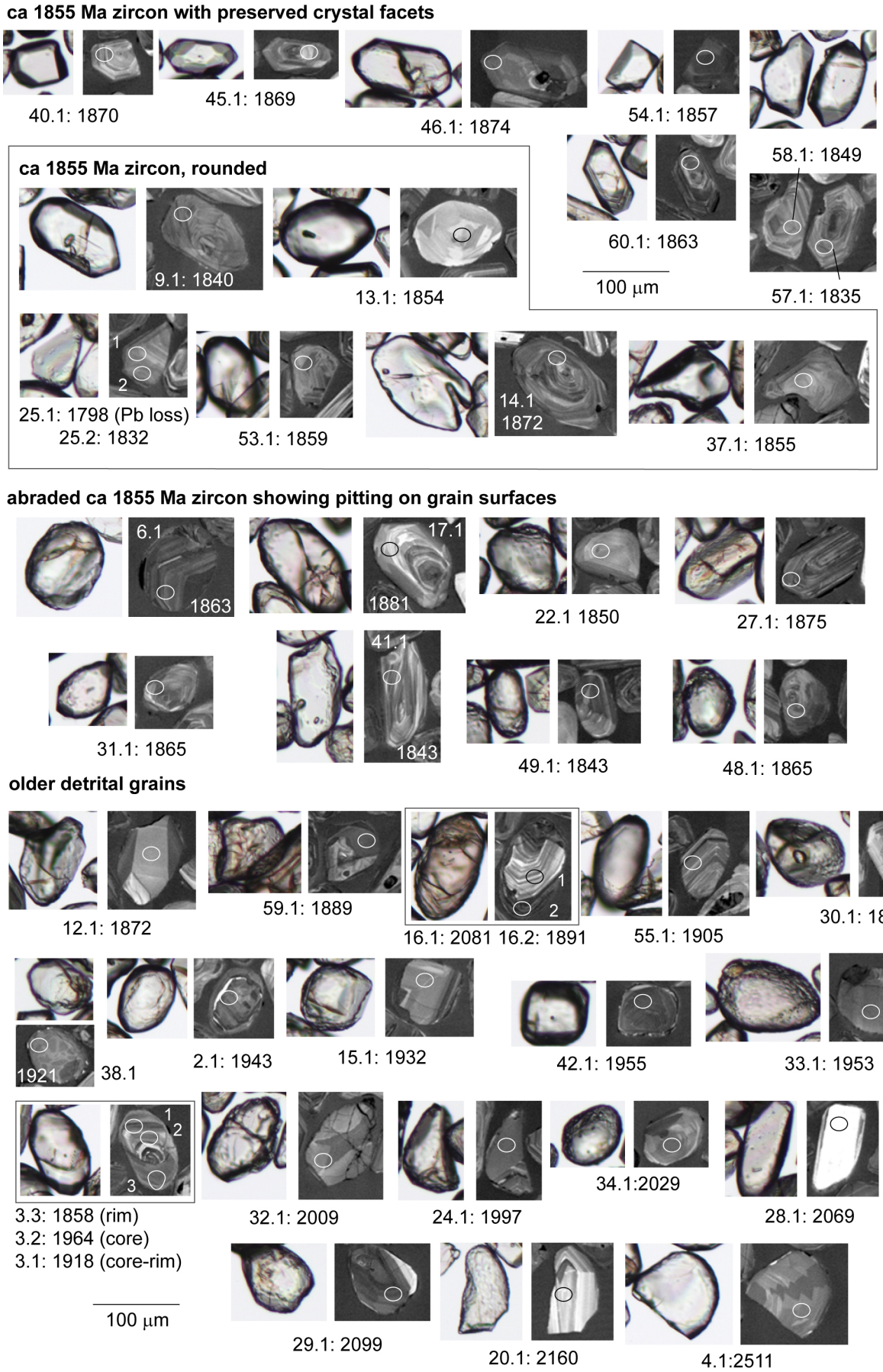

Figure 15. Representative zircon from sample R1708858 showing the location of analyses, annotated with their IMF-corrected $^{207}Pb/^{206}Pb$ ages. Transmitted light (left) and CL images (right). All analysis numbers are prefixed by 858.

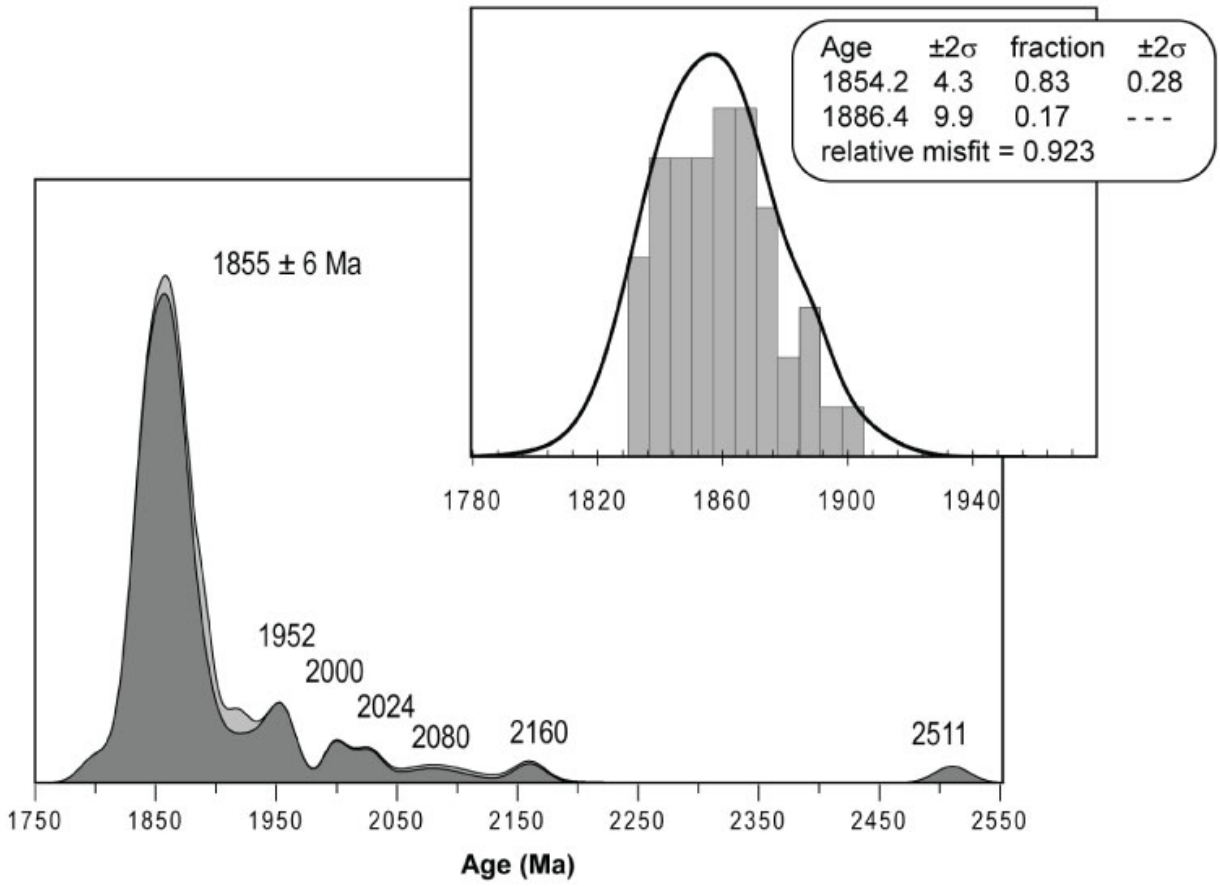

Figure 16. Probability density diagram for all analyses from the 'felsic gneiss' (R1708858), generated using AgeDisplay (Sircombe 2004). The light grey curve represents all data. The dark grey curve represent are filtered for > 5% discordance. Inset shows the mixture modelling algorithm of Sambridge and Compston (1994) applied to the main peak, illustrating 5 slightly older analyses producing a tail on the high side of the 1855 Ma population. These analyses might indicate minor ca 1885 Ma inheritance.

The fabric within the metasediment must have formed between c. 1850 Ma and the intrusion of the diorite at 1740 Ma. The major Palaeoproterozoic deformational event in the Gawler Craton is the Kimban Orogeny, a transpressional event associated with amphibolite to granulite-facies metamorphism, tight to isoclinal folding and mylonitisation, and is accompanied by syn- to post-deformational felsic and mafic magmatism (Parker, 1980; Parker, 1993; Vassallo and Wilson, 2002). Recognised metamorphic ages for the Kimban Orogeny typically lie within the range 1690 and 1730 Ma, and have been published for the southern Gawler Craon (Dutch et al., 2008; Reid et al., 2007) the Nawa Domain in the northern Gawler Craton (Howard et al., 2011; Payne et al., 2008) and the eastern Eyre Peninsula (Fraser and Neumann, 2010). However, a number of older metamorphic ages have been obtained for rocks on the eastern Eyre Peninsula whose fabric is interpreted to have formed during the Kimban Orogeny. A c.1790 Ma foliated granite at Murninnie Mine has a metamorphic age of 1764±5 Ma, and the Minbrie Gneiss at Mt Ghearthy has a metamorphic age of 1762±43 Ma (Fraser and Neumann, 2010). Excepting two analyses of the Warrow Quartzite at Sleaford Bay which were dated to ~1730 Ma, no metamorphic zircons have been observed and dated in the many other geochronology samples of the 1790 Ma Hutchison Group from the Cleve Hills and the Broadview Schist (Fraser and Neumann, 2010; Szpunar et al., 2011). It may be that some of the deformation observed in the eastern Eyre Peninsula occurred earlier than the1730-1690 Ma Kimban deformation on the southern Eyre Peninsula and the Nawa Domain.

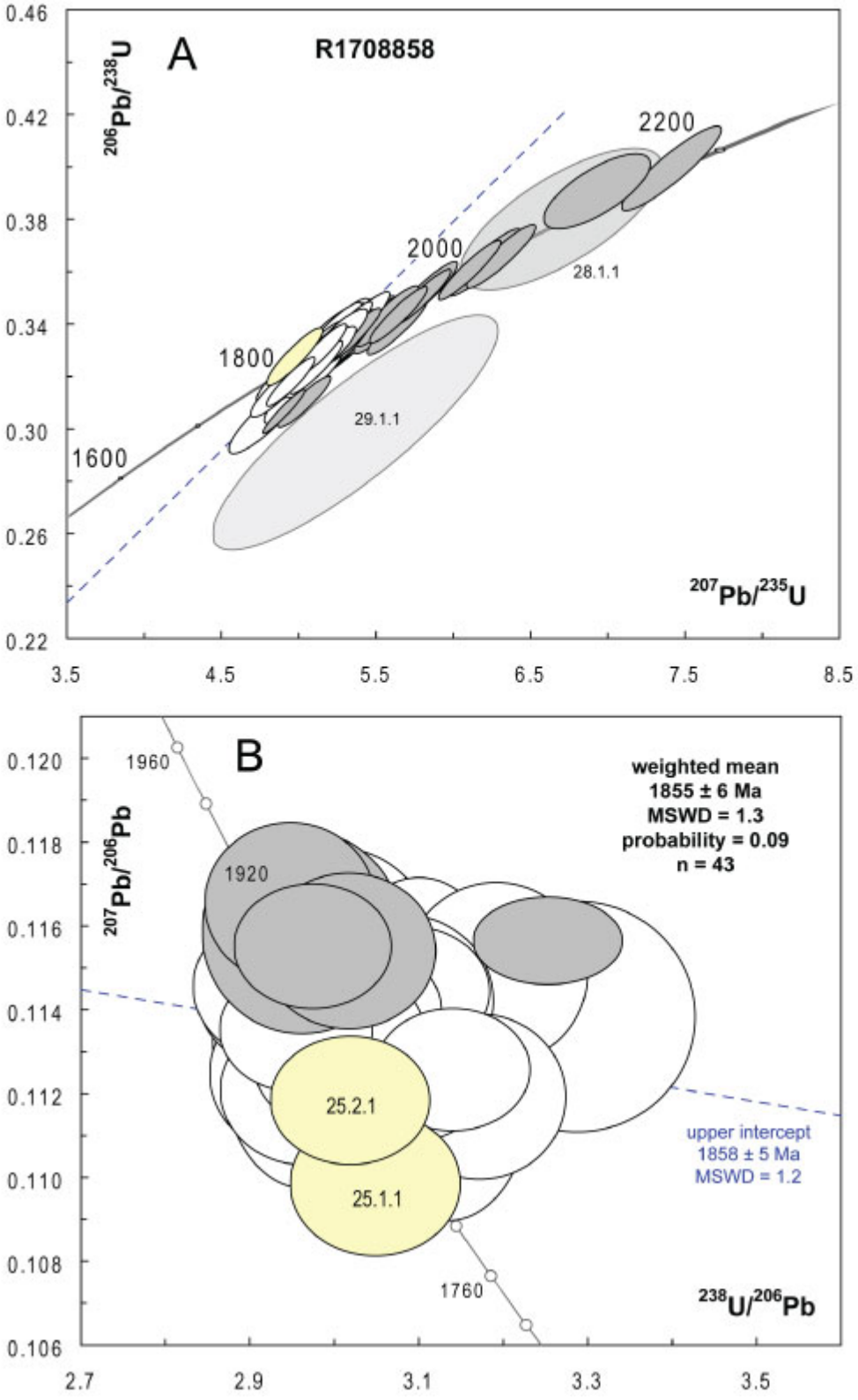

Figure 17. (a) Concordia diagram for sample R1708858. One analysis (4.1.1: 2508 Ma) lies beyond the range of this figure. White error ellipses represent the dominant population used in the age calculation. Grey error ellipses represent older analyses. One slightly young analysis (25.1.1) is highlighted in yellow. (b) The upper Concordia intercept age is generated on a Tera-Wasserburg Concordia diagram and calculated using the IMF-corrected 207Pb/206Pb ratios. The age agrees well with the weighted mean age of the dominant population. The lower intercept intersects the origin.

5. DOLERITE AND AMPHIBOLE SCHIST

Within the diorite there are two mafic bodies which appear to be intruded by it; a hornblende schist at 83.3–85.0 m and a dolerite at 595.0–603.0 m (see Fig. 2 and Table 1) and are presumably either large xenoliths or part of the country rock sequence along with the metasediment described above. The contacts of the amphibole schist with the granodiorite phase of the diorite pluton are at broken core (Fig. 19a), however there is a vein of granodiorite which intrudes the dolerite and is presumed to be part of the larger diorite pluton (Fig. 19b). Enclaves of the dolerite occur within the diorite at 595 m directly above the contact between the dolerite and diorite (Figs 19e and 19f), and diorite veins intrude the dolerite.

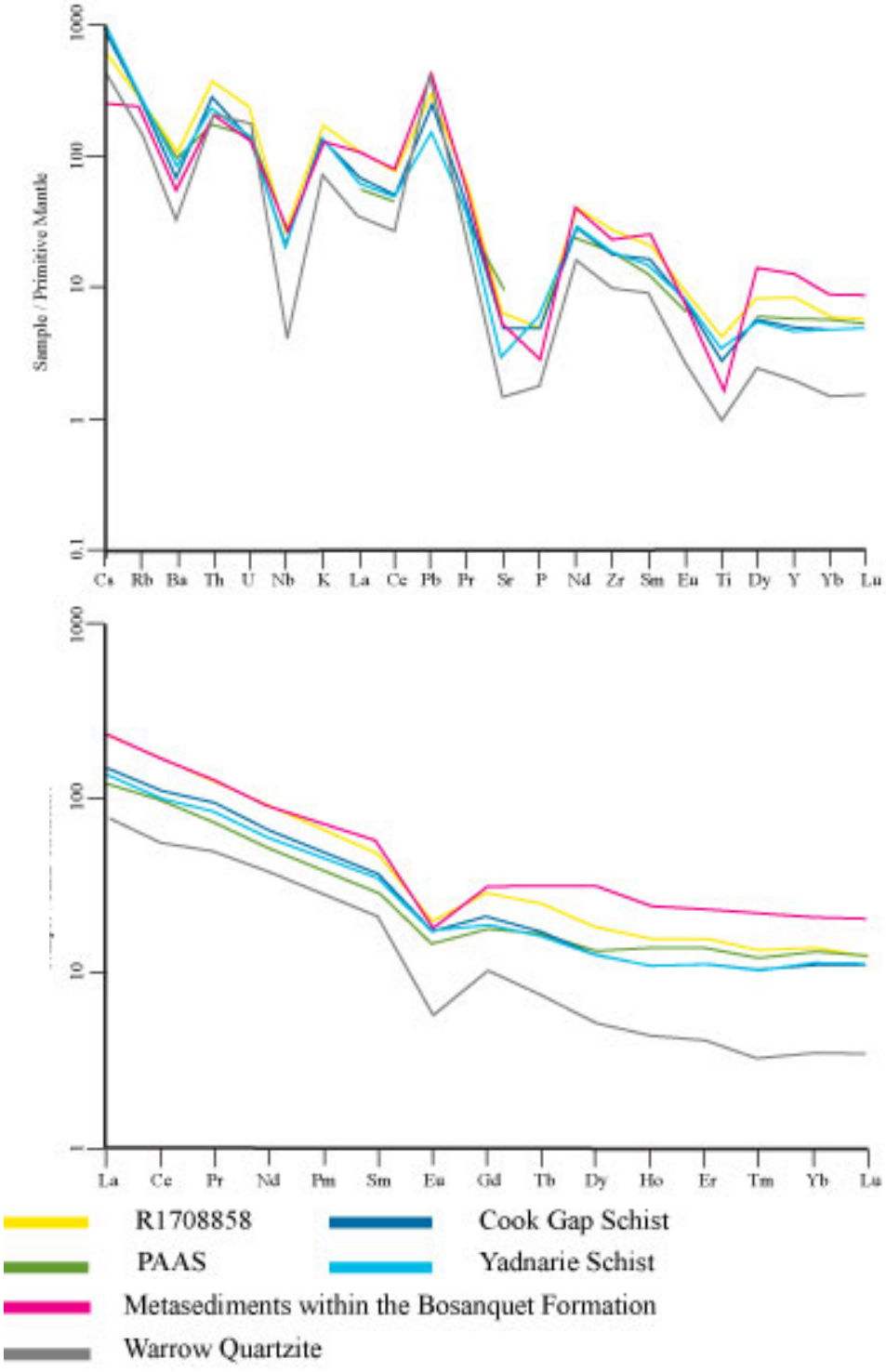

Figure 18. (a) Trace element spidergram of sample 1708858 normalised to primitive mantle (Sun and McDonough, 1989) and (b) REE spidergram normalised to chondrite (Bonython, 1984), compared to selected members of the Hutchison Group

(Szpunar et al., 2011) and PAAS (Post Archaean Australian Shales; (Taylor and McLennan, 1985) (Janousek, 2008).

5.1 PETROLOGY

The amphibole schist is irregularly layered, and is composed predominantly of inequigranular pale green amphibole, (90–95%) with minor chlorite and leucoxene after primary biotite, feldspar and oxides (Figs 19c and 19d). The amphibole is inequigranular and commonly microcrystalline but is up to 1 mm in some layers, and is partly foliated (Purvis, 2010). Disseminated spots of chlorite and titanite up to 0.5 mm in diameter are interpreted to represent former biotite. Some layers contain minor to common interstitial feldspar (Purvis, 2010). The precursor of this rock is may have been a pyroxenite.

The dolerite is microcrystalline, and is composed of unaligned plagioclase laths typically 100 μm in diameter and 250 μm in length, which show simple twinning. The plagioclase is surrounded by pyroxene which occurs both as euhedral phenocrysts up to 800 μm in diameter to smaller interstitial subhedral and anhedral grains, interstitial biotite and minor oxides.

5.2 GEOCHEMISTRY

Both the hornblende schist and dolerite plot as subalkaline/tholeiitic basalts on a TAS diagram (Fig. 20). They each have distinct trace and REE signatures. Relative to primitive mantle the amphibolite schist is depleted in Rb, Ba, Th, U, Nb and Zr and enriched in Pb (Fig. 21a). The dolerite is depleted in Nb, Zr and Ti and enriched in Pb. The amphibole schist has a steeper REE signature, compared to the much flatter signature of the dolerite, which has a small negative Yb anomaly (Fig. 21b).

5.3 DISCUSSION

Both the dolerite and amphibole schist must be older than crystallisation of the diorite at ~1740 Ma. The presence of a fabric within the amphibole schist suggests that it is older than the undeformed dolerite, although it is uncertain whether the foliation in the amphibole schist formed at the same time as that in the ~1850 Ma metasediment xenolith. The dolerite may be a Kimban mafic slightly older than the diorite which intrudes it.

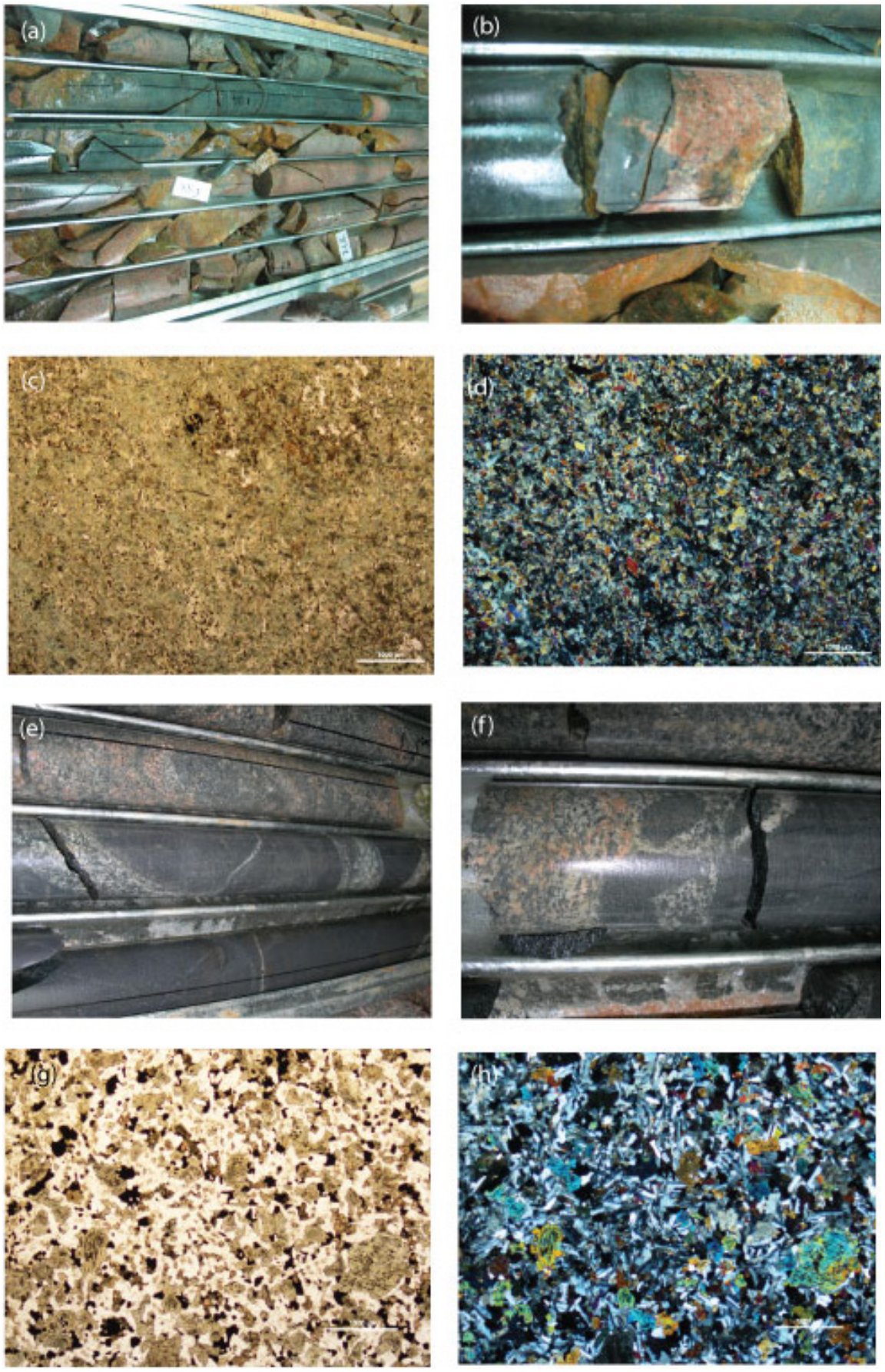

Figure 19. Photos of xenoliths/country rock in diorite; amphibole schist at 83.30–85.0 m (a-d) and dolerite at 595.0–603.0 m (e–h). (a) Core interval (left to right is down hole) containing hornblende schist in first three rows intruded by diorite below. (b) Vein of granodioritic phase of diorite within dolerite. Amphibole schist under (c)

plane polarised and (d) cross polarised light. (e and f) Core intervals (left to right is down hole) showing enclaves of dolerite within diorite in bottom two rows. Dolerite under plane (f) and cross polarised light.

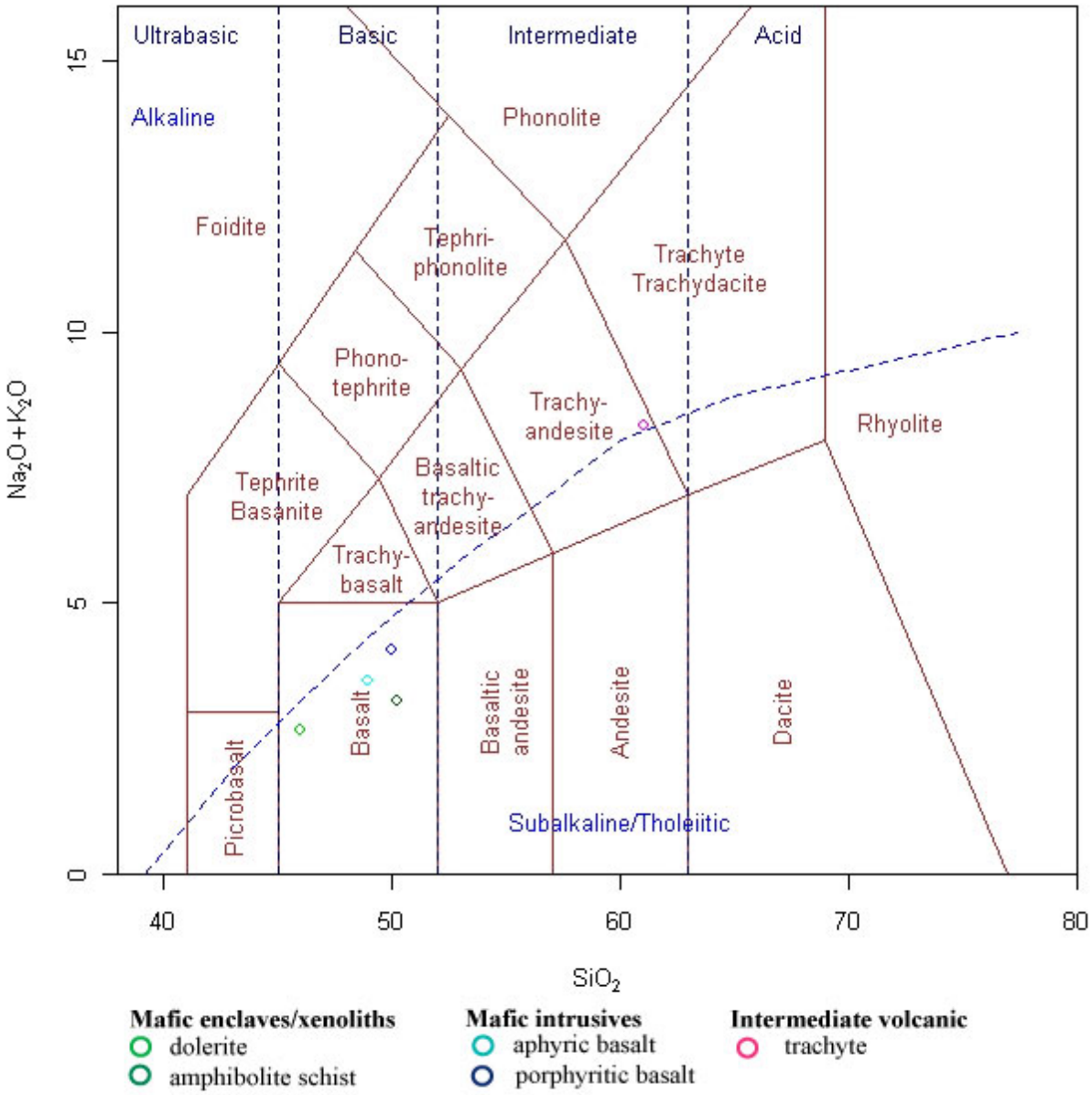

Figure 20. TAS (Total Alkali vs Silica) classification plot (Le Bas et al., 1986) for mafic xenoliths/country rock and mafic and intermediate intrusives in diorite. Plotted in GCDkit v2.3 (Janousek, 2008). Refer to table 1 and graphic log (Fig. 2) for units.

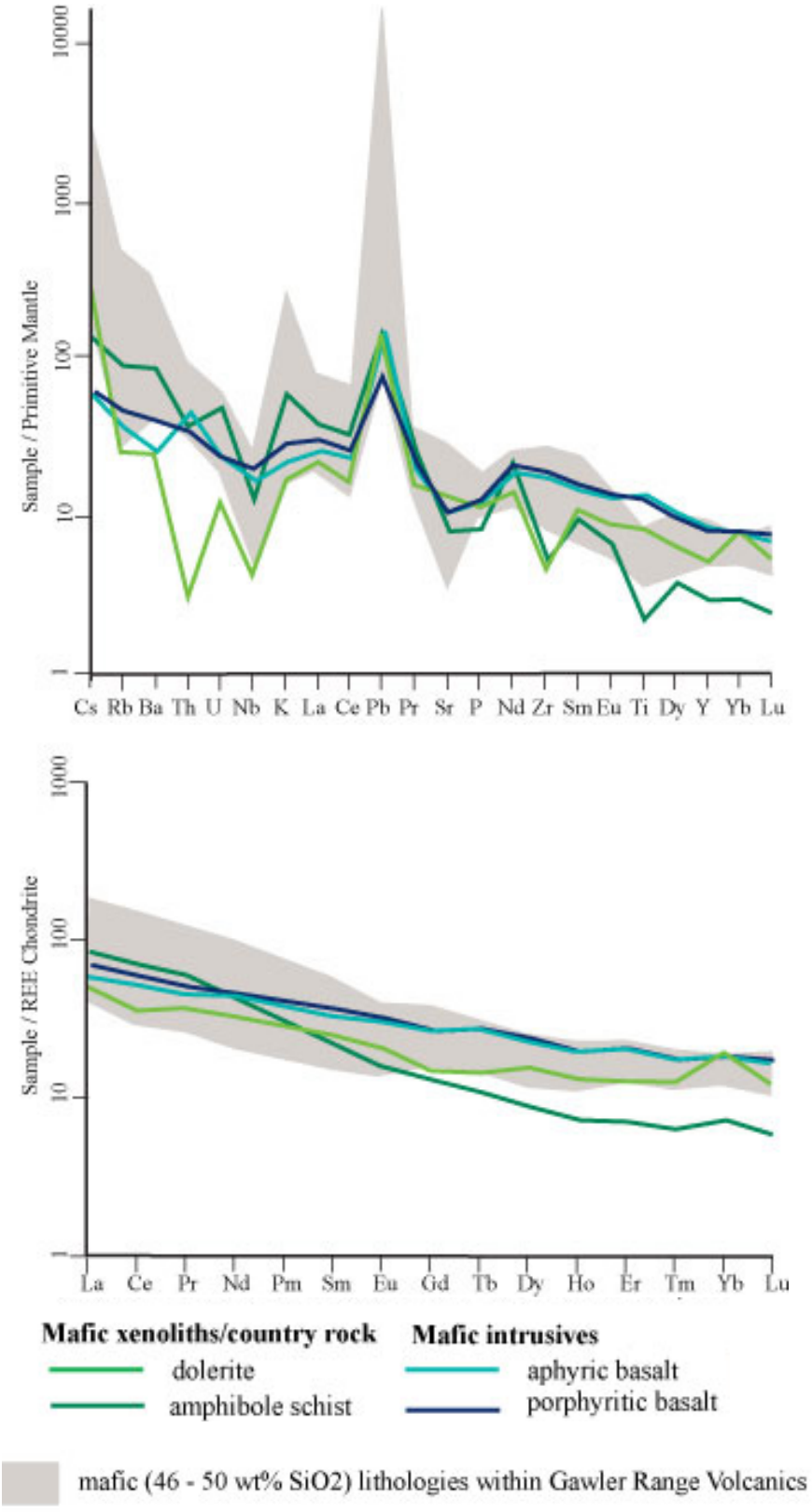

Figure 21. (a) Trace element spidergram normalised to primitive mantle and (b) REE spidergram normalised to chondrite of both mafic xenoliths and mafic volcanics in diorite compared to mafic lithologies (46–50 wt% SiO_2) from the Gawler Range Volcanics [N=16, data from (Fricke, 2005; Giles, 1980)].

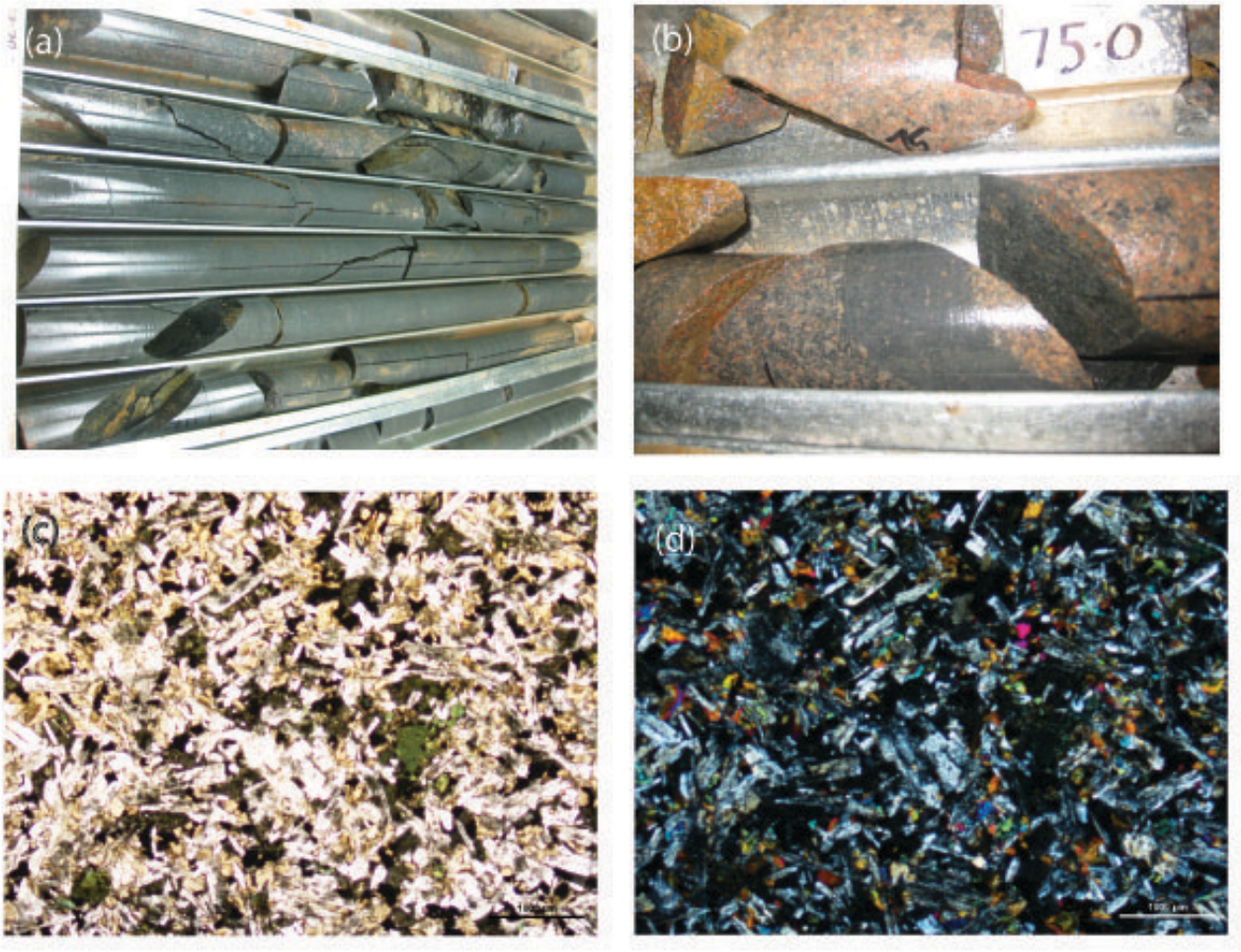

Figure 22. Photos of basalt intrusives. (a) Interval of core (left to right is down hole) showing diorite and sharp contact with porphyritic basalt in the second row at broken core (b) Vein of basalt intruding granodiorite at 74.05 – 74.15 m. Photomicrographs of porphyritic basalt at 108.90–131.70 m in (c) plane and (d) cross polarised light.

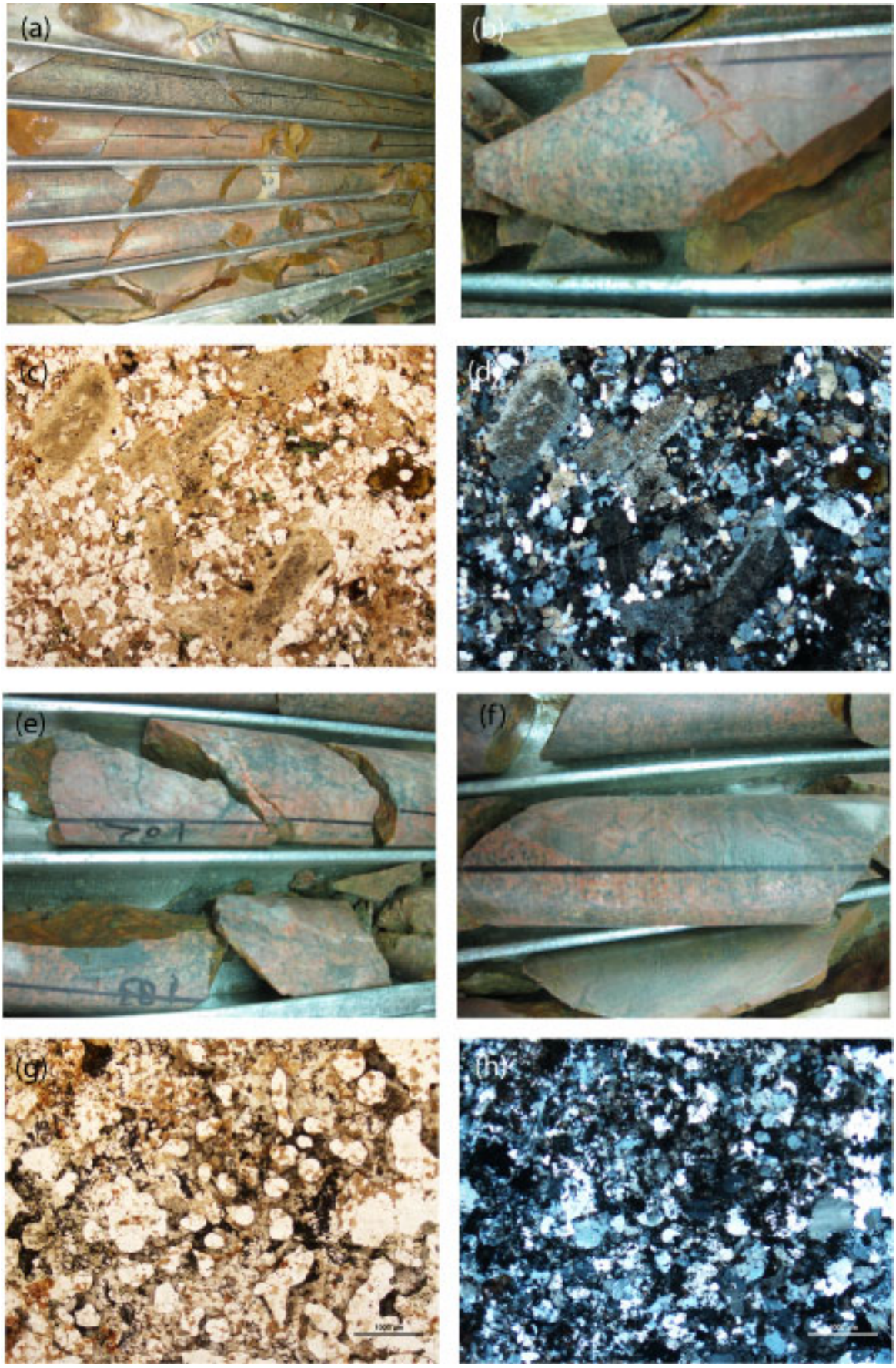

Figure 23. Photos of dacite at 80.0–81.30 m and associated breccia at 81.70–83.30 m. (a) Interval of core (left to right is down hole) showing granododiorite (top left) and dacite. (b) Contact between dacite (left) and granodiorite (right), showing recrystallisation of biotite in granodiorite at contact. Photomicrographs of dacite under (c) plane and (d) cross polarised light. (e) Volcanic breccia. (f) Contact

between granodiorite (left) and volcanic breccia (right). Photomicrographs of volcanic breccia under (g) plane and (h) cross polarised light.

6. VOLCANIC INTRUSIVES

The diorite is intruded by a number of mafic and intermediate volcanics (see Fig. 2 and Table 1). The mafic volcanics consist of an aphyric basalt extending from the beginning of the cored hole (55.70 m) to 72.50 m, a porphyritic basalt at 108.90–131.70 m and 137.40–140.30 m and an aphyric basalt at 220.0–229.25 m (Fig. 22). The intermediate volcanics consist of a porphyritic dacite at 80.0–81.3 m (Fig. 23), a porphyritic trachyte (Fig. 24) at 250.8–280.0 m, and an andesite at 400.0–405.9 m and 483.9–485.8 m (Fig. 25) and two volcanic breccias at 81.70–83.30m (Fig. 22) and 420.0–422.40 m (Fig. 25).

There are clear intrusive relationships observed in the drill core for most of the volcanics. The contacts between the shallowest aphyric basalt and diorite are at broken core, but the thin vein of basalt at 74.05–74.15 m appears to be part of the same body and chloritic alteration of the larger basalt occurs at its contact with the diorite which is presumed to represent a cooling margin. The porphyritic basalt has sharp contacts with the diorite, which are typically at broken core, but alteration is observed in the upper 10 cm of the basalt and is interpreted to be a cooling margin. The contacts between the larger body of aphyric basalt are broken and invaded by a calcite vein, but the vein of apyric basalt at 218.65–218.85 m is intrusive and appears to be part of the same body.

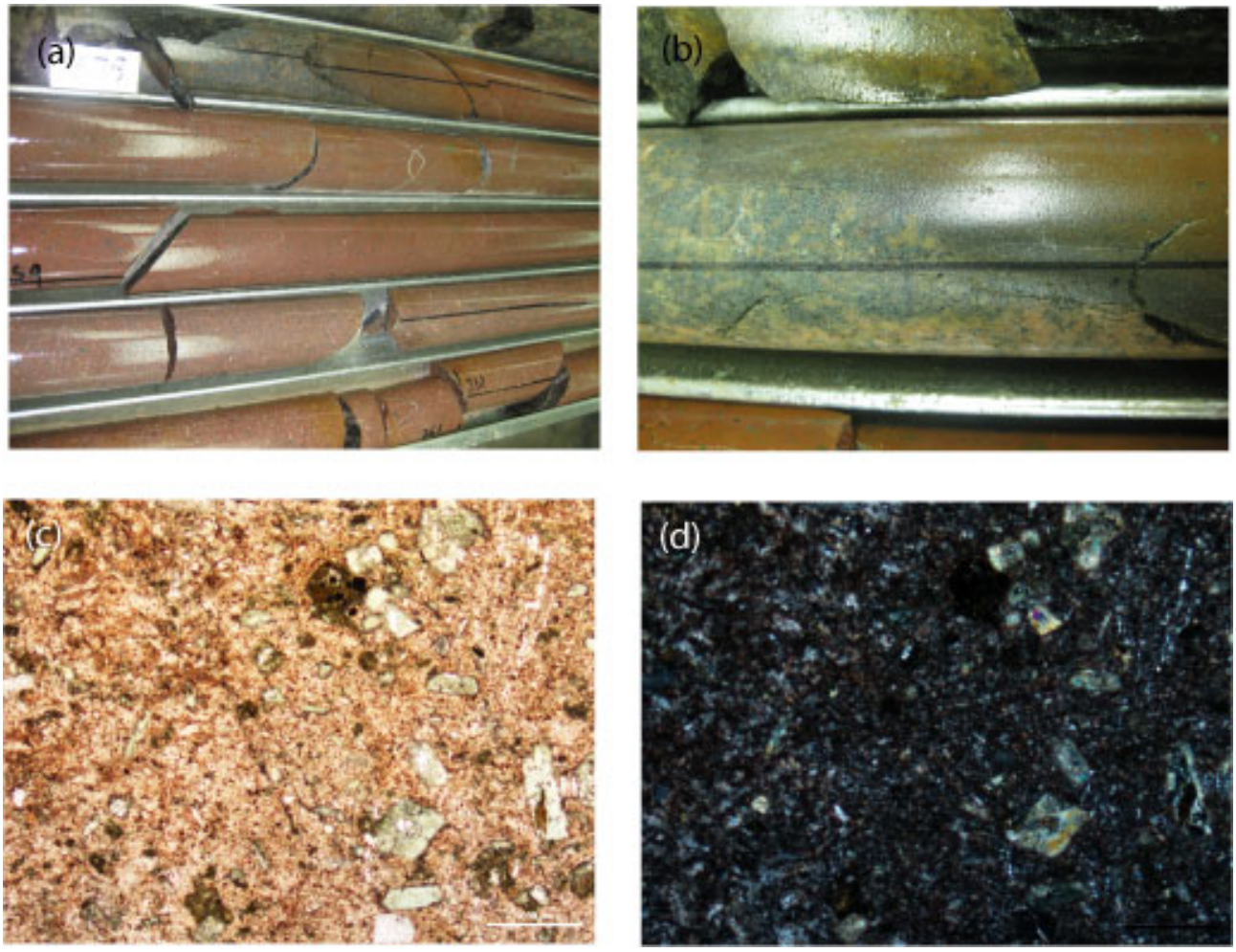

Figure 24. Photos of trachyte at 250.8–280.0 m. (a) Interval of core (left to right is down hole) showing diorite (top left) and trachyte. (b) Contact between diorite (left) and trachyte (right) showing chloritic alteration trachyte in. Photomicrographs of trachyte under (c) plain and (d) cross polarised light.

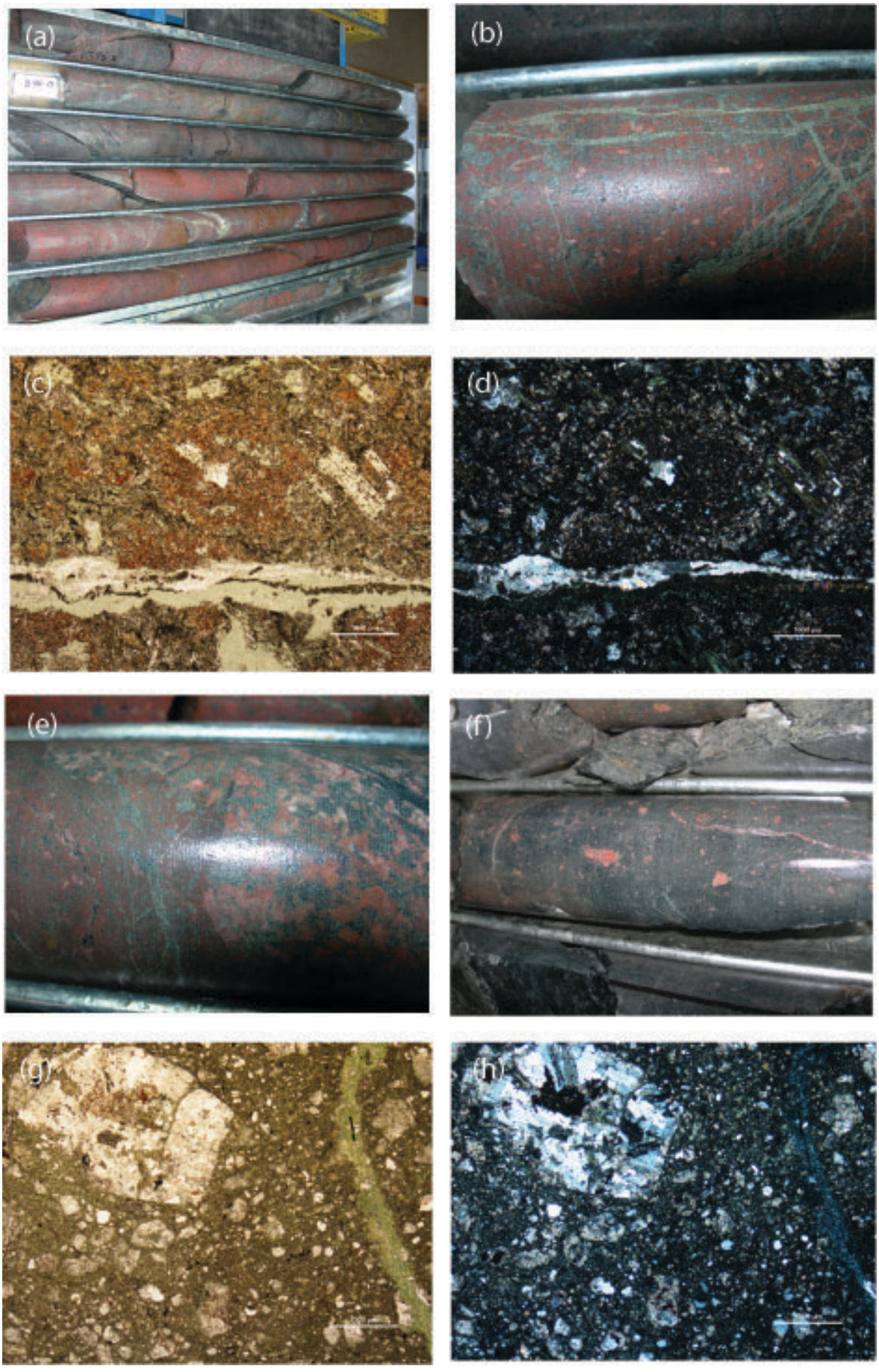

Figure 25. Photos of andesite at 400.0–405.90 m and associated volcanic breccia at 420.0–422.40 m. (a) Interval of core (left to right is down hole) showing diorite (top three rows) and andesite (bottom three rows). (b) Andesite, with chlorite veining. Photomicrographs of andesite under (c) plane and (d) cross polarised light. (e)

Contact between andesite and diorite. (f) Volcanic breccia. Photomicrographs of breccia under (g) plane and (h) cross polarised light.

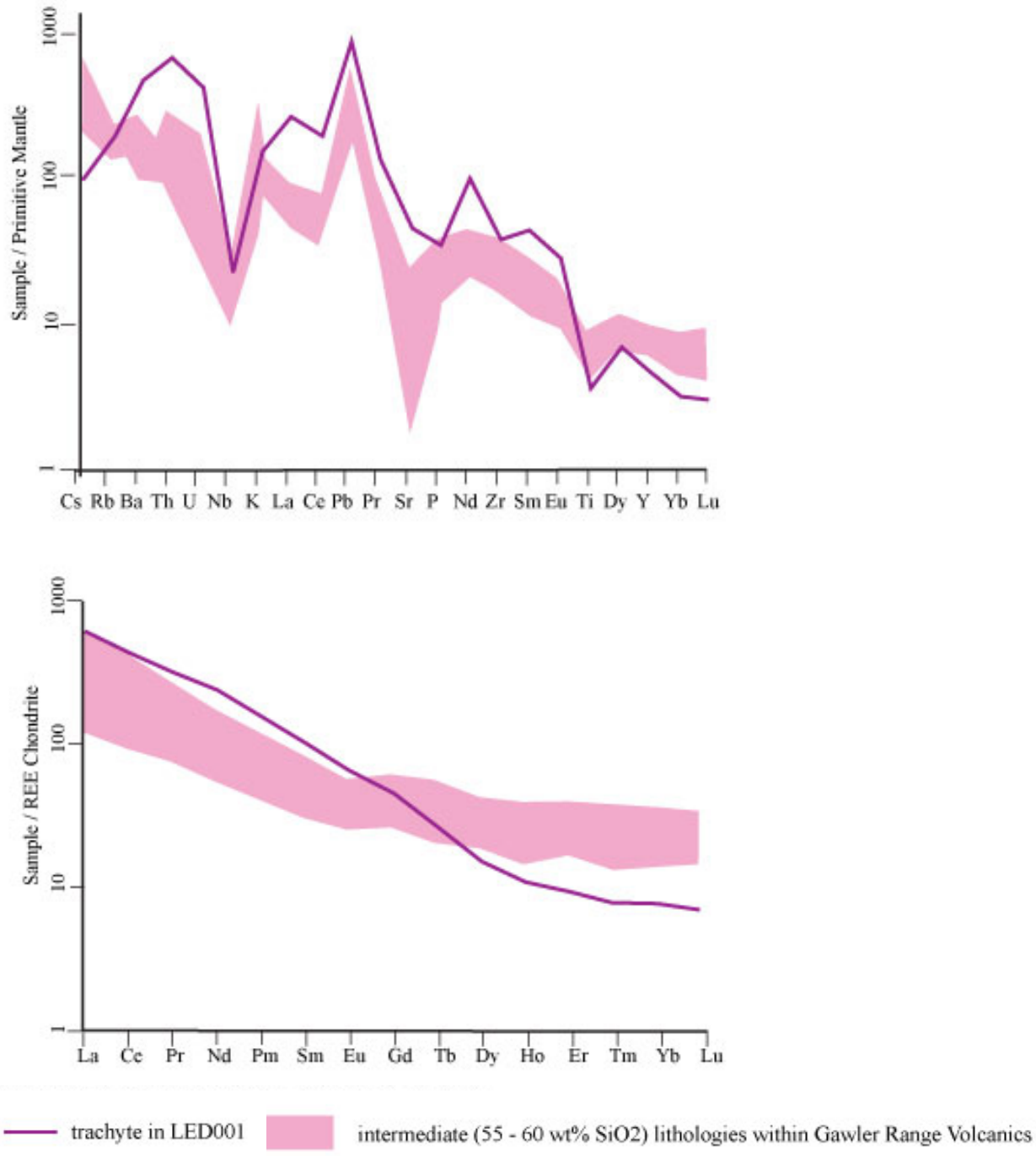

Figure 26. (a) Trace element spidergram normalised to primitive mantle and (b) REE spidergram normalised to chondrite of trachyte in LED001 compared to intermediate lithologies (55–60 wt% SiO_2) from the Gawler Range Volcanics [N=17, data from (Creaser, 1989; Fricke, 2005; Giles, 1980; Jagodzinski, 2005)].

At the lower contact between the porphyritic dacite and diorite a thin layer of biotite has recrystallised in the diorite, presumably caused by intrusion of the volcanic (Fig. 23b). The dacite may be associated with the volcanic breccia at 81.70 m, which has sharp contacts with the hornblende schist and granodiorite and contains fragments of granodiorite and schist in a volcanic groundmass (Figs 23e and 23f). The porphyrytic trachyte (Fig. 24a) has intruded in three layers;

250.8–254.7 m, 256.85–276.4 m and 278.65–280.0 m. At its contacts with the diorite the trachyte often exhibits a purple-brown cooling margin (Fig. 24b), and apophyses of the trachyte are observed intruding the diorite. The andesite (Figs 25a and 25b) intrudes in three layers; at 400.0–403.5 m, 404.9–405.9 m and 483.9–485.8 m, and may all be part of the same intrusion. At its contacts with the diorite, apophyses of both these andesites intrude the diorite (Fig. 25e). The volcanic breccia at 420.0–422.4 m (Fig. 25f) may be associated with the andesite.

6.1 PETROLOGY

The porphyritic basalt is fine grained and composed of plagioclase, clinopyroxene and possible orthopyroxene and olivine and mesostasis (Figs 22c and 22d; Purvis, 2010). The plagioclase occurs as inequigranular euhedral laths up to 1.5 mm in diameter, and is commonly clouded by sericite±chlorite. The clinopyroxene is subophitic, with some grains up to 1.5 mm in diameter and sparse microspherulitic aggregates. Patches of smectite±chlorite±carbonate may represent altered olivine or orthopyroxene. The patches of mesostasis are largely indetermine, but swallow-tail plagioclase microlites and dendritic opaque oxide occur in some areas.

The aphyric basalt is fine grained and composed of plagioclase and Ti-bearing clinopyroxene with minor possible olivine and oxide and quenched mesostasis (Purvis, 2010). The plagioclase occurs as laths up to 2.5 mm long which are locally fritted with inclusions of opaque oxide and clinopyroxene and locally altered with sericite. Clinopyroxene occurs as granular to subophitic grains up to 1 mm long, and is partly interstitial to plagioclase. Small patches of clay may be altered olivine or pyroxene. The mesostasis occurs in patches up to 5 mm in diameter, and contains swallow-tailed plagioclase microlites, dendritic and microcrystalline oxide, needles of titanaugite and feathery clouded possible alkali feldspar and clay.

The dacite porphyry is composed of plagioclase phenocrysts up to 6 mm long, altered biotite and possible hornblende phenocrysts up to 1.5 mm long in a groundmass of plagioclase, quartz, potassium feldspar and biotite with trace opaque oxide, titanate, apatite and zircon (Figs 23c and 23d; Purvis, 2009). The associated hydrothermal breccia at 81.7–83.3 m is composed of an inequigranular mosaic of quartz and haematite-stained albite-sericite altered plagioclase and minor chloritised biotite and contains fragments of hornblende schist (Figs 23g and 23h; Purvis, 2010).

The porphyritic trachyte is composed of orthoclase, clinopyroxene and biotite phenocrysts in a groundmass of potassium feldspar and opaque oxide with minor quartz and apatite (Figs 23c and 23d; Purvis, 2009). Orthoclase phenocrysts are round and up to 7 mm long. Clinopyroxene phenocrysts are up to 3 mm long and partly replaced by actinolite and/or chlorite. Biotite occurs as phenocrysts up to 2 mm long and is partly or completely altered to clay, chlorite and leucoxene ± quartz. The potassium feldspar in the groundmass occurs as laths 0.5 mm long with pale cores and haematite-rich rims. Opaque oxides and quartz are microcrystalline and occur in the groundmass, and apatite is granular and prismatic and up to 0.6 mm in diameter.

The andesite is composed of plagioclase phenocrysts up to 3 mm long and lesser biotite phenocrysts in a groundmass composed of unorientated to weakly flow-orientated plagioclase laths and disseminated biotite, epidote and leucoxene and small quartz aggregates (Figs 24c and 24d). It has undergone albite-epidote-chlorite-leucoxene-hematite-alteration and later epidote ± calcite ± albite veining (Purvis, 2009). The breccia (Figs 24f to 24h) is a heterogeneous rock composed of abundant unsorted fragments which range in size from microcrystalline to over 10 mm in diameter, in a matrix of sericite, carbonate, chlorite and minor leucoxene (Purvis, 2009). Most of the fragments are composed of plagioclase laths, secondary chlorite ± leucoxene replacing ferromagnesian minerals, interstitial quartz and minor sericite and/or carbonate, and appear to be derived from the diorite. There are also monomineralic fragments, such as smectite or illite fragments up to 4 mm long probably replacing feldspar, and single crystal quartz grains. The breccia has been effected by sericite-carbonate-leucoxene and clay alteration, and is intruded by a set of early carbonate veins and later chlorite and quartz veins, both of which contain earthy haematite (Purvis, 2009).

6.2 GEOCHEMISTRY

The mafics plot as sub-alkaline tholeiitic basalts on a TAS discrimination diagram (Fig. 20). They share a near-identical trace element signature with a depletion in Nb and Sr and enrichment in Pb relative to primitive mantle and a fairly flat REE signature, which fits within the trend of mafic lithologies of Gawler Range Volcanics (Fig. 21). Geochemistry is available only for the trachyte, which plots at the boundary between trachyte and trachyandesite on a TAS discrimination diagram (Fig. 20; Le Bas et al., 1986). Compared to intermediate (55–60 wt% SiO_2) lithologies of the Gawler Range Volcanics the trachyte is more enriched in Ba, Th, U and Nd, and has a steeper REE trend, in particular with a greater depletion of HREE (Fig. 25).

6.3 DISCUSSION

The volcanics are likely to be part of the Gawler Range Volcanics (GRV), a succession of felsic and lesser mafic lavas which were extruded over the centre of the Gawler Craton at ~1590 Ma (Allen et al., 2008; Blissett et al., 1993). The southernmost exposure of the lava sheets of the upper GRV crops out 10 km to the north of drill hole LED001, and a plug or dyke of GRV lava is observed only 5 km to the southeast of the hole (Fig. 1). There are no basalts observed within this upper GRV sequence to the north of the hole, but approximately 40 km to the west at Roopena H.S. is a localised volcanic centre of fine-grained amygdaloidal amdesite to trachyandesite lavas which belong to the lower GRV (Allen et al., 2008; Dalgarno et al., 1968; Fricke, 2005).

CONCLUSION

The geological history of drill hole LED001, as suggested by the contact relationships, petrology, geochronology, geochemistry and regional geology presented above appears as follows:

A sequence of metasediments which may belong to the Cleve Group was deposited after c.1850 Ma. The basement to this metasediment may be the sequence of interlayered orthogneisses, amphibolites and minor paragneisses which are exposed to the west of the drill hole on the northern shore of Lake Gilles, and have been dated to 2529±4 Ma (Fraser and Neumann, 2010). Based on their evolved ε_{Nd} signature the basement to this sequence is interpreted to be the c. 3150 Ma Cooyerdoo Granite (Fraser et al., 2010). The age and relationship of the amphibole schist relative to the metasediment is uncertain. The metasediment and amphibole schist were deformed during a pre 1740 Ma metamorphic event, which although slightly older than the recognised age is likely to have been during the Kimban Orogeny. Following deformation, a dolerite intruded these foliated rocks. These rocks were then intruded by a large diorite pluton which incorporated xenoliths of the basement sequence. The diorite was itself intruded by a bimodal volcanic sequence comprising dacite, andesite, trachyte and basalt lavas and breccias, and the fluids associated with these lavas caused haematite-chlorite-albite-sericite-carbonate alteration in the diorite.

APPENDIXES

1. MINERALOGICAL REPORT 9483
2. MINERALOGICAL REPORT 9691
3. GEOCHEMISTRY TABLE

1. MINERALOGICAL REPORT 9483

Pontifex & Associates Pty Ltd

MINERALOGY – PETROLOGY · SECTION PREPARATION

A.B.N. 25 007 521 084

26 Kensington Rd, Rose Park
South Australia 5067
Tel: +61 8 8332 6744
Fax: +61 8 8332 5062

PO Box 91
Kent Town SA 5071
AUSTRALIA

Email:
ian@pontifexpetrographics.com.au
Website:
www.pontifexpetrographics.com.au

MINERALOGICAL REPORT No. 9483

by Alan C. Purvis, PhD

February 16th, 2009

Summary Comments

Samples 1661810-1661817 (without 1661813) include andesites (1661810-11), poorly preserved volcanic (1661812), gabbro (1661814), altered poorly preserved material (1661815) and brecciated quartz microdiorite (1661816-17). The gabbro has hornblende-actinolite-epidote-carbonate-clay-hematite alteration bur the other samples have low-temperature hydrothermal alteration with albite-epidote-chlorite or sericite-carbonate-chlorite-quartz-leucoxene alteration ± clay.

Table 1: Samples described in Report No. 9483

1661810	Andesite?	ab-ep-chl-lx-hem	ep-cc-ab/cbt veins
1661811	Andesite?	ab-chl-ep-hem-lx	qtz-cbt/cbt veins
1661812	Volcanic	ksp-chl-ep-cbt-hem ± ab, qtz	cbt, chl, ep, qtz veins
1661814	Gabbro	act-hb-ab-ep-cc	ep-cc-clay-hem veins
1661815	Unknown	ser-cbt-qtz-chl-lx	cbt, qtz/qtz-chl veins
1661816	Microdiorite breccia	ser-cbt-chl-lx	cbt/chl-qtz vns
1661817	Microdiorite breccia	ser-cbt-chl-lx-clay	cbt/qtz-chl veins

Key: ab: albite; act: actinolite; bi: biotite; bn: bornite; cbt: carbonate; cc: calcite; chc: chalcocite; chl: chlorite; cpy: chalcopyrite; ep: epidote; gr: graphite; hb: hornblende; hem: hematite; ilm: ilmenite; lx: leucoxene/anatase; mv: muscovite; po: pyrrhotite; py: pyrite; qtz: quartz; rut: rutile; sd: sulphide; ser: sericite; tm: tourmaline

SAMPLE	1661810
ROCK NAME (from TS)	Albite-epidote-chlorite-leucoxene-hematite-altered probable andesite with veins of epidote ± calcite ± albite and carbonate veins.

PETROGRAPHY:

A visual estimate of the modal mineral abundances:

In this sample, albitised plagioclase phenocrysts to 2mm long (7-8%) are more abundant than chloritised biotite phenocrysts to 2mm long (2-3%) and rare chlorite-epidote-altered phenocrysts. The groundmass is largely composed of partly flow-oriented albitised plagioclase laths with weak hematite staining as well as 10% disseminated chlorite after biotite, minor epidote and sparse leucoxene. Small quartz-rich aggregates are also disseminated, with epidote and leucoxene. Abundant mostly narrow veins are filled with epidote ± calcite with carbonate-rich lenses to 3mm wide containing minor epidote and albite. Late irregular veins to 2mm wide contain carbonate and rare quartz. This sample may represent altered andesite.

SAMPLE	1661811
ROCK NAME (from TS)	Albite-chlorite-epidote-hematite-leucoxene-altered probable andesite with late magmatic or secondary quartz, quartz-rich veins and lenses with less abundant carbonate, quartz-carbonate veins and carbonate veins.

PETROGRAPHY:

Hematite-stained albitised plagioclase phenocrysts are scattered irregularly through this thin section (mostly towards one end) and are as much as 3mm long. There are also less abundant but more evenly disseminated chloritised biotite phenocrysts and chlorite-epidote-leucoxene-altered possible amphibole or pyroxene phenocrysts (± hematite). The groundmass is rich in unoriented albitised plagioclase laths with interstitial quartz as well as chlorite, epidote, calcite and oxidised opaque oxide. Some of the chlorite is in albitised plagioclase, with diffuse earthy hematite, but some is separate and possibly ex-biotite. The host-rock is probably andesitic.

Irregular veins and lenses to 4mm wide contain unoriented quartz prisms to 2mm long as well as carbonate and interstitial hematite ± chlorite. There are also later narrow quartz-carbonate veins and late crosscutting carbonate veinlets mostly about 0.4mm wide.

SAMPLE	1661812
ROCK NAME (from TS)	K-spar-chlorite-epidote-carbonate-hematite-altered probably biotite-pyroxene porphyritic volcanic with veins containing carbonate, chlorite, epidote and quartz

PETROGRAPHY:

Irregularly disseminated phenocrysts in this thin section include chlorite-leucoxene-altered biotite to 2mm long and chlorite-leucoxene ± carbonate aggregates apparently derived from pyroxene phenocrysts to 2mm long. The groundmass is made up of reddish microcrystalline K-spar-rich domains, rarely with poorly preserved microspherulitic patches, accompanied by chlorite-leucoxene-altered possible biotite microlites and disseminated fine-grained carbonate. Areas between these domains are rich in chlorite, carbonate and leucoxene, locally with K-spar or albite and/or quartz. Early veins contain carbonate and chlorite or epidote and chlorite, rarely with albite in carbonate veins and quartz in chlorite-rich areas. Later veins contain carbonate ± quartz.

This sample represents altered biotite-pyroxene-porphyritic volcanic rock of uncertain original composition. Some geochemistry may be needed to further classify this sample.

SAMPLE 1661814

ROCK NAME (from TS) Actinolite-hornblende-albite-epidote-altered apatite-bearing gabbro with a possibly pegmatoidal albite-calcite-actinolite-epidote vein, epidote-calcite veins and fractures or shears with clays, epidote, carbonate and hematite.

PETROGRAPHY:

A visual estimate of the modal mineral abundances in the host-rock (there are also veins):

Mineral [Host Rock]	***Abundance***	***Origin/location***
Albite with sericite, hematite and epidote	55%	Ex-plagioclase
Actinolite, hornblende and titanite	40-45%	Ex-pyroxene
Opaque oxide	1-2%	Oxidised?
Apatite	1%	Primary

The host-rock in this thin section is composed of altered metamorphosed gabbro with zoned actinolite and green probable hornblende replacing clinopyroxene to 5mm in grainsize and albitised plagioclase to 4mm in grainsize with minor sericite, epidote and earthy hematite. Very minor opaque oxide seems to have been oxidised and is locally rimmed by epidote. Apatite is disseminated as prisms to 1mm long.

The host-rock passes into a pegmatoidal vein 8mm wide with abundant albite to 10mm in grainsize accompanied by less abundant carbonate and minor actinolite. Epidote is disseminated through the albite and carbonate as small prisms and there are very small patches of reddish possible K-spar in the albite.

Irregular veins and patches in the gabbro contain epidote and carbonate with later fractures or microshears with lamellae of clay as well as epidote, carbonate and earthy hematite.

SAMPLE	1661815
ROCK NAME (from TS)	Heterogeneous sericite-carbonate-quartz-chlorite-leucoxene-altered rock with poor textural preservation (fragmental?), cut by carbonate veins, carbonate-quartz veins and quartz-chlorite veins with Fe-rich chlorite.

PETROGRAPHY:

This sample is heterogeneous, highly veined and has poor textural preservation. It has minor disseminated single-crystal quartz grains to 1mm in diameter as well as areas variously rich in sericite, carbonate, leucoxene and earthy hematite ± partly microcrystalline quartz, suggesting possible fragments to 1mm in diameter, in a hematite-stained matrix. Small carbonate grains may also represent fragments and there are irregular areas apparently flooded by chlorite. One possible fragment seems to have feldspar shapes, now sericite, and interstitial quartz. Early carbonate veins to 2mm wide are present as well as veins to 4mm wide rimmed by chlorite and microsparry fine-grained quartz and infilled with coarse-grained carbonate, locally with fine prismatic quartz and sparse chlorite. Later veins are more irregular (0.2mm to 2mm wide) and filled by unoriented mostly prismatic quartz to 1.5mm long with interstitial moderately Fe-rich chlorite.

SAMPLE	1661816
ROCK NAME (from TS)	Fragmental rock with clasts of possible quartz microdiorite with sericite-carbonate-chlorite-leucoxene alteration and leucoxene ex-opaque oxide in a chlorite-rich matrix; cut by carbonate veins and chlorite-quartz veins.

PETROGRAPHY:

This sample contains abundant unsorted fragments from microcrystalline to 4mm in diameter in a matrix of chlorite and leucoxene ± quartz. The fragments contain abundant plagioclase laths with minor sericite and/or carbonate and interstitial quartz, locally with chlorite ± leucoxene derived from mafic material. Small fragments may be monomineralic and include single-crystal quartz grains. Small opaque oxide grains have been altered to leucoxene and there is rare zircon 0.05mm in grainsize. The fragments may have been derived from quartz microdiorite.

Early carbonate veins are present as well as irregular veins rich in chlorite, with less abundant unoriented quartz prisms than in the analogous veins in the previous sample. All of these veins contain fine-grained earthy hematite. Some areas between carbonate veins seem to have sericite and carbonate rather than chlorite.

SAMPLE	1661817
ROCK NAME (from TS)	Fragmental rock with unsorted fragments of quartz microdiorite in a matrix of sericite, carbonate, chlorite and leucoxene, with sericite-carbonate-leucoxene and clay alteration.

PETROGRAPHY:

This sample is similar to 1661816 but has fragments to 10mm long rich in plagioclase to 3mm in grainsize with interstitial quartz, partly veined and flooded by sericite and/or carbonate. Some fragments also contain leucoxene ex-opaque oxide and carbonate-chlorite-leucoxene derived from mafic silicates. There are also fragments to 4mm long totally altered to possible smectite or illite and composed of elongate former grains of possible feldspar. The matrix seems to be mostly sericite and carbonate with minor leucoxene and chlorite. Rare zircons to 0.1mm long occur in the matrix and in fragments. The fragments again seem to represent quartz microdiorite,

Narrow carbonate veins are followed by much narrower quartz-chlorite veins compared to the previous samples.

2. MINERALOGICAL REPORT 9691

Pontifex & Associates Pty Ltd

MINERALOGY – PETROLOGY · SECTION PREPARATION

A.B.N. 25 007 521 084

26 Kensington Rd, Rose Park
South Australia 5067
Tel: +61 8 8332 6744
Fax: +61 8 8332 5062

PO Box 91
Kent Town SA 5071
AUSTRALIA

Email:
ian@pontifexpetrographics.com.au
Website:
www.pontifexpetrographics.com.au

MINERALOGICAL REPORT No. 9691

by Alan C. Purvis, PhD

April 19th, 2010

SUMMARY COMMENTS

Eighteen core samples from drillhole LED001 are described in this report from normal thin sections. These are labelled 1690554 and 1708855 to 1708871 (with two samples labelled 1708864A and B, and no sample 1708867). Several lithological groups are identified, as listed below.

Diorite Group (1708859, 862, 863, 864B, 866, 868, 869 and 870)

The largest group of 8 samples consists of weakly to intensely altered, partly veined and brecciated diorite, and quartz-diorite, partly transitional to quartz monzodiorite, commonly with biotite and hornblende or with clinopyroxene and minor biotite. Common accessory minerals are magnetite, titanite, apatite and zircon. Some samples are porphyritic but most are inequigranular or even-grained. Interstitial quartz and K-feldspar. Large interstitial orthoclase grains occur in sample (1708870). The single breccia (1708864B) is adjacent to quenched basalt and may be a contact or hydrothermal breccia including a fragment of possible altered basalt. Sample 1708868 is highly foliated and protomylonitic apparently from a shear zone.

Alteration in these samples consists of various combinations of albite, sericite, hematite, chlorite, epidote, carbonate and leucoxene and there are veins variously with epidote, calcite and quartz. Rare pyrite occurs in 1708869 and 870.

Granodiorite Porphyry (1708855)

This single sample of granodiorite porphyry represents the only quartz-rich intrusive rock in this batch. It has albite-sericite-chlorite-epidote alteration and fractures variously with clay, sericite, adularia, epidote and albite.

The mineralogies of the diorite and granodiorite samples are illustrated in Fig. 1, below, with the classification illustrated by a quartz-alkali feldspar-plagioclase diagram (Fig. 2)

Trachyte (1708865)

This single sample is a K-feldspar-clinopyroxene-biotite porphyritic trachyte with alteration to hematite-actinolite-chlorite and clay.

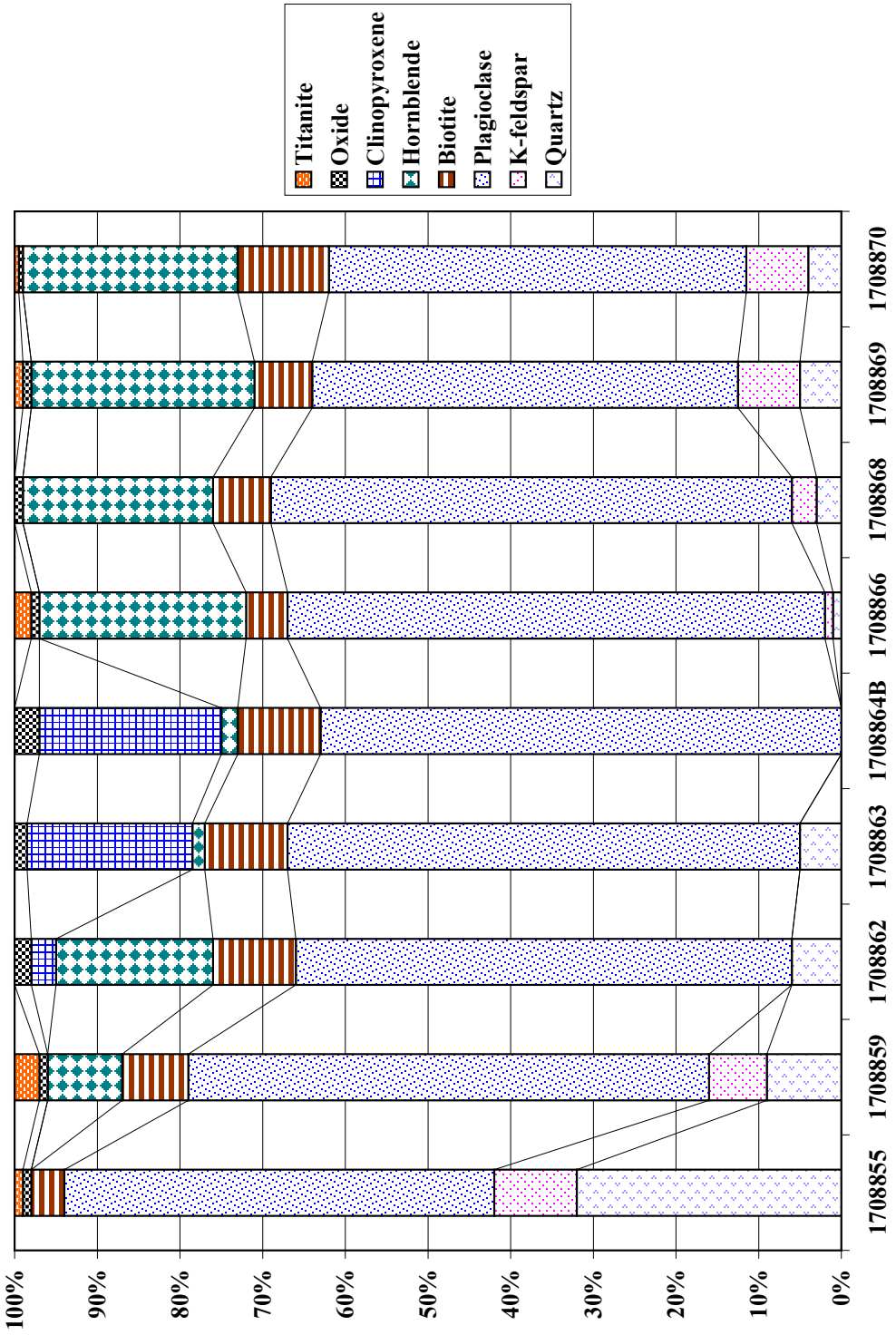

Fig. 1: Estimated primary mineralogy of granodiorite and diorite samples, Report No. 9691

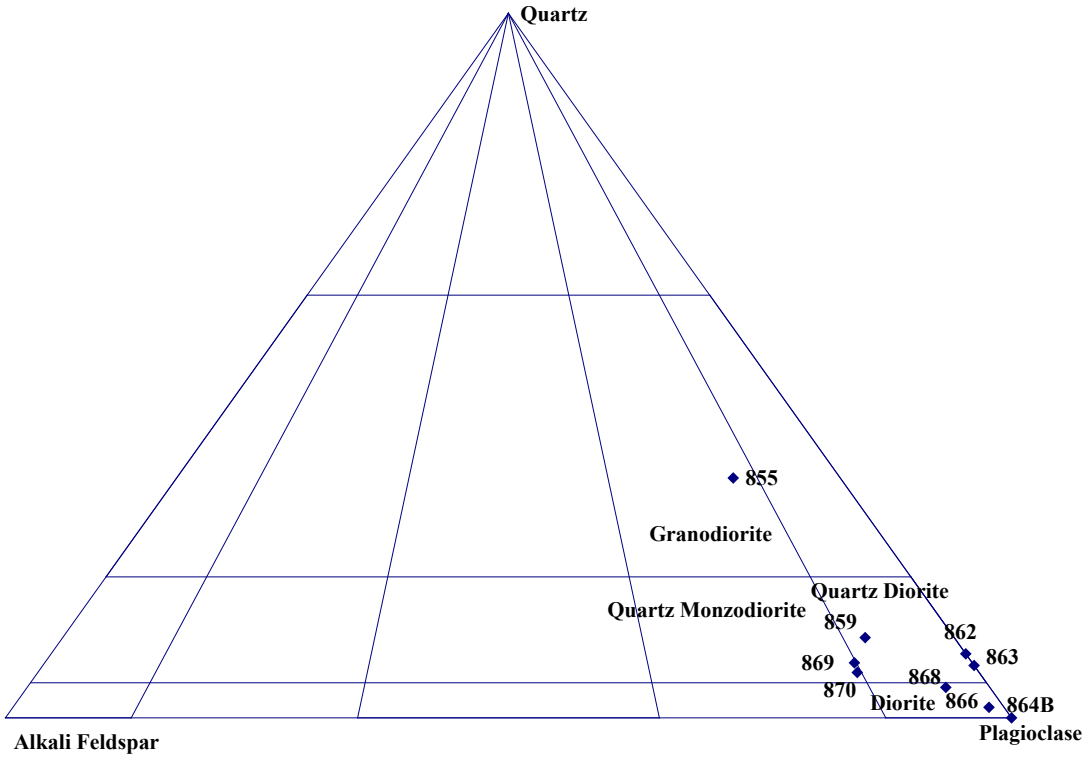

Fig. 2: Quartz-Alkali feldspar-Plagioclase diagram for granodiorite and diorite samples, Report No. 9691. All sample numbers have the prefix 1708, not shown above

Mafic Igneous Lithologies (1690554, 1708860, 861, and 864A)

These four mafic samples include basalt and dolerite with patches of mesostasis (1690554, 1708861) also quenched basalts, with small scale heterogeneity in sample 1708864A, adjacent to brecciated diorite. The quenched basalts have chlorite ± clay alteration and may have been partly glassy. These samples seem to represent intrusions as they are not metamorphosed but show low temperature hydrothermal alteration.

Amphibole schist (1708857)

This sample is actinolite or hornblende schist with feldspar ± hematite and chlorite ex-biotite. Some geochemistry may be required to explain the origin of this sample.

Quartz-rich quartzofeldspathic lithologies (1708856, 858 and 871)

These samples are quartz-rich but varied:
1708856: Altered quartz-rich quartzofeldspathic micromosaic with minor chloritised biotite and lenses or fragments of actinolite-rich material ± chloritised biotite: possible metasandstone or silicified igneous lithology.
1708858: Altered fine-grained laminated quartz-feldspar-biotite gneiss with sericitised and albitised plagioclase and chloritised biotite: possibly metamorphosed laminated quartzofeldspathic sandstone
1708871: Quartz-rich granofels with altered feldspar(s), and biotite and minor green hornblende, accompanied by opaque oxide, apatite and altered accessory grains: chlorite-sericite alteration is seen and the rock may be metasandstone or an unusual vein.

Selected geochemistry may be useful in elucidating these samples.

INDIVIDUAL DESCRIPTIONS

Sample No	***1690554***
Rock type from TS	Weakly altered basalt or dolerite with weakly altered plagioclase, minor chlorite, Ti-bearing clinopyroxene, oxide and areas of quenched mesostasis.
Hand specimen	Grey massive unfoliated rock (mafic?)

Field Note: *Biotite-rich metasediment? LED001, ~225m*

PETROGRAPHY

Visually estimated mineralogy and components:

Component	***Abundance***
Plagioclase as small phenocrysts and laths to 2.5mm long; locally fritted with inclusions of opaque oxide and clinopyroxene and locally altered with patches of sericite.	50-55%
Granular and subophitic pale brownish clinopyroxene to 1mm long, partly interstitial to plagioclase.	30%
Small patches of green clay possibly ex-olivine or pyroxene	2%
Granular opaque oxide to 0.5mm in grainsize (titanomagnetite?)	5%
Irregular areas of feldspathic mesostasis to 5mm in diameter with partly swallow-tailed plagioclase microlites, dendritic and microcrystalline opaque oxide and needles of purplish titanaugite as well as feathery clouded possible alkali feldspar and clays.	10%

Interpretation:

This sample may represent Fe-Ti-rich basalt or dolerite with unusually abundant areas of mesostasis as well as opaque oxide and augite-titanaugite.

Sample No	***1708855***
Rock type from TS	Granodiorite porphyry with albite-sericite-chlorite-epidote alteration and fractures with clay, sericite, adularia, epidote and albite
Hand specimen	Mottled reddish and greenish-grey rock

Field Note: *Felsic volcanic*

PETROGRAPHY

Visually estimated mineralogy:

Mineral	***Abundance***	***Origin/location***
Plagioclase phenocrysts	19%	Sericite-clouded phenocrysts
Quartz	32%	In groundmass
Plagioclase, fine-grained	33%	In groundmass, sericite-clouded
K-feldspar	10%	In groundmass, inequigranular
Chlorite-hematite-leucoxene ± epidote	4%	Ex-decussate biotite ± hornblende
Leucoxene and titanite	~1%	With biotite
Apatite, zircon	Trace	Accessory

Sericite-clouded, albitised plagioclase phenocrysts to 6mm long are abundant in this thin section, occurring singly and in aggregates. There are also altered biotite flakes and possible hornblende grains to 1.5mm long. The groundmass has abundant sericite-clouded albitised plagioclase and quartz and less abundant K-feldspar and chloritised biotite, mostly 0.1mm to 0.7mm in grainsize. Small aggregates of opaque oxide and partly leucoxenised titanite are disseminated, with apatite and rare fine-grained zircon (~0.05mm long) in and adjacent to biotite, possible hornblende, opaque oxide and titanite. Narrow fractures contain sericite, hematite, adularia, albite and epidote.

Interpretation:

The visually estimated mineralogy and texture indicate plagioclase porphyritic granodiorite porphyry of intrusive origin with low temperature hydrothermal alteration and veining.

Sample No	***1708856***
Rock type from TS	Altered quartz-rich quartzofeldspathic micromosaic with minor chloritised biotite and lenses or fragments of actinolite-rich material ± chloritised biotite.
Hand specimen	Heterogeneous rock with green lenses or fragments in a fine-grained reddish matrix

Field Note: *Adjacent to contact of granite with mafic – brecciated margin of granite? Core broken at contact*

PETROGRAPHY

Visually estimated mineralogy:

Mineral	***Abundance***	***Origin/location***
Quartz	~65-70%	In reddish matrix
Albite, sericite and hematite	~25-30%	Altered, reddish plagioclase
Chlorite	2-3%	Ex-biotite, disseminated and in lenses
Actinolite	2-3%	In lenses or fragments

Much of this sample is an inequigranular mosaic of quartz and hematite-stained albite-sericite-altered plagioclase as well as minor chloritised biotite. Most of the quartz is less than 0.5mm in grainsize, with mostly finer-grained quartz, but some quartz-rich lenses have quartz to 2mm long and one patch has plagioclase to 1.5mm in grainsize. The proportion of altered plagioclase seems to vary from ~5% to possibly 35% and some of the biotite is in possible fractures in various orientations. Minor altered biotite is also disseminated. Altered biotite is also a minor .component in lenses to 8mm long dominated by fine-grained green actinolite. Rare zircon 0.05mm in diameter occurs in the quartzofeldspathic areas.

Late hairline fractures contain reddish feldspar and minor quartz.

Interpretation:

This sample is too quartz-rich to represent granite and may be of hydrothermal origin, or modified by silicification. The amphibole-rich lenses could be fragments of sample 1708857 (actinolite schist).

Sample No	***1708857***
Rock type from TS	Actinolite or hornblende schist with feldspar ± hematite and chlorite ex-biotite.
Hand specimen	Grey-green amphibole-rich rock

Field Note: *Fine-grained mafic*

PETROGRAPHY

Visually estimated mineralogy:

Mineral	***Abundance***	***Origin/location***
Actinolite/hornblende	Dominant 90-95%?	Metamorphic, partly foliated
Chlorite-leucoxene	5-7%	Ex-biotite
Feldspar(s) ± limonite	2-3%	Disseminated and in lenses
Oxide	Trace	accessory

This sample is irregularly layered but is dominated by inequigranular pale green amphibole (actinolite or hornblende), commonly microcrystalline but as much as 1mm in grainsize in some layers and lenses. Some layers also have disseminated spots to 0.5mm in diameter composed of various types of chlorite and minor titanite. These spots seem to represent former biotite. Several layers have minor to common interstitial feldspar, partly hematite-stained and possibly including adularia ± albite. Rare opaque oxide is present.

Interpretation:

This sample is largely composed of fine-grained amphibole, either actinolite or hornblende, but is of uncertain origin. Some geochemistry may be useful in interpreting the origins of this sample, but the amphibole-rich lenses in the previous sample may represent fragments of this lithology in a quartz-rich or silicified matrix.

Sample No	***1708858***
Rock type from TS	Altered fine-grained laminated quartz-feldspar-biotite gneiss with sericitised and albitised plagioclase and chloritised biotite: possibly metamorphosed laminated quartzofeldspathic sandstone
Hand specimen	Banded fine-grained greenish grey rock

Field Note: *Fine-grained orthogneiss*

PETROGRAPHY

Visually estimated mineralogy:

Mineral	***Abundance***	***Origin/location***
Quartz	Major (in layers)	More abundant (to 65% in quartz-rich layers)
Sericite	Abundant (in layers)	Ex-plagioclase in plagioclase-rich layers (to 70%)
Albite, hematite-stained ± sericite	Common to abundant	Ex-plagioclase in quartz-rich layers (to 30%)
Chlorite ± leucoxene	Sparse to minor	Ex-biotite in layers and fractures
Leucoxene and opaque oxide	2-3%	Ex-detrital opaque oxide?
Apatite and zircon	Rare	Accessories

This material has lenticular layers from less than 1mm wide to 7mm wide, with a micromosaic mostly less than 0.25mm in grainsize. These layers are alternately rich in quartz and in weakly hematite-stained sericitised or albitised plagioclase. Plagioclase-rich layers have sericitised plagioclase but quartz-rich layers commonly contain at least some albitised feldspar. Minor foliated biotite has been altered to chlorite and leucoxene and is more abundant informer plagioclase-rich layers. There is also some chlorite in fractures at a low angle to the layering. Minor leucoxene and opaque oxide are disseminated.

Interpretation:

This sample has an overall quartz content possibly more than 50% and would seem to represent layered quartzofeldspathic metasandstone rather than orthogneiss (of igneous origin) as suggested in the notes quoted above.

Sample No	***1708859***
Rock type from TS	Altered hornblende-biotite quartz diorite to quartz monzodiorite with albite-sericite-hematite-chlorite-titanite alteration
Hand specimen	Pinkish feldspathic rock with mafic clots

Field Note: *Granite*

PETROGRAPHY

Visually estimated mineralogy:

Mineral	***Abundance***	***Origin/location***
Albite-sericite-hematite	63%	Inequigranular plagioclase
Quartz	9%	Interstitial primary
K-feldspar	7-8%	Mostly interstitial, primary
Chlorite-titanite/leucoxene	8%	Ex-biotite ± hornblende
Hornblende	8-9%	Primary igneous
Titanite (sphene)	3%	
Magnetite	1%	
Apatite, rare zircon	<1%	Accessories

Euhedral crystals of albite-sericite-hematite-altered plagioclase are abundant in this thin section and range from 0.5mm to 6 or 7mm long. Interstitial quartz is mostly less than w2mm in grainsize, with mostly interstitial K-feldspar to 4mm long, locally enclosing plagioclase, opaque oxide and quartz. Mafic grains and clots are scattered and contain or consist of chloritised biotite to 1.5mm long and mostly fresh brown hornblende as much as 2mm long, rarely overprinted by fine-grained green hornblende. Grains and aggregates of magnetite and/or titanite are also common, with apatite commonly in and adjacent to oxide or mafic silicates. Apatite occurs as prisms to 0.5mm long and there are rare zircons to 0.15mm long.

Interpretation:

The visually estimated mineralogy of this sample suggests quartz diorite transitional to quartz monzodiorite with albite-sericite-hematite and chlorite-titanite alteration.

Sample No	***1708860***
Rock type from TS	Chlorite-clay-carbonate-hematite-altered amygdaloidal, possibly olivine-pyroxene porphyritic basalt with fractures containing carbonate and/or clay.
Hand specimen	Dark grey-green fine-grained rock

Field Note: *Altered mafic volcanic adjacent to the contact of mafic with granodiorite/ granite? Core broken at contact*

PETROGRAPHY

This sample has the following components:

Component	***Abundance***
Patches of chlorite ± smectite ± carbonate to 2mm long possibly representing former phenocrysts and aggregates of olivine, commonly enclosing microcrystalline probable chromite	Minor (5%)
Elongate aggregates to 3mm long composed of possible chlorite-smectite ± limonite with carbonate and/or quartz, possibly derived from pyroxene	Minor (5%)
Patches to 4mm in diameter composed of carbonate with quartz and/or plagioclase with pyrite in one aggregate: possibly representing amygdales the largest patch has decussate coarse-grained chlorite or chlorite-smectite with interstitial pale green chlorite and minor pyrite	Very minor (3-4%)
Heterogeneous fine-grained green and orange hematite-stained clays with minor opaque oxide and visible microcrystalline apatite: the green clays seem to represent former feldspar laths with clouded orange material ex-pyroxene or interstitial glass.	Abundant
Fractures filled with clays or with carbonate and quartz/feldspar ± apatite ± hematite	Very minor

This may represent altered olivine-pyroxene porphyritic basalt with amygdales and late clay and/or carbonate-rich fractures.

Sample No	***1708861***
Rock type from TS	Altered basalt with sericite-chlorite-clay alteration and clouded areas of mesostasis.
Hand specimen	Dark grey fine-grained rock

Field Note: *Fine-grained mafic*

PETROGRAPHY

The minerals and other components in this thin section are:

Component	***Abundance***
Plagioclase as inequigranular euhedral laths as much as 1.5mm long, commonly clouded by sericite ± chlorite.	50-55%
Mostly pale brownish subophitic clinopyroxene (Ti-bearing?) with some colourless grains to 1.5mm long and sparse microspherulitic aggregates.	25-30%
Green possible smectite ± chlorite with leucoxene-like spots, possibly ex-olivine or Ca-poor pyroxene (orthopyroxene or pigeonite)	5%
Very fine-grained opaque oxide (titanomagnetite ± ilmenite?)	5%
Clouded patches of largely indeterminate mesostasis with swallow-tail plagioclase microlites and dendritic opaque oxide in some areas: may contain apatite.	10%

Interpretation:

This sample represents altered fine-grained basalt with sericite-chlorite-clay alteration and areas of clouded mesostasis.

Sample No	***1708862***
Rock type from TS	Altered and veined quartz-bearing diorite with albite-hematite-actinolite-chlorite-epidote alteration and a large epidote-calcite vein passing into a finely brecciated zone. Narrow epidote veins are also present.
Hand specimen	Granular rock with pink feldspar(s), green mafic spots and possible epidote veins

Field Note: *Altered granitoid*

PETROGRAPHY

Visually estimated mineralogy of the host rock:

Mineral	***Abundance***	***Origin/location***
Albite-hematite-epidote	60%	Ex-coarse-grained plagioclase
Quartz	5-6%	Interstitial and with epidote
Actinolite and hornblende	20-25%	Primary and ex-pyroxene?
Chlorite	6%	Ex-biotite, ± epidote
Epidote	4%	Ex-biotite and with actinolite and quartz
Oxide	1-2%	Partly fractured and fragmented and veined by chlorite
Apatite, possible allanite and zircon	<1%	Accessories, with epidote rims on allanite

This thin section is divided into two by a large wedge-shaped vein 0.5mm to 20mm + in width, filled with fine-grained granular to prismatic epidote with a large lens of coarse-grained calcite. The epidote-rich zone contains fragments of albite and actinolite derived from the host rock, passing laterally into zones of breccia with fine-grained fragmented epidote, actinolite, albite-epidote-hematite-altered plagioclase etc in clouded microcrystalline epidote.

The host rock is rich in hematite-stained albitised plagioclase grains to 4mm long and 3-4mm wide with disseminated very fine-grained epidote commonly rimmed by earthy hematite. Aggregates of actinolite and olive-green hornblende are also abundant and may represent altered pyroxene that was composite with primary hornblende, and there are rare aggregates of actinolite interlaminated with chlorite to 4mm long, also derived from pyroxene. Chlorite-epidote

aggregates with minor leucoxene/titanite have replaced common to abundant biotite to 3 or 4mm in grainsize. Minor granular quartz is commonly rimmed and veined by epidote. Relatively fine-grained magnetite has been fractured and veined by chlorite and is accompanied by apatite. Some apatite is separate from the opaque oxide, however. Narrow epidote veins also extend into areas of altered diorite.

Interpretation:

This sample represents altered and veined quartz-bearing diorite with albite-hematite-actinolite-chlorite-epidote alteration and veins of epidote ± calcite as well as lenses with comminuted albite, represent and actinolite in microcrystalline epidote.

Sample No	***1708863***
Rock type from TS	Weakly altered quartz-bearing biotite-augite diorite with actinolite, sericite and prehnite.
Hand specimen	Grey-green granular rock

Field Note: ***Granodiorite***

PETROGRAPHY

Visually estimated mineralogy:

Mineral	***Abundance***	***Origin/location***
Plagioclase + sericite	60-65%	
Clinopyroxene + actinolite	20%	Partly altered igneous grains
Biotite ± clay-prehnite	10%	
Quartz	5%	Late magmatic
Hornblende	1-2%	
Magnetite	1-2%	Magmatic, minor/accessory
Apatite, zircon	<1%	

Partly sericitised plagioclase laths to 6mm long and mostly 2-3mm wide are abundant in this sample and are weakly aligned, although some grains are oblique to or at a high angle to the overall layering. Granular clinopyroxene is mostly 1-4mm in grainsize and is locally mottled and rimmed by brownish green hornblende or replaced by actinolite. Separate hornblende grains are rare, however. Minor magnetite is disseminated, commonly composite with apatite, although some apatite occurs separately, and there is rare zircon to 0.25mm long. Poikilitic biotite to 4mm in grainsize is interstitial to earlier minerals as is minor quartz, which is optically continuous over areas to 4mm in diameter. Some of the biotite has possible clay alteration and/or lenses of prehnite parallel to the cleavage.

Interpretation:

This sample is composed of quartz-bearing biotite-augite diorite with actinolite, sericite and minor prehnite as secondary minerals.

Sample No	*1708864A*
Rock type from TS	Heterogeneous altered basalt with partly crystalline and possibly glassy zones, partly fractured and fragmented and veined by chlorite: alteration to albite and chlorite ± leucoxene is evident.
Hand specimen	Irregularly layered rock with grey-green and dark grey layers and lenses

Field Note: ***Altered mafic volcanic intruding granodiorite***

PETROGRAPHY

This sample has irregular lenses and layers with albitised, partly sericite-clouded plagioclase, partly as phenocrysts and partly as microlites, together with chloritised mafic phenocrysts in some areas. The plagioclase phenocrysts have maximum lengths varying from 1mm to 2.5mm between lenses and layers, but some layers have only sparse plagioclase and others lack visible plagioclase. One large plagioclase lath, about 2mm long, is attached to uralitised clinopyroxene and may have been detached from the adjacent diorite.

The groundmasses may have been glassy and are composed of chlorite, microcrystalline opaque oxide, brown clay and possibly some albite. These areas are brownish in low-angle incident light and seem to pass into areas that are pale or whitish in low-angle incident light and seem to contain leucoxene as well as or instead of opaque oxide. These pale areas are commonly around fractures and in lenses and zones lacking plagioclase laths. Some areas with abundant plagioclase are also pale in low-angle incident light, however. The crystal-free areas may have been glassy and some have been fractured and fragmented and veined by chlorite. Some of the fragments are pale throughout and some have cores that are pale in low-angle incident light and pale rims against the veins. Hairline fractures with pale margins also extend into crystal-bearing darker zones. There is also a wider chlorite-filled vein that extends 6mm into the thin section and terminates against a pale zone.

Interpretation:

This sample is basaltic but seems to represent complex partly crystalline and totally glassy zones that have had alteration to albite and chlorite ± leucoxene and partly fractured and fragmented and veined by chlorite. It may indicate several separate or semi-continuous pulses of intrusion allowing the development of zones with various proportions of plagioclase laths and phenocrysts and mafic grains. Contraction on cooling and possibly devitrification of the crystal-free zones may have allowed chlorite veining at low temperatures.

Sample No	***1708864B***
Rock type from TS	Breccia of albite-sericite-actinolite-clay-leucoxene-altered diorite and porphyritic fine-grained diorite, as well as a patch or altered fragment of basalt, with albite-hematite-clay-leucoxene alteration, in a sparse matrix of hematite-stained feldspar and chlorite: hydrothermal or contact breccia?
Hand specimen	Contact between pale granular rock and partly darker material

Field Note: ***Altered mafic volcanic intruding granodiorite***

PETROGRAPHY

The pale zone at one end of this thin section is composed of altered porphyritic fine-grained diorite with possibly 60-65% sericite-clouded albitised plagioclase phenocrysts partly as phenocrysts to 5mm long and partly as groundmass grains 0.5mm to 1.5mm long. Common to abundant clinopyroxene to 3mm long has been totally altered to actinolite, and there are clay-leucoxene-limonite-altered biotite flakes to 4mm long. There is no quartz but opaque oxide and apatite are disseminated, with granular apatite partly composite with magnetite and acicular apatite in plagioclase. Other large fragments, to 25mm or more in diameter, are composed of more uniformly coarse-grained diorite similar to those described above but again lacking quartz. These fragments have about 60-65% albitised and weakly sericitised plagioclase as well as mafic grains and aggregates. The mafic material is largely actinolite ex-clinopyroxene with less abundant clay-leucoxene-limonite ex-biotite. Magnetite and apatite also occur in mafic clots and disseminated, as in the other diorite samples in this drillhole..

There is a zone between the porphyritic microdiorite fragment and the other fragments with mostly smaller fragments, from 0.2mm to 8mm long. These fragments contain or consist of albitised plagioclase, actinolite, clays and leucoxene, magnetite and apatite as in the larger, mostly more even-grained fragment, with more clearly hematite-stained zones in the altered plagioclase, mostly on the margins of the fragments. The matrix is rich in hematite-stained feldspar and/or chlorite with rare microcrystalline opaque oxide.

On one side of the thin section there is a patch or fragment of altered mafic material 6mm wide. This material has abundant albitised, hematite-stained plagioclase laths and minor chloritised mafic grains in a clouded dark groundmass of khaki or olive-green clay with fractures apparently rich in leucoxene. This material is partly interstitial to fragments of diorite.

Interpretation:

This sample may represent an intrusion-generated or hydrothermal breccia and may be related to the complex basaltic rock in 1708864A. Similar breccias occur adjacent to more felsic dykes in southern New South Wales, where they locally contain sulphides.

Sample No	***1708865***
Rock type from TS	K-feldspar-clinopyroxene-biotite porphyritic trachyte with hematite-actinolite-chlorite-clay alteration.
Hand specimen	Red fine-grained rock with mostly darker possible phenocrysts: the stained offcut shows abundant K-feldspar partly as phenocrysts

Field Note: *Rhyolite*

PETROGRAPHY

Visually estimated mineralogy:

Mineral	***Abundance***	***Origin/location***
K-feldspar as phenocrysts	5%	Rounded phenocryst to 7mm long.
Clinopyroxene + actinolite and/or chlorite	10%	Partly altered phenocrysts to 3mm long
Biotite with clays, chlorite and leucoxene ± quartz	3-4%	Partly or completely altered phenocrysts to 2mm long
Apatite	<1%	Granular and prismatic, to 0.6mm
K-feldspar ± hematite	~80%	Laths to 0.5mm long with pale cores and hematite-rich rims and interstitial material
Opaque oxide	2-3%	In the groundmass: microcrystalline
Quartz	~1%	In the groundmass: microcrystalline

This sample has a varied phenocryst population, originally orthoclase-clinopyroxene-biotite-apatite, with alteration to actinolite, chlorite and clays, in a K-feldspar-rich groundmass largely lacking quartz. The abundance of apatite is consistent with possible trachyte.

Interpretation:

The visually estimated mineralogy indicates former trachyte with ‘red-rock’ alteration.

Sample No	1708866
Rock type from TS	Altered biotite-bearing plagioclase porphyritic hornblende microdiorite with sericite and minor chlorite
Hand specimen	Fine-grained greenish grey rock

Field Note:

PETROGRAPHY

Visually estimated mineralogy:

Mineral	***Abundance***	***Origin/location***
Plagioclase phenocrysts	5%	Partly sericitised phenocrysts
Plagioclase + sericite	60%	Groundmass grains
Hornblende	25%	Granular, in the groundmass
Biotite ± chlorite	5%	Ragged flakes ± quartz
Quartz and K-feldspar	1-2%	interstitial
Titanite	1-2%	Fine-grained, primary
Oxide	1%	Microcrystalline
Apatite	<1%	Accessory

Partly sericitised plagioclase phenocrysts to 4mm long are scattered through this sample, locally in aggregates with hornblende and partly chloritised biotite. Moderately flow-oriented sericite-clouded plagioclase to 1mm or more in grainsize is the main groundmass mineral together with less abundant granular hornblende. Some of the hornblende has cores of actinolite probably derived from former clinopyroxene. Minor biotite is also disseminated but is not obviously foliated. There is also minor partly euhedral titanite, disseminated microcrystalline opaque oxide and small needles of apatite. Sparse to quartz occurs in some areas and interstitial orthoclase is also evident, mostly adjacent to plagioclase phenocrysts.

Interpretation:

This sample is sparsely plagioclase porphyritic microdiorite with sericite-chlorite alteration.

Sample No	***1708868***
Rock type from TS	Heterogeneous hornblende-diorite gneiss with a protomylonitic texture and albite-hematite-chlorite-leucoxene-sericite alteration: contains carbonate veins and lenses.
Hand specimen	Pinkish granular rock with dark spots

Field Note: *Altered granitoid*

PETROGRAPHY

This sample is foliated and highly deformed but shows variation across the thin section. It has possibly 60-65% hematite and sericite-clouded albitised plagioclase as anhedral grains and augen, varying in maximum grainsize across the thin section, from 2mm in one corner to 6mm in the opposite corner. In the finer-grained area there is also fresh greenish brown hornblende mostly less than 2mm in grainsize as well as minor chloritised biotite, opaque oxide, titanite and apatite. Lamellae of quartz and/or K-feldspar are interstitial to the plagioclase, hornblende and biotite with hematite-staining in the feldspar and a recrystallised almost mylonitic character in the quartz. Further across the thin section the hornblende becomes altered to chlorite and leucoxene without the lamellar texture seen in chlorite-leucoxene-altered biotite. Mylonitic lamellae of quartz or of hematite-stained K-feldspar become more abundant and there are rare grains of K-feldspar. The widest mylonitic lens is 2mm wide and has microcrystalline quartz, feldspar and chlorite. In the coarse-grained area there are undeformed patches of the chlorite that locally contain carbonate or actinolite (mostly in chlorite ex-hornblende) or epidote (in chlorite ex-biotite) and the plagioclase becomes on the whole coarser-grained. Some areas have lenses of quartz that are not highly deformed, however. This area also has conformable carbonate veins and lenses of carbonate to 1.5mm wide. Hairline carbonate veins occur in other parts of the thin section.

Interpretation:

This sample represents highly deformed and altered biotite-bearing hornblende diorite with a protomylonitic texture and albite-hematite-chlorite-sericite-leucoxene alteration.

Sample No	***1708869***
Rock type from TS	Altered and veined quartz-K-feldspar-bearing hornblende diorite to monzodiorite with albite-hematite-chlorite-leucoxene alteration, veins with quartz, carbonate and epidote and rare pyrite.
Hand specimen	Pinkish granular rock with pale veins

Field Note: *Altered granitoid*

PETROGRAPHY

This sample contains areas of altered quartz-bearing diorite-monzodiorite and a complex vein set. The visually estimated mineralogy below refers to the less altered parts of the diorite.

Mineral	***Abundance***	***Origin/location***
Plagioclase + hematite + sericite	50-52%	Altered primary plagioclase
Hornblende and chlorite-leucoxene	34%	Partly fresh hornblende and chloritised biotite and hornblende
K-feldspar	7-8%	Interstitial
Quartz	5%	Interstitial
Oxide, pyrite and titanite	1-2%	Minor components
Apatite and zircon	Sparse	Accessories

The freshest areas have weakly altered plagioclase to 5mm in grainsize (mostly less than 3mm) as well as fresh hornblende to2.5mm and smaller flakes of chloritised biotite. Interstitial poikilitic K-feldspar and mostly fine-grained quartz are also disseminated and there is very minor fine-grained pyrite as well as opaque oxide, titanite, apatite and rare zircon to 0.25mm long. Further alteration sees hornblende also altered to chlorite and leucoxene and minor epidote in late magmatic quartz. More altered rock on the other side of most of the veins has more heavily hematite-stained plagioclase and totally altered mafic silicates. This area has interstitial quartz but little or no K-feldspar. Trace pyrite is also disseminated.

Lenses of hematite-stained microcrystalline feldspar, containing smaller lenses of carbonate and epidote, occur in the less altered part and are adjacent to a narrow carbonate vein with sparse hematite, pyrite to 0.5mm in grainsize, quartz and chlorite. A screen of altered diorite separates this vein from a possibly boudinaged vein 3-5mm wide, dominated by coarse-grained carbonate but with irregular quartz-rich lenses. Minor epidote occurs in this vein. Along one side of this

vein, adjacent to the more altered diorite, there is a zone 1.5mm to 3mm wide dominated by granular to prismatic epidote with minor quartz and carbonate. Narrower veins, with carbonate ± quartz, are parallel or oblique to the main veins, mostly within the more highly altered diorite,

Interpretation:

This sample represents altered and veined quartz and K-feldspar-bearing hornblende diorite with albite-hematite-sericite-chlorite-leucoxene alteration and veins variously rich in quartz, carbonate and epidote. Traces of pyrite are disseminated.

Sample No	***1708870***
Rock type from TS	Quartz-bearing biotite-hornblende quartz diorite to quartz monzodiorite with albite-hematite-chlorite alteration, epidote veins and rare pyrite.
Hand specimen	Pinkish granular rock with dark spots

Field Note: *Altered granitoid*

PETROGRAPHY

Visually estimated mineralogy:

Mineral	***Abundance***	***Origin/location***
Albite with epidote and hematite	~50%	Altered plagioclase
Hornblende ± chlorite ± leucoxene	25-30%	Partly altered primary hornblende
Lamellae chlorite-leucoxene	10-15%	Altered biotite
Quartz	3-5%	Interstitial, late magmatic
Orthoclase	7-8%	Coarse-grained interstitial
Pyrite	<1%	Secondary
Titanite, apatite and oxide	<1%	Accessories

Albitised plagioclase to 4mm in grainsize is abundant in this thin section and contains fine-grained epidote and patches of hematite as well a diffuse pale hematite. Granular hornblende is partly or largely altered to chlorite and leucoxene, with lamellar chlorite and leucoxene replacing biotite flakes. Interstitial quartz is disseminated and there are large interstitial orthoclase grains about 5mm to 8mm in diameter along two edges of the thin section, providing a monzonitic texture to these areas. Veins of epidote are 0.2mm to 0.5mm wide and there are very narrow albite veins.

Interpretation:

This sample is composed of altered diorite to monzodiorite with minor pyrite.

Sample No	***1708871***
Rock type from TS	Quartz-rich granofels with altered feldspar(s), and biotite and minor green hornblende, accompanied by opaque oxide, apatite and altered accessory grains: chlorite-sericite alteration is seen and the rock may be metasandstone or an unusual vein.
Hand specimen	Pale, hard lithology, possibly quartz-rich

Field Note: *Calcite/feldspar vein in granite?*

PETROGRAPHY

Visually estimated mineralogy:

Mineral	***Abundance***	***Origin/location***
Quartz	Dominant	Recrystallised
Albite ± sericite + K-feldspar?	Minor (10-15%)	Metamorphic?
Clay-chlorite-leucoxene ± prehnite	Minor (~5%)	Ex-biotite
Hornblende	<1%	Metamorphic, in one corner
Limonitised and clay-altered grains	Trace	Accessories
Apatite	Trace	Accessory: prisms and needles

This sample is predominantly inequigranular quartz to 5mm in grainsize showing some exaggerated grain growth, with mostly fine-grained interstitial sericite-clouded albite and chlorite or clay-altered fine-grained decussate biotite. Plagioclase to 1.5mm in grainsize occurs in one corner of the thin section with disseminated prismatic hornblende to 2mm long. A flake of altered biotite in this area contains a lens of prehnite. Rare fresh opaque grains occur, but their composition is uncertain. Disseminated small grains have been altered to limonite or orange clay and may include opaque oxide and possible allanite. Minor apatite is disseminated, most abundantly in areas close to hornblende, with granular and acicular textures. Much of the apatite is enclosed in quartz

Interpretation:

This lithology would normally be interpreted as metasandstone, but the context, together with the presence of apatite makes this questionable. However, the texture and mineralogy would be very unusual in a vein. It is unfoliated and classified as granofels.

3. GEOCHEMISTRY TABLE

					Majors											
					Al_2O_3	CaO	Fe_2O_3	K_2O	MgO	MnO	Na_2O	P_2O_5	SiO_2	TiO_2	H_2O	LOI
				Units	%	%	%	%	%	%	%	%	%	%	%	%
				Scheme	IC4	IC4	IC4	IC4	IC4	IC4	IC4	IC4	IC4	IC4	GRAV5A	GRAV7
				Detection Limit	0.01	0.01	0.01	0.01	0.01	0.01	0.01	0.01	0.01	0.01	0.01A	0.01A
Sample Number	**Lithology**	**Depth from** (m)	**Depth to** (m)													
1708854	granodiorite	79.00	79.25		17.5	4.19	7.02	3.23	3.26	0.13	4.24	0.44	55.7	0.84	0.37	1.73
1708858	metasediment	90.00	91.40		19.3	1.22	7.48	5.28	3.26	0.07	2.2	0.1	57.8	0.93	0.74	1.01
1708859	granodiorite	98.30	98.75		17	3.05	6.61	3.38	3.04	0.11	4.38	0.37	57.2	0.88	0.42	2.86
1708863	diorite	158.70	160.15		15.8	8.09	10.7	1.77	6.32	0.18	2.9	0.41	49.7	0.88	0.5	2.31
1708866	porphyritic diorite	326.58	327.00		17.3	6.7	9.73	2.29	3.76	0.15	4.02	0.62	51.5	1.12	1.44	1.7
1661813	diorite	415.20	415.52		16.1	3.77	5.31	4.11	1.82	0.08	4.08	0.21	62.3	0.69		2.14
1661818	diorite	434.12	434.60		16.4	5.08	7.02	3.62	3.71	0.12	4.55	0.33	56.7	0.76		2.6
1661819	diorite	466.45	466.80		17.8	7.42	8	1.63	3.99	0.12	4.55	0.38	55	0.75		1.29
1661823	diorite	508.05	508.70		17.3	4.99	6.73	2.94	5.2	0.15	4.8	0.26	54.2	0.68		3.92
1661824	diorite	522.04	522.45		16.9	6.3	7.36	2.16	3.66	0.12	4.53	0.31	56.9	0.76		1.43
1661825	diorite	541.33	541.63		18.1	9.47	10.4	1.49	4.88	0.13	3.3	0.82	49.6	0.84		1.54
1661826	leucocratic band in diorite	555.62	556.04		13.3	1.4	1.39	4.93	0.22	0.01	3.67	<0.01	74.5	0.12		0.76
1661827	mafic enclave in diorite	603.88	604.11		14.9	11.5	17.1	0.51	5.95	0.23	2.16	0.24	46.3	1.74		0.52
1661828	diorite	627.10	627.40		17.7	6.25	7.77	2.4	2.84	0.11	4.65	0.39	55.4	1.04		1.56
1661829	diorite	630.08	630.34		18.1	7.89	8	1.29	3.83	0.11	4.4	0.36	52.7	0.77		1.38

		Trace Elements															
		Ag	As	Ba	Be	Bi	Cd	Co	Cr	Cs	Cu	Ga	Hf	In	Mo	Nb	Ni
	Units	ppm	ppm	ppm	ppm	ppm	ppm	ppm	ppm	ppm	ppm	ppm	ppm	ppm	ppm	ppm	ppm
	Scheme	IC3M	IC3M	IC4M	IC4M	IC3M	IC3M	IC3M	IC4	IC3M	IC3M	IC3M	IC4M	IC3M	IC4M	XRF1	IC3M
	Detection Limit	0.1	0.5	10	0.5	0.1	0.1	0.2	20	0.1	0.5	0.1	1	0.5	2	2	2
Sample Number	**Lithology**																
1708854	granodiorite	0.2	0.5	1200	1.5	<0.1	<0.1	21	25	1.9	14	21.5	5	<0.5	<2	11	26
1708858	metasediment	0.3	1	750	3.5	0.1	<0.1	22	170	4.9	11.5	26.5	8	<0.5	<2	17	55
1708859	granodiorite	0.2	2.5	1600	1.5	<0.1	0.2	16.5	40	1.6	41	21	6	<0.5	<2	13	19
1708863	diorite	0.2	1.5	550	1	<0.1	0.1	43	125	2.1	100	18.5	2	<0.5	<2	4	105
1708866	porphyritic diorite	0.2	0.5	1100	2	<0.1	<0.1	27.5	25	1.7	44.5	22.5	6	<0.5	<2	11	21
1661813	diorite	0.2	1.5	1300	1.5	<0.1	<0.1	11.5	<20	0.6	50	23.5	5	<0.5	<2	12	12
1661818	diorite	0.2	2	800	1.5	<0.1	0.1	21	30	0.3	39.5	22	3	<0.5	<2	9	40
1661819	diorite	0.2	29	850	1	<0.1	0.1	24.5	35	1.1	80	26.5	2	<0.5	<2	7	46
1661823	diorite	0.2	2.5	550	1	<0.1	<0.1	17.5	25	1.1	38	27.5	3	<0.5	<2	8	35
1661824	diorite	0.2	1.5	900	1.5	<0.1	0.2	21.5	30	1.3	40.5	25	3	<0.5	<2	9	43
1661825	diorite	0.1	1.5	445	0.5	<0.1	<0.1	35	35	1.7	110	26	1	<0.5	<2	2	50
1661826	leucocratic band in diorite	0.1	1.5	1200	1.5	<0.1	<0.1	2.2	<20	0.9	28.5	15.5	3	<0.5	<2	3	2
1661827	mafic enclave in diorite	0.1	7	170	1	<0.1	0.1	55	20	2.2	75	26.5	1	<0.5	<2	3	60
1661828	diorite	0.3	0.5	1400	1	<0.1	0.1	17.5	20	1	70	27.5	7	<0.5	<2	14	21
1661829	diorite	0.2	1	800	1.5	<0.1	0.2	24	40	1.2	70	26.5	1	<0.5	<2	4	42

		Trace Elements																
		Pb	Rb	Sb	Sc	Se	Sn	Sr	Ta	Te	Th	Tl	U	V	W	Y	Zn	Zr
	Units	ppm	ppm	ppm	ppm	ppm	ppm	ppm	ppm	ppm	ppm	ppm	ppm	ppm	ppm	ppm	ppm	ppm
	Scheme	IC3M	IC4M	IC3M	IC4	IC3M	IC4M	IC4M	IC4M	IC3M	IC4M	IC3M	IC4M	IC4	IC4M	IC4M	IC3M	XRF1
	Detection Limit	0.5	0.5	0.5	5	0.5	10	5	2	0.2	0.5	0.1	0.5	20	3	1	0.5	4
Sample Number	**Lithology**																	
1708854	granodiorite	19.5	95	<0.5	15	<0.5	<10	800	<2	0.2	11.5	0.7	3	105	<3	18	105	220
1708858	metasediment	21.5	175	<0.5	20	<0.5	<10	135	2	0.2	31	0.9	5	90	<3	37	145	300
1708859	granodiorite	20.5	95	<0.5	10	<0.5	<10	750	<2	0.4	10.5	0.8	2	90	<3	19	120	295
1708863	diorite	25.5	60	<0.5	25	<0.5	<10	750	<2	0.4	5	0.3	1	180	<3	14	120	60
1708866	porphyritic diorite	15	65	<0.5	20	<0.5	<10	950	<2	0.4	8.5	0.4	1.5	160	<3	22	135	265
1661813	diorite	39	90	<0.5	10	<0.5	<10	900	<2	<0.2	19.5	0.6	3	70	<3	13	75	245
1661818	diorite	19	90	<0.5	15	<0.5	<10	750	<2	<0.2	8.5	0.8	1.5	100	<3	12	160	150
1661819	diorite	30.5	31.5	<0.5	15	<0.5	<10	1200	<2	<0.2	3.5	0.2	<0.5	125	<3	12	110	80
1661823	diorite	13	80	<0.5	10	<0.5	<10	1100	<2	<0.2	8	0.5	1	110	<3	12	170	115
1661824	diorite	30.5	49.5	<0.5	15	<0.5	<10	1000	<2	<0.2	7	0.3	1	115	<3	12	115	135
1661825	diorite	20.5	39	<0.5	15	<0.5	<10	1400	<2	<0.2	3.5	0.2	0.5	190	<3	10	110	45
1661826	leucocratic band in diorite	45	85	<0.5	2.5	<0.5	<10	550	<2	<0.2	33	0.4	8	<20	<3	1	23.5	130
1661827	mafic enclave in diorite	10.5	15.5	<0.5	40	<0.5	<10	280	<2	<0.2	<0.5	0.1	<0.5	375	<3	22	205	50
1661828	diorite	24.5	50	<0.5	10	<0.5	<10	1200	<2	<0.2	11	0.3	2	105	<3	18	115	350
1661829	diorite	24.5	23	<0.5	15	<0.5	<10	1300	<2	<0.2	3	0.2	1	125	<3	13	110	60

		Rare Earth Elements													
		La	Ce	Pr	Nd	Sm	Eu	Gd	Tb	Ho	Dy	Er	Tm	Yb	Lu
	Units	ppm	ppm	ppm	ppm	ppm	ppm	ppm	ppm	ppm	ppm	ppm	ppm	ppm	ppm
	Scheme	IC4M	IC4M	IC3R	IC3R	IC3R	IC3R	IC3R	IC3R	IC3R	IC3R	IC3R	IC3R	IC3R	IC3R
	Detection Limit	1	1	0.05	0.02	0.02	0.02	0.05	0.02	0.02	0.02	0.05	0.05	0.05	0.02
Sample Number	**Lithology**														
1708854	granodiorite	75	150	17	65	10	2.5	7	0.86	0.66	4	1.75	0.25	1.45	0.2
1708858	metasediment	70	140	15	55	9.5	1.5	7.5	1.2	1.15	6	3.3	0.45	2.9	0.42
1708859	granodiorite	75	165	18	65	10	2.4	6.5	0.82	0.64	3.8	1.75	0.25	1.5	0.18
1708863	diorite	38	80	9.5	36.5	6.5	1.85	4.6	0.62	0.5	2.9	1.4	0.2	1.2	0.88
1708866	porphyritic diorite	75	160	18	70	11	2.8	7.5	0.94	0.78	4.5	2.1	0.3	1.8	0.28
1661813	diorite	70	110	11.5	41	7.5	1.7	3.7	0.5	0.46	2.7	1.25	0.15	2.8	0.16
1661818	diorite	55	90	12	43	7.5	2	4.1	0.54	0.48	2.9	1.3	0.15	2.8	0.16
1661819	diorite	55	90	11.5	42.5	8	2.2	4.2	0.54	0.46	2.8	1.25	0.15	2.5	0.14
1661823	diorite	70	105	13.5	50	9	2.3	4.7	0.58	0.46	2.8	1.25	0.15	2.7	0.16
1661824	diorite	55	90	11.5	42.5	8	2	4.2	0.56	0.48	3	1.3	0.15	2.5	0.16
1661825	diorite	42	75	10.5	40.5	7.5	2.1	4	0.5	0.4	2.5	1.05	0.1	2.6	0.1
1661826	leucocratic band in diorite	50	65	6	16.5	2.1	0.72	0.8	0.08	0.06	0.38	0.2	<0.05	1.8	0.04
1661827	mafic enclave in diorite	15	28	4.4	19	4.7	1.45	3.8	0.66	0.92	4.7	2.6	0.4	3.8	0.38
1661828	diorite	85	140	17.5	65	11.5	2.6	5.5	0.76	0.66	4	1.75	0.2	3.2	0.2
1661829	diorite	55	90	11.5	44	8	2.3	4.5	0.58	0.5	3.1	1.35	0.15	2.5	0.16

REFERENCES

Allen, S.R., McPhie, J., Ferris, G. and Simpson, C., 2008. Evolution and architecture of a large felsic Igneous Province in western Laurentia: The 1.6 Ga Gawler Range Volcanics, South Australia. Journal of Volcanology and Geothermal Research, 172: 132-147.

Black, L. P., Kamo, S. L., Allen, C. M., Aleinikoff, J. N., Davis, D. W., Korsch, R. J. and Foudoulis, C., 2003. TEMORA 1: a new zircon standard for Phanerozoic U-Pb geochronology. Chemical Geology 200(1-2): 155-170.

Blissett, A.H., Creaser, R.A., Daly, S.J., Flint, R.B. and Parker, A.J., 1993. Gawler Range Volcanics. In: J.F. Drexel, W.V. Preiss and A.J. Parker (Editors), The Geology of South Australia. Vol. 1, The Precambrian. South Australia Geological Survey. Bulletin 54, pp. 107-124.

Bonython, W.V., 1984. Geochemistry of the Rare Earth Elements: Meteorite Studies. In: P. Henderson (Editor), Rare Earth Element Geochemistry. Elsevier, pp. 63-114.

Dalgarno, C.R., Johnson, J.E., Forbes, B.G. and Thomson, B.P., 1968. Port Augusta 1:250 000 Geological Atlas Series Map. Sheet SI/53-4. Geological Survey South Australia. .

Dutch, R., Hand, M. and Kinny, P.D., 2008. High-grade Palaeoproterozoic reworking in the southeastern Gawler Craton, South Australia. Australian Journal of Earth Sciences, 55: 1063-1081.

Fanning, C.M., Reid, A.J. and Teale, G.S., 2007. A Geochronological Framework for the Gawler Craton, South Australia. South Australia Geological Survey. Bulletin 55.

Faulkner, L., 2007. EL 3466 and 3467. Lake Gilles and Corunna North. PACE Initiative: Theme 2, Year 4. Drilling partnership - eastern margin of Gawler Range Volcanic Province mineral prospects. Project final report., Open File Envelope 11458. Geological Survey Branch. Primary Industries and Resources South Australia.

Fraser, G., McAvaney, S., Neumann, N., Szpunar, M. and Reid, A., 2010. Discovery of early Mesoarchaean crust in the eastern Gawler Craton, South Australia. Precambrian Research, 179: 1-21.

Fraser, G. and Neumann, N., 2010. New SHRIMP U-Pb zircon ages from the Gawler Craton and Curnamona Province, South Australia, 2008 - 2010. Geoscience Australia, Record, 2010/16.

Fricke, C.E., 2005. Source and origin of the lower Gawler Range Volcanics (GRV), South Australia: Geochemical constraints from mafic magmas, Honours theisis, Monash University, Clayton.

Gifkins, C., Herrmann, W. and Large, R., 2005. Altered volcanic rocks: a guide to description and interpretation. Centre for Ore Deposit Research, Hobart.

Giles, C.W., 1980. A Comparative Study of Archaean and Proterozoic Felsic Volcanic Associations in Southern Australia, University of Adelaide.

Howard, K.E. et al., 2011. U-Pb zircon, zircon Hf and whole-rock Sm-Nd isotopic constraints on the evolution of Palaeoproterozoic rocks in the northern Gawler Craton. Australian Journal of Earth Sciences, 58: 615-638.

Janousek, V., 2008. GCDkit version 2.3, pp. Geochemical Data Toolkit for Windows.

Le Bas, M.J., Le Maitre, R.W., Streckiesen, A. and Zanettin, B., 1986. A chemical classification of volcanic rocks based on the total alkali-silica diagram. Journal of Petrology, 27: 745-750.

Ludwig, K.R. 2001. SQUID 1.02. A User's Manual. Berkeley Geochronology Center Special Publication number 2, 21 pp.

Ludwig, K.R. 2003. Isoplot 3.00 - a geochronological toolkit for Microsoft Excel. Berkeley Geochronology Center Special Publication No. 4.

McAvaney, S., 2012. The Cooyerdoo Granite: Palaeo- and Mesoarchaean basement of the Gawler Craton

MESA Journal, 65, in press.

Middlemost, E.A.K., 1985. Magmas and Magmatic rocks: An Introduction to Igneous Petrology. Longman, London.

Parker, A.J., 1980. The Kalinjala Mylonite Zone, eastern Eyre Peninsula. Quarterly Geological Notes, 76: 6-11.

Parker, A.J., 1993. Kimban Orogeny. In: J.F. Drexel, W.V. Preiss and A.J. Parker (Editors), The geology of South Australia. Vol. 1, The Precambrian. South Australia Geological Survey.

Parker, A.J. and Flint, R.B., 1983. WHYALLA, South Australia. Sheet SI/53-08, International Index. 1:250 000 Geological Series Geological Survey of South Australia.

Payne, J.L., Hand, M., Barovich, K. and Wade, B.P., 2008. Temporal constraints on the timing of high-grade metamorphism in the northern Gawler Craton: implications for assembly of the Australian Proterozoic. Australian Journal of Earth Sciences, 55(623-640).

Purvis, A., 2009. Mineralogical Report No.9483. Pontifex and Associates Pty. Ltd.

Purvis, A., 2010. Mineralogical Report No. 9691. Pontifex and Associates Ltd.

Reid, A., Vassallo, J., Wilson, C. and Fanning, C.M., 2007. Timing of the Kimban Orogeny on southern Eyre Peninsula, Report Book 2007/005. Primary Industries and Resources of South Australia.

Reid, A.J., McAvaney, S.O. and Fraser, G.L., 2008. Nature of the Kimban Orogeny across northern Eyre Peninsula. MESA Journal, 51: 25-34.

Stacey, J.S. and Kramers, J.D. 1975. Approximation of terrestrial lead isotope evolution by a two-stage model. *Earth and Planetary Science Letters* 26: 207-221

Steiger, R.H. and Jäger, E. 1977. Subcommission of geochronology: convention on the use of decay constants in geo- and cosmochronology. *Earth and Planetary Science Letters* 36: 359-362

Stern, R.A., Bodorkos, S., Kamo, S.L., Hickman, A.H. and Corfu, F. 2009. Measurement of SIMS Instrumental Mass Fractionation of Pb Isotopes During Zircon Dating. Geostandards and Geoanalytical Research 33(2): 145-168.

Sun, S.S. and McDonough, W.F., 1989. Chemical and isotopic systematics of oceanic basalts: implications for mantle composition and processes. In: A.D. Saunders and M.J. Norry (Editors), Magmatism in ocean basins. Geological Society of London Special Publication 42, pp. 313-345.

Szpunar, M., Hand, M., Barovich, K. and Jagodzinski, E.J., 2011. Isotopic and geochemical constraints on the Palaeoproterozoic Hutchison Group, southern Australia: Implications for Palaeoproterozoic reconstructions. Precambrian Research, 187: 99-126.

Taylor, S.R. and McLennan, S.M., 1985. The Continental Crust: Its composition and evolution. Blackwell Scientific Publications.

Vassallo, J.J. and Wilson, C.J.L., 2002. Palaeoproterozoic regional-scale non-coaxial deformation: an example from eastern Eyre Peninsula, South Australia. Journal of Structural Geology, 24: 1-24.

Weste, G., 1996. Geology of the Roopena and Uno 1:100 000 scale mapsheet areas, eastern Gawler Craton, South Australia. Department of Primary Industries and Resources. Open File Envelope, 9025.